IS&T imaging.org

November 7-8, 2025 Tokyo, Japan

Advances in Printing Technology

EXPLORING CUTTING EDGE PRINTING TECHNOLOGY

PAPERS BEING PRESENTED AT ADVANCES IN PRINTING TECHNOLOGY 2025

November
7 (Fri) - 8 (Sat), 2025

Japan Printing Center
1 Chome-16-8 Shintomi-cho, Chuo-ku, Tokyo

Organizer: Society for Imaging Science and Technology

Co-Organizer: IS&T Tokyo-Japan Chapter
Sponsor: Imaging Society of Japan

APT2025 Technical Program

7-Nov

	Time	Country	name	Affiliation	Title	Exhibit
Opening Remarks	9:00-9:05	USA	Jonathan B. Phillips	Executive Director, Society for Imaging Science & Technology	Opening remarks 1	-
	9:05-9:10	Japan	Masahiko Fujii	President, the Imaging Society of Japan	Opening remarks 2	-
"Electrophotography and Metrology"						
Opening Keynote	9:10-10:10	USA	Chieh-Min Cheng	Xerox Corporation (Retired)	Reimagining Toner: Vibrant Effects, Greener Materials, and Smarter Manufacturing at Xerox	-
1	10:10-10:35	Japan	Koichiro Yuasa, Yutaka Kiuchi	FUJIFILM Business Innovation Corp.	Contact and Non-contact Hybrid Static Elimination Technology to adapt High Resistance Media in Electrophotography	-
2	10:35-11:00	Japan	Yosuke Tsukiyama	Niigata University	Effect of Paper Dust (Lint) and Evaluation of Paper Dust Release	-
Author's interview & Break (15min)						
lunch: 11:15-13:00						
"Novel Products and Solutions" (Prodct Introductoin)						
3	13:00-13:25	Japan	Nobuhiko Hosobata	KNF Japan Co., Ltd.	KNF Diaphragm pumps and applications	-
4	13:25-13:50	Japan	Futa Kawagoe	HIROX Co.,Ltd	Utilization of Digital Microscopes in the Printing Industry	With exhibit
5	13:50-14:15	Japan	Genta Koori	KONICA MINOLTA, INC.	Measurement Technologies Supporting Color Management in the Growing Industrial Printing Industry	-
Author's interview & Break (15min)						
"Latest Inkjet Technology and Trends 1"						
6	14:30-14:55	United Kingdom	Tri Tuladhar	Trijet Limited	TriPAV: A High-Frequency Rheometer for Precision Inkjet Characterisation and Waveform Optimisation	With exhibit
7	14:55-15:20	Germany	Ramon Borrell	Quantica GmbH	Novel Additive Manufacturing Applications Enabled by Modular Integration of Ultra High Viscosity Technology	-
8	15:20-15:45	South Korea	Jaeyong Choi	ENJET Co.,LTD.	Development of a Multi-Nozzle Hybrid Inkjet Printhead Enabling Droplet Ejection up to 200 cP Using Piezoelectric–Electrohydrodynamic Mechanism	-
Author's interview & Break (15min)						
"AI-Driven Research"						
9	16:00-16:25	Kazakhstan	Altynay Kadyrova	KIMEP University	Text-to-Image Generation AI Tools for 2.5D Prints: Preliminary Observations	-
10	16:25-16:50	Switzerland	Fernando Rodriguez Llorente	HES-SO University of Applied Sciences and Arts Western Switzerland	The role of nozzle acoustic sensing in inkjet printing, an Artificial Intelligence perspective.	-
11	16:50-17:15	Japan	Takahiro Tsujimoto	KONICA MINOLTA, INC.	Next-generation Intelligent Media Sensor System: Automating Operations and Enhancing Productivity through Paper Type Identification	-
Focal Talk	17:15-17:45	Norway	Marius Pedersen	Norwegian University of Science and Technology	Exploring the Future Potential of Artificial Intelligence for Printing	-
Author's interview & Break (15min)						
(All attendees will wait outside the room.)						
Reception	19:00-21:00					

8-Nov

		Country	name	Affiliation	Title	Exhibit
Announcements	9:00-9:05					
"Latest Inkjet Technology and Trends 2"						
12	9:05-9:30	Japan	Yosuke Konishi	RICOH Company Ltd.	Observation of Pore Formation in Binder Jetting with Granulated Ceramics Particles	-
13	9:30-9:55	USA	Shane O'Neill	FUJIFILM Dimatix	PERFORMANCE, PRODUCTIVITY, DURABILITY- The recipe for productivity in high-speed inkjet	-
Author's interview & Break (10min)						
"Technologies for Aesthetic Expression"						
14	10:05-10:30	Japan	Masaya Takahashi	ALPS ALPINE CO., LTD.	Development of metal decoration technology using on-demand thermal transfer printing	With exhibit
15	10:30-10:55	Japan	Hiroya Nishida	KYOCERA Corporation	A New 12-inch, 1200dpi Thermal Printhead for Digital Decorative Film Printing	-
16	10:55-11:20	Japan	Nobuyuki Kamitani	Dai Nippon Printing Co., Ltd.	Peripheral technologies for enhancing the print quality of the Ki-Re-i ID photo booth	-
Author's interview & Exhibition (1hour10min, 11:20-12:30)						
lunch: 12:30-14:00						
"Significance and Value of Printing"						
17	14:00-14:25	Estonia	Enn Kerner	Board member of ENGINEERS EUROPE	Enhancing Quality and Standardisation in Flexographic Printing: the need to embrace Big Data	-
18	14:25-14:50	Switzerland	Patrick Le Galudec	PLG Consultant for DiatecX	GREEN a sincere approach to Ecology applied to inkjet printing	-
Author's interview & Break (10min)						
Focal Talk	15:00-15:30	Japan	Katsuhiko Nishimura	CrossMINDS Co., Ltd.	The Enduring Value of Electrophotography in the Digital Age: Pioneering New Frontiers	With exhibit
Focal Talk	15:30-16:00	Japan	Yoheita Yoshihara, Yoshihiro Miura	KENBUNSYA CO.,LTD.	RGB workflow and high-value-added decorative printing initiatives	With exhibit
Closing Keynote	16:00-17:00	Netherland	Charles Lissenburg	Keypoint Intelligence	The Future of Print: Value, Volume—or Both?	-
Closing Remarks	17:00-17:05	Japan	Natsuko Minegishi	KONICA MINOLTA, INC.	Closing Remarks	-

Reimagining Toner: Vibrant Effects, Greener Materials, and Smarter Manufacturing at Xerox

Chieh-Min Cheng (Retired); Xerox Corporation; Webster, New York, USA

Abstract

Toner technology is at a transformative crossroads. With heightened demands for vivid print quality, sustainability, and cost-efficient manufacturing, Xerox has reimagined its toner development pipeline. This paper presents a comprehensive overview of Xerox's innovative work in three pillars: (1) specialty toners enabling new color and functional effects, (2) sustainable toners incorporating bio-based and low-impact materials, and (3) advanced manufacturing via the Continuous Emulsion Aggregation (EA) toner process, with new solvent-free techniques for resin emulsification. Together, these advances push the boundaries of what's possible in electrophotographic printing.

Specialty Toners – Expanding the Color and Function Palette

Xerox's specialty toners are designed not only to expand the CMYK color gamut but also to introduce unique visual and functional effects. These include:

1. Gamut Extension Toners: Beyond CMYK, Xerox has developed orange, green, and violet toners for extended-gamut printing. These enable higher color accuracy in packaging, branding, and photo applications—achieving up to 90% Pantone® coverage in certain workflows.

2. Clear Toner: Clear toners enable tactile and visual enhancement through spot varnish effects, watermarking, and protective overcoats. Precise EA particle size control ensures uniform gloss modulation, and the resin system is optimized for transparency and low haze.

3. White Toner: High-opacity white toner is essential for printing on dark or transparent substrates, particularly in packaging and specialty print applications. Xerox's formulation provides superior coverage with fewer layers, reducing cost and print time.

4. Metallic Toners (Gold and Silver): Metallic toners offer a cost-effective alternative to foil stamping and metallic inks. Xerox metallic toner integrates reflective pigments into a stable carrier system, enabling high-shine finishes while maintaining fuser compatibility.

5. Fluorescent Toners: Fluorescent cyan, magenta, yellow, and white toners glow under UV light and have found applications in event tickets, promotional materials, and youth-focused marketing. These toners require precise pigment dispersion and stability control, which has been a focus of Xerox's R&D [1].

6. Security and Anti-Counterfeiting Toners: Xerox has developed specialty toners that incorporate taggants—chemical markers that are invisible to the naked eye but detectable under specific conditions. This enables track-and-trace, authenticity verification, and brand protection features.

7. Phosphorescent Toners: Unlike fluorescent toners, phosphorescent toners glow after exposure to light. These are used in emergency signage, novelty printing, and limited-edition designs. Xerox has optimized pigment loading and particle morphology to ensure charge stability and fusing performance.

Table 1: Xerox Specialty Toner Portfolio.

Specialty Toners		Color
	White	
	Clear	
Metallic	Silver	
	Gold	
Fluorescent	Cyan	
	Magenta	
	Yellow	
	White	
Security	IR taggant	
	Invisible fluorescent	Under UV
	Light Black	
	Conductive	

Figure 1: Xerox specialty toners enable a wider range of possibilities.

While Table 1 summarizes the attributes of Xerox's specialty toner portfolio, Figure 1 illustrates their translation into real-world applications [2]. Examples include the use of white and metallic toners for high-contrast invitations, fluorescents for attention-grabbing signage, and clear overlays for visual and tactile effects on menus and postcards. Together, these capabilities demonstrate how specialty toners expand the creative and functional boundaries of digital printing, enabling new value propositions for both commercial and security-sensitive markets.

Sustainable Toners – Toward Greener Printing

As the printing industry confronts its environmental impact, Xerox has prioritized sustainability in toner development. Three major directions are being pursued:

1. Biomass-Based Polyester Resin Using Rosin Feedstocks: Xerox has successfully synthesized polyester toner resin using rosin-based feedstocks derived from pine trees [3]. These resins contribute to a higher bio-based content (over 30%) while maintaining essential properties like fusing, gloss, and triboelectric performance. In this approach, rosin acids are first esterified with reactive diols and subsequently copolymerized with monomers such as terephthalic acid (TPA), propylene glycol (PG), and sebacic acid (SA) to form tailored polyesters. These resins maintain the mechanical strength and thermal stability essential for emulsion aggregation while embedding a renewable carbon backbone. The resulting chemistry enables bio-based EA toners that achieve significant lifecycle carbon footprint reductions without sacrificing print quality or performance.

2. Microorganism-Derived Resin Systems: Biotechnology now enables the fermentation of bio-based monomers by engineered microorganisms. Xerox is exploring these bio-resins, particularly polyhydroxyalkanoates (PHAs), for use in hybrid toner systems [4]. Early prototypes show comparable performance to petrochemical-based polyester with a significantly reduced carbon footprint.

3. Steps Toward Carbon-Neutral Toner: Through a combination of renewable energy sourcing in production, recycled packaging, bio-derived resins, and improved energy efficiency in printing (lower fusing temperatures), Xerox is progressing toward carbon-neutral toner offerings. Life Cycle Analysis (LCA) tools are being integrated into toner formulation protocols to quantify and minimize environmental impact from raw material to printed page.

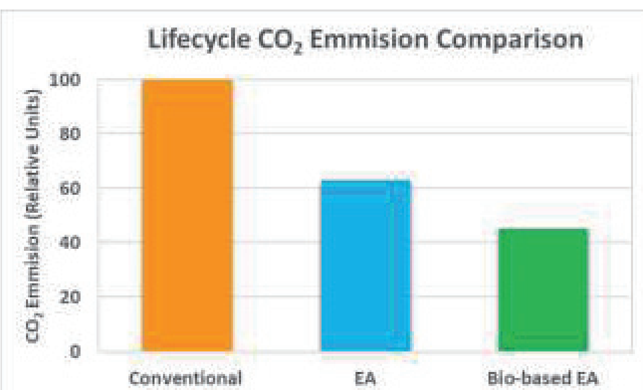

***Figure 2**:* Life cycle CO_2 emissions comparison between conventional pulverized toner, EA toner, and biomass-based EA toner.

Lifecycle assessment highlights how both process innovation and renewable resin substitution contribute to lowering the carbon footprint of toner systems. As shown in Figure 2, conventional pulverized toners carry the highest CO_2 emissions, normalized to 100 relative units. Emulsion aggregation (EA) toners already reduce emissions by roughly 35–40% due to their lower fusing energy requirements. When renewable resins are incorporated into EA systems, emissions are reduced even further—by more than half compared to conventional toners. Importantly, the EA process maintains tight particle size distribution and effective pigment encapsulation, ensuring that advances in sustainability do not come at the expense of print quality, color gamut, or durability.

Manufacturing Breakthroughs – Continuous EA Toner Process

Emulsion Aggregation (EA) technology remains at the core of Xerox's toner platform. It produces uniform, spherical toner particles with narrow size distribution and tunable surface properties. This leads to improved image quality, lower toner consumption, and faster fusing.

1. Transition to Continuous Processing:

Traditional batch EA processing suffers from variability and limited scalability. Xerox's continuous EA toner process allows for uninterrupted production with real-time control of particle size, charge, and morphology [5]. Key advantages include:

• Consistent product quality
• Higher throughput and reduced downtime
• Lower energy and water use per toner kilogram
• Integrated real-time quality monitoring

This shift from batch to continuous process represents a major milestone in toner manufacturing, aligning with the demands of both high-volume production and sustainable operations.

2. Solvent-Free for Polyester Resin Emulsification Latex

One of the major innovations in resin preparation is Xerox's continuous solvent-free emulsification (SFE) process for polyester latex [6].

• Elimination of organic solvents: Conventional latex production uses organic solvents or co-solvents to emulsify resins into nanoscale particles. Xerox's new solvent-free process eliminates these hazardous components entirely, aligning with green chemistry principles.

• Continuous operation advantages: The process allows for precise control of latex particle size and distribution, resin molecular weight, and thermal and rheological properties. This process reduces the overall carbon footprint of toner production and improves workplace safety and environmental compliance.

• Application to specialty and sustainable toners: This latex can be directly used in both specialty and sustainable toner formulations. Its tunability allows the incorporation of metallic pigments, fluorescent dyes, and bio-resins without compromising stability or print performance.

Integration Across the Value Chain

As illustrated in Figure 3, the transition from conventional to advanced toner platforms delivers quantifiable performance improvements across multiple dimensions. Pantone coverage increases by approximately 20%, enabled by the incorporation of specialty pigments such as metallics and fluorescents that broaden the accessible color gamut. Resin substitution with renewable feedstocks achieves up to 50% biomass incorporation, directly displacing fossil-based polyesters and lowering lifecycle emissions.

Process innovations, including continuous emulsion aggregation, shorten synthesis cycle times by ~30%, improving scalability and consistency. Most notably, solvent-free emulsification reduces organic solvent use by nearly 90%, representing a step-change in environmental compliance and sustainability. Collectively, these gains highlight how Xerox toner technology simultaneously advances print quality, manufacturing efficiency, and carbon reduction goals.

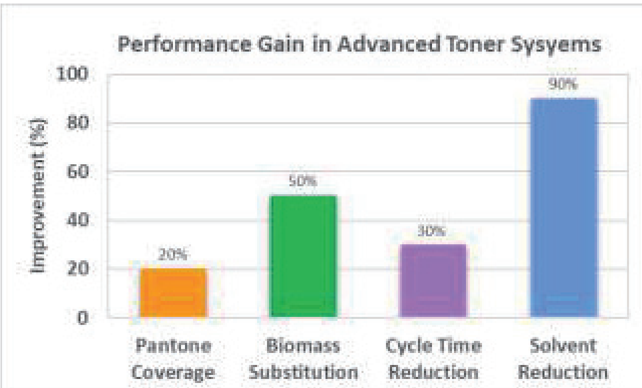

Figure* 3:* Measured performance improvements in advanced toner systems.

Xerox's toner innovations extend beyond material breakthroughs to embrace system-level integration across the entire imaging ecosystem. The convergence of specialty effects with sustainable resins presents unique challenges, as pigment loading, transparency, and charge control must remain compatible with bio-based chemistries. Xerox has addressed this by demonstrating proof-of-concept fluorescent and metallic toners formulated entirely with rosin-derived resins – proving that vibrancy and sustainability can coexist.

From a manufacturing perspective, the adoption of continuous EA processing in combination with solvent-free latex emulsification lowers production costs while strengthening sustainability metrics. This dual advantage establishes Xerox toners as both technologically advanced and environmentally responsible, in alignment with evolving regulations and market expectations.

Importantly, these innovations are integrated across the value chain:

• Printer hardware: New toner formulations are co-developed with fusing and charging subsystems to ensure optimal transfer and image fidelity.

• Workflow software: Specialty toner layers are integrated into prepress tools allowing designers to specify white, clear, or metallic effects easily.

• Packaging and logistics: Toners are packaged in recyclable containers with minimal overwrap, and shipping logistics are optimized using AI to reduce emissions.

• Customer enablement: Xerox provides training and support for print providers to maximize the creative and functional potential of specialty and sustainable toners.

Conclusion and Future Directions

Xerox's ongoing toner innovation program is reimagining what toner can do—not only in print quality and visual effects but also in sustainability and manufacturing efficiency [7]. Future directions include:

• Bioengineered toner particles with programmed degradation pathways.
• AI-driven toner formulation to optimize color, cost, and carbon.
• Decentralized microfactories using continuous processes for localized toner production.

These advances will redefine the role of toner in a circular, digital-first, and design-rich printing ecosystem.

References

[1] Qi, Y et al.; US Patent 11199786 (2021).
[2] Expand Your Opportunities Beyond CMYK; https://www.xerox.com/en-us/digital-printing/insights/beyond-cmyk
[3] Farrugia, V et al.; US Patent 8580472 (2013).
[4] McAneney-Lannen, G et al.; US Patent 8187780 (2012).
[5] Lawton, D et al.; US Patent 9182691 (2015).
[6] Faucher, S et al.; US Patent 8207246 (2012).
[7] Transformative Production Print Ecosystem; https://www.xerox.com/en-us/digital-printing

Author Biography

Dr. Chieh-Min Cheng, ACS Fellow, former Xerox Fellow and Area Manager, spent 29 years advancing toner and inkjet technologies, leading Xerox's Materials Technology Area. He holds 134 U.S. patents and 18 publications across polymers, imaging, inks, toners, e-paper, and 3D printing. With an M.S. in Chemical Engineering and a Ph.D. in Polymer Science and Engineering from Lehigh University, his career reflects a lasting commitment to innovation and advancing printing material sciences.

Contact and Non-contact Hybrid Static Elimination Technology to adapt High Resistance Media in Electrophotography

***Koichiro YUASA*[1] *and Yutaka KIUCHI*[2]**

[1]KeyTechnology Development, [2] Production Product Development, FUJIFILM Business Innovation Corp;Japan

Abstract

There has been increasing demand for digital printing using dry electrophotography especially to adapt high-resistance media such as transparent film or waterproof paper made from synthetic resin. In dry electrophotography, charging through the second transfer process causes electrostatic adhesion between each media for their high resistance, which lead to poor storage quality and electric shocks to operators. These prevent post-processing and limit the number of storable sheets. We have developed an elimination technology which improve these issues by utilizing the advantages of both a contact and a non-contact static elimination of static electricity. The contact static elimination is highly responsive to speed by supplying charge in narrow gap, and the non-contact is capable of uniform elimination of static electricity by supplying charge through corona discharge.

This technology is installed as a paper output option for products of Fujifilm, Revoria Press PC1120, EC2100S/EC2100, SC285S/SC285. As a result of introducing the technology to the market, it was found that it is necessary to accommodate static elimination for various types of media. When evaluating media resistance for each region's media using the charge decay half-life as an indicator, no regional differences were observed among Western countries, Asia, and Japan. For representative high-resistance media such as films, hologram films, label paper, and water-resistant paper, it was found that static elimination is required when the surface resistivity exceeds a certain value. This technology improves the work of printers with high resistance materials such as film and waterproof paper, reduces the need for the previous work of peeling off stuck paper, avoids operators from large amounts of static electricity. So, this technology enables digital printing using dry electrophotography to handle a variety of media, enabling printing companies to add value and expand the market.

1. Introduction

In recent years, digital printing using dry electrophotographic technology has enabled the creation of high-value-added images by combining conventional YMCK toners with special color toners such as metallic (gold and silver), white, and fluorescent pink. This combination expands expressive capabilities through various patterns. As a result, the demand for value enhancement using diverse media, as shown in Fig. 1, has been increasing. There is a growing need to support high-resistance media such as transparent films and waterproof paper [1]. However, due to the characteristics of the image formation process in dry electrophotography, issues such as electrostatic adhesion between high-resistance media and electric shocks to operators may occur. These prevent post-processing and limit the number of storable sheets.

Fig.1 *Image example of digital media.*

A typical dry electrophotographic process is illustrated in Fig. 2. This process consists of a primary transfer, in which a toner image developed on the photoconductor drum is transferred to an intermediate transfer belt, and a second transfer, in which the image on the belt is transferred onto the media. In the second transfer, toner is transferred to the media by applying a bias voltage to the charged toner, thereby forming an electric field.

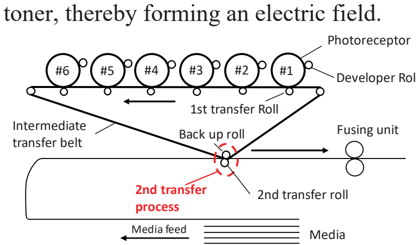

Fig.2 *Electrophotographic process.*

In the case of high-resistance media, the influence of the second transfer bias, as illustrated in Fig. 3, causes the surface potential of the media to become negatively charged after passing through the second transfer nip (Fig. 4), while the backside becomes positively charged.

This charge distribution leads to electrostatic adhesion, where the negative surface and positive backside attract each other (Fig. 5(a)). As a result, when the sheets overlap in the output tray, the films become misaligned, reducing stacking performance (Fig. 5(b)). Additionally, since charge accumulates on the film, operators may experience electrostatic discharge when touching the media, resulting in an electrical shock to fingers or other contact points.

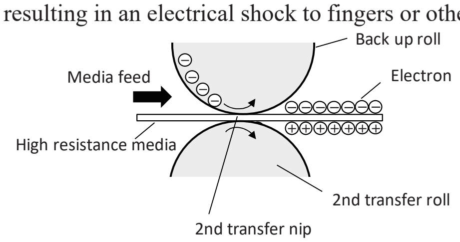

Fig.3 *2nd transfer process.*

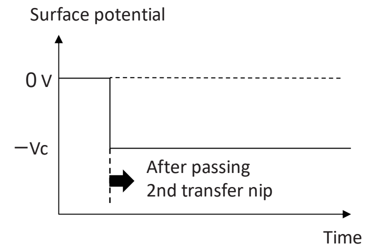

Fig.4 *Media surface potential.*

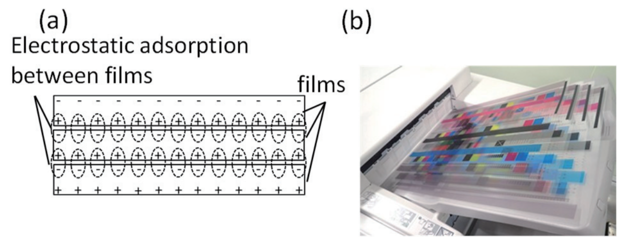

Fig. 5 *(a) Electrostatic adsorption between films (b) poor storage quality of film.*

To suppress the charging of the film, it is necessary to neutralize the electric charge on its surface. While a general-purpose ionizer (MJ-B04, manufactured by Keyence) [2] provides a certain level of effectiveness, its performance is insufficient for high-resistance media such as films. Therefore, we aimed to develop a static elimination technology compatible with high-resistance media that can be widely applied to production digital printing machines [10].

2. Study on Static Elimination Technology

Static elimination methods can be broadly categorized into contact-type and non-contact-type approaches. The contact-type method involves directly grounding static charges by bringing conductive brushes or wires into physical contact with the charged object. Alternatively, it can neutralize surface charges by supplying counterbalancing positive or negative charges.

In contrast, the non-contact-type method—typically employing corona discharge—utilizes high voltage to ionize ambient air, thereby generating bipolar ions (± charges) that neutralize static electricity on the target surface. Each method exhibits distinct discharge characteristics, and when applied to high-resistance media such as transparent film, neither approach alone provides sufficient static electricity elimination performance. Consequently, we investigated a hybrid static elimination system that integrates both contact and non-contact techniques to enhance overall discharge efficacy for high-resistance media.

2.1 Contact-type Static Elimination Technology

In general, when an electric field is applied to an insulator via contact with a roller, discharge occurs in microscopic air gaps. In electrophotography, a contact-based charging process is employed for photoconductive drums, where discharge is induced in the micro-gap regions formed before and after the nip area between the charging roller and the photoconductor, thereby enabling charge transfer [3]. The onset voltage for atmospheric discharge between parallel plate electrodes is known to follow Paschen's Law [4], which defines the breakdown voltage as a function of gap distance, pressure, and applied voltage. The discharge phenomena observed in the charging process can be reasonably approximated by this law.

While the above process is designed to impart charge, the same discharge mechanism can be utilized to remove existing charges by applying an opposite polarity to the charged media. Figure 6 illustrates a contact-type static eliminator based on this principle. The media is conveyed through a nip formed between a bias roll and a counter roll, where positive charges are supplied from the bias roll to neutralize negative charges on the media surface.

This method offers high responsiveness to charge variation and demonstrates significant surface potential reduction even under high-speed conditions typical of electrophotographic systems, as shown in Figure 7. However, contact-type static eliminator alone is insufficient to mitigate issues such as media adhesion and electrostatic shock. These limitations arise due to factors such as stress from gap discharge, surface roughness of the bias roll, surface irregularities and resistance non-uniformity of the media, and fluctuations in charge distribution during transport. These factors contribute to residual micro-scale potential fluctuations post-discharge.

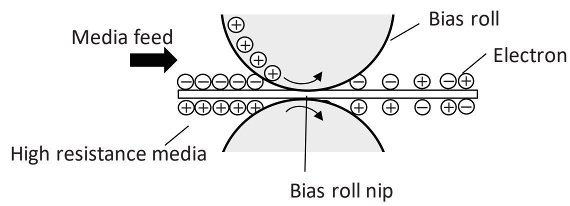

Fig. 6 *Contact-type static eliminator.*

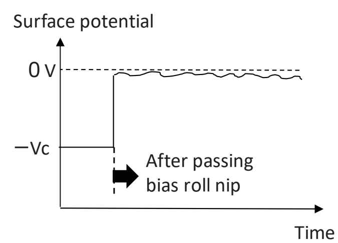

Fig. 7 *Media surface potential after contact-type static eliminator.*

2.2 Non-contact-type Static Elimination Technology

The non-contact-type static elimination involves applying a high voltage to a wire, thereby generating corona discharge in the vicinity of the wire surface. The corotron charging method, commonly used in electrophotography as a non-contact charging technique, charges the photoconductor by directing discharged particles along an electric field formed by the grid and shield electrodes.

Although non-contact static eliminator such as corotron are generally less effective in neutralizing strongly charged high-resistance films, they offer advantages over contact-based discharge techniques. Specifically, they are less susceptible to geometric constraints of the components involved, which can affect discharge uniformity in a contact-type static eliminator. Furthermore, the charged particles generated by corona discharge can selectively neutralize regions with higher potential differences, enabling in-plane charge uniformity across the media surface.

2.2.1 Counter electrode

In a non-contact-type static eliminator, the uniformity of charge neutralization is significantly influenced by the presence of a counter electrode on the reverse side of the media. Figure 8(a) illustrates the discharge effect of a non-contact ionizer equipped with a grounded counter electrode positioned opposite the discharge wire. In this configuration, the positive ions generated near the discharge wire are predominantly attracted toward the grounded electrode, thereby contributing to the neutralization of negative surface charges on high-resistance media.

Conversely, as shown in Figure 8(b), when no grounded counter electrode is installed opposite the discharge wire, the ions generated by corona discharge disperse into the surrounding space without being actively directed toward the negatively charged media surface. As a result, effective charge neutralization is not achieved[5].

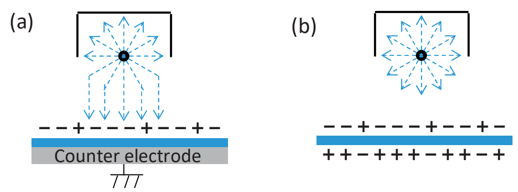

Fig. 8 *(a) Counter electrode (b)non counter electrode.*

2.2.2 AC Discharge Bias

To enhance the efficiency of non-contact static eliminator, the contribution of the AC component in the applied bias voltage is significant. Accordingly, the discharge bias is configured by superimposing an alternating voltage component onto a DC voltage, resulting in the generation of both positive and negative ions near the media surface. These ions contribute to the neutralization of both negative and positive surface charges, thereby reducing the surface potential toward zero, as illustrated in Figure 9(a).

In contrast, when a discharge bias consists solely of a DC voltage component, only positive ions are generated around the discharge wire. These ions can neutralize negative surface charges on the media; however, no negative ions are produced to neutralize positive surface charges. As a result, the positive charges remain on the media surface, as shown in Figure 9(b).

Based on these observations, the adoption of an AC discharge bias enables non-contact-type static eliminator (Figure 10) to effectively neutralize both positive and negative surface charges, even when they coexist on high-resistance media. This leads to a more uniform surface potential, as demonstrated in Figure 11.

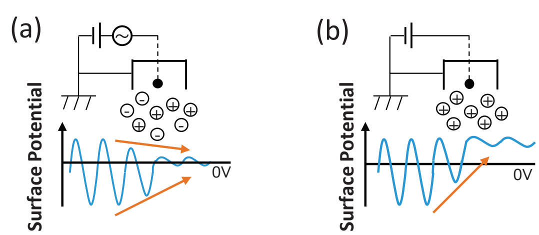

Fig.9 *(a) Alternating static eliminator bias (b) direct current static eliminator bias.*

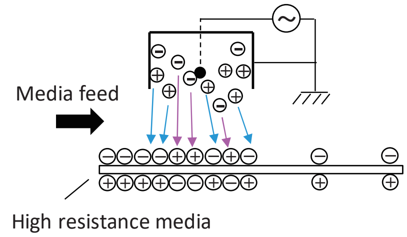

Fig. 10 *Non-contact-type static eliminator.*

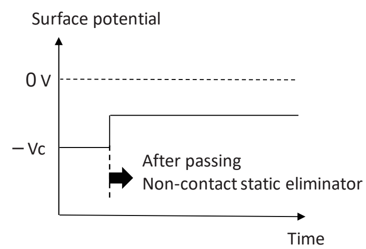

Fig. 11 *Media surface potential after non-contact-type static eliminator.*

3. Verification of Static Elimination Performance

3.1 Verification of Charge Uniformity

To visualize the distribution of electrostatic charges on the surface of a film, we devised a method that involves applying two types of toners with opposite charging polarities. Specifically, magenta toner was used for positively charged particles, and cyan toner for negatively charged particles. Depending on the polarity of the surface charge on the film, toners of different colors adhere to the surface, enabling visual identification of the charge distribution.

Figure 12 shows the visualization results for (a) before static elimination, (b) after contact-type static elimination, and (c) after both contact-type and non-contact-type static elimination. Prior to discharge, the film surface is uniformly covered with magenta toner, indicating a homogeneous distribution of negative surface charges (Fig. 12(a)). After contact-type static elimination, most of the negative charges are neutralized; however, residual negative charges appear as uneven clusters, and small regions of positive surface charge are also observed (Fig. 12(b)). In contrast, after applying both contact and non-contact static elimination, the surface charges are almost completely neutralized, as shown in Fig. 12(c).

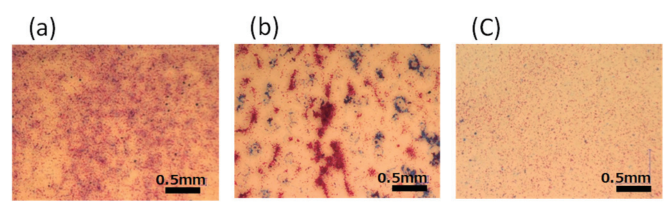

Fig.12 *Visualization of the film surface potential (a) before static elimination (b) after contact-type static elimination (c) after contact-type and non-contact-type static elimination.*

3.2 Verification of Electrostatic Adhesion and Electrostatic Shock

To evaluate the effectiveness of contact and non-contact-type static elimination in mitigating electrostatic adhesion and electrostatic shock, we conducted performance verification tests. Electrostatic adhesion was assessed by measuring the force required to separate overlapped film layers, while electrostatic shock was evaluated by quantifying the residual charge using a commercially available electrometer. These measurements served as proxy indicators for discharge performance before and after treatment (Fig. 13(a), (b)).

Both measurements showed significant improvement after static elimination, confirming that the overall handling and storage quality of the film was substantially enhanced (Fig. 14).

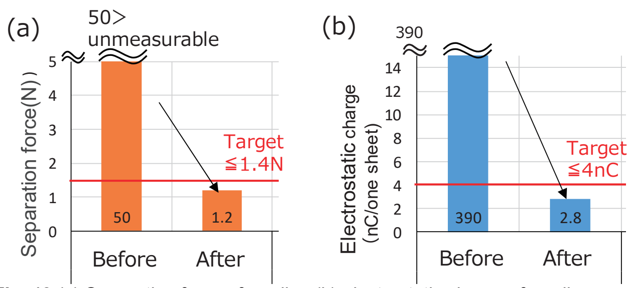

Fig. 13 *(a) Separation force of media (b) electrostatic charge of media.*

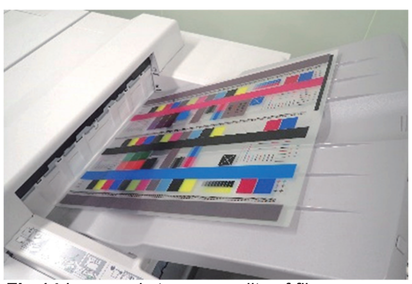

Fig.14 *Improved storage quality of film.*

3.3 Market Introduction

The static eliminator equipped with this technology was launched in 2021 as a paper output option for Fujifilm products Revoria Press PC1120 (Fig. 15) [6], and its static elimination performance has been highly rated in the market. As a result of its introduction to the market, it was found that it is necessary to accommodate the static elimination of various types of media.

Fig. 15 *Revoria Press PC1120.*

Figure 16 shows the relationship between the surface resistivity of media and charge decay. The vertical axis represents charge decay, which is defined as the time it takes for the initial charge potential to be reduced by half. A longer charge decay time indicates that once the media becomes charged, it takes longer to discharge, and when stacked, the media tends to stick together—this serves as an indicator of such behavior. Although high charge decay can be observed even under standard room temperature and humidity conditions, it tends to increase in low-humidity environments, a trend that is consistent across Japan, Asia, and Western countries.

Charge decay shows a strong correlation with surface resistivity: the higher the surface resistivity, the more difficult it becomes to eliminate static electricity. When the surface resistivity exceeds a certain value, quality problems will occur and measures to remove static electricity will be required.

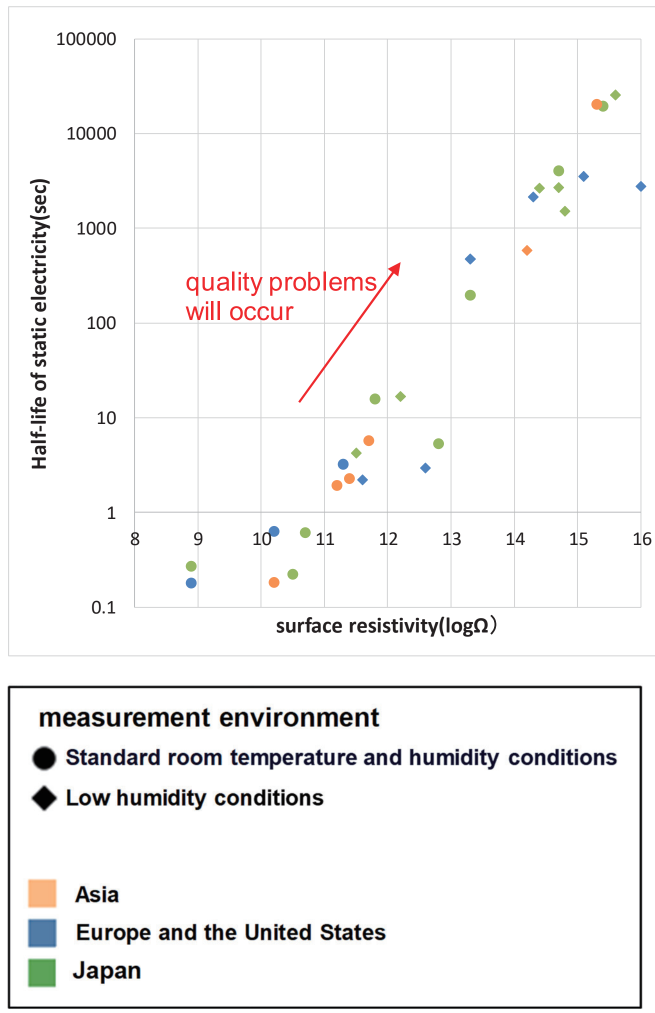

Fig.16 *surface resistivity vs Half-life of static electricity.*

Figure 17 shows the surface and reverse-side resistivity maps of each media type. In the market, it is necessary to properly eliminate static electricity from high-resistance media such as single-layer films, hologram films, film label paper, synthetic/water-resistant paper, and coffee pouch.

This technology enables static elimination by adjusting and appropriately applying a discharge bias, thereby resolving issues such as “reduced media storage performance due to electrostatic adhesion” and “electric shock,” and making it possible to handle the high-resistance media.

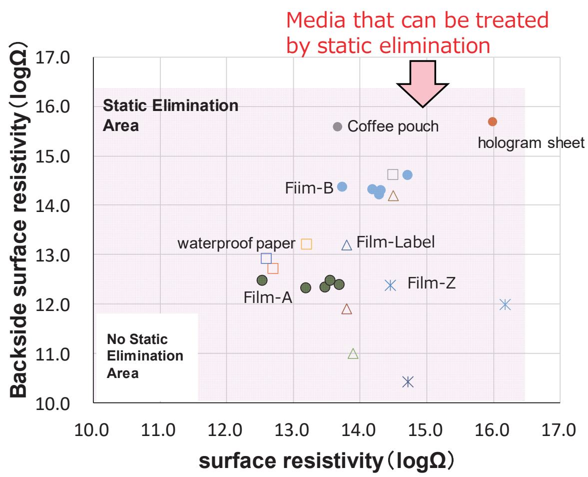

Fig.17 *Media resistivity map.*

4. Conclusion

This paper presented the phenomenon of media charging that occurs when forming images on high-resistance substrates using dry electrophotography, along with the associated challenges. We demonstrated the effectiveness of both contact and non-contact-type static elimination while also showing that neither method alone provides sufficient discharge performance. To address this, we proposed a hybrid discharge technology that combines both approaches, compensating for their individual limitations and achieving effective charge neutralization.

By implementing this technology, we resolved key issues such as media adhesion due to electrostatic attraction and electrostatic shock, which can hinder post-processing and reduce productivity due to limitations in sheet stacking capacity. Furthermore, by leveraging techniques commonly used in electrophotographic charging processes, we were able to utilize shared components, facilitating easy integration into commercial products.

This technology is installed as a paper output option for Fujifilm products Revoria Press PC1120, EC2100S/EC2100, SC285S/SC285, thereby expanding media compatibility. It improves handling of materials prone to adhesion—such as films, synthetic paper, waterproof paper, and label stock—reducing the need for manual separation and protecting operators from high levels of static electricity [7, 8, 9]. These high resistance media, which are required for high value-added applications, are used worldwide without regional differences.

In conclusion, this technology enables digital printing using dry electrophotography handle a wide variety of high-resistance media required for high-added value production worldwide, satisfying the needs of various applications.

References

[1] Y. Kiuchi, A. Tanaka, H, Kuge, and T. Baba, “Challenge to B2 paper printing by dry electrophotographic technology,” Journal of the Imaging Society of Japan, 64, pp. 43-53 (2025) [in Japanese]. https://doi.org/10.11370/isj.64.43

[2] KEYENCE CORPORATION, “Bar unit MJ-B040,” https://www.keyence.co.jp/products/static/ionizer/mj/models/mj-b040/, (accessed 2025-04-01).

[3] M. Ohmori and M. Ohshima, “Measurement techniques of micro region discharge current for analysis discharge mode of contact charging roller,” Journal of the Imaging Society of Japan, 56, pp. 98-106 (2017) [in Japanese]. https://doi.org/10.11370/isj.56.98

[4] M. Takeuchi, “Introduction to electromagnetism and electrostatics (III) -Electrostatics-,” Journal of the Imaging Society of Japan, 45, pp.283-298 (2006) [in Japanese]. https://doi.org/10.11370/isj.45.283

[5] H. Tanaka (FUJIFILM Business Innovation Corp.), “Joden souchi oyobi kore wo mochiita baitai shori souchi,” Japanese Patent Office, No. 2021-111526 (2021), 35 p [in Japanese].

[6] FUJIFILM Business Innovation Corp., “Revoria Press PC1120,” https://www.fujifilm.com/fb/product/publishing/rev_pc1120, (accessed 2025-04-01).

[7] NEWPRINTING co., ltd., https://www.newprinet.co.jp/special/%E5%AF%8C%E5%A3%AB%E3%83%95%E3%82%A4%E3%83%AB%E3%83%A0bi%E3%80%80%E6%9C%AA%E7%9F%A5%E3%81%AA%E3%82%8B%E5%B8%82%E5%A0%B4%E3%82%92%E6%8E%98%E3%82%8A%E8%B5%B7%E3%81%93%E3%81%99%E3%80%8Crevoria-press-pc11, (accessed 2025-04-01).

[8] Kyoshinsha, https://www.kik.co.jp/blog/%E3%82%AA%E3%83%B3%E3%83%87%E3%83%9E%E3%83%B3%E3%83%89%E5%8D%B0%E5%88%B7%E6%A9%9F%E3%80%8Crevoria%E3%80%8D%E5%B0%8E%E5%85%A5/, (accessed 2025-04-01).

[9] PRINT JOURNAL DIGITAL co., ltd., https://www.pjl.co.jp/report/2025/07/19044.html, (accessed 2025-09-01).

[10] K. Yuasa and Y Kiuchi, "Contact and Non-contact Hybrid Static Elimination Technology to Improve Storage Quality of High Resistance media," Proceedings of the 135th Annual Conference of the Imaging Society of Japan (Imaging Conference Japan 2025), PR-02, pp. 103-106 [in Japanese].

Author Biography

Koichiro Yuasa received his master’s degree in applied Electronics from the Graduate School of Basic Engineering, Tokyo University of Science in 2004. In the same year, he joined Fuji Xerox Co., Ltd. (now FUJIFILM Business Innovation Corp.), where he has been engaged in the development of electrophotographic digital printing technologies.

Kiuchi, Yutaka holds BS and MS degree in Applied Physics from Tsukuba Univ. (1998) and a MA degree in Business Administration from Waseda Univ. (2020). In 1998, he joined Fuji Xerox Co., Ltd., where he has been engaged in research on electrophotography process and is currently developing electrophotography products in FUJIFILM Business Innovation Corp. He is a member of the Imaging Society of Japan.

Effect of Paper Dust (Lint) and Evaluation of Paper Dust Release

Yosuke Tsukiyama; Niigata University, Niigata city, Niigata prefecture, Japan

Abstract

This study investigates the influence of paper lint adhesion on the frictional characteristics of rubber rollers used in multifunction printers (MFPs). Contamination of roller surfaces by fine paper particles after extensive operation is recognized as a major cause of paper-feeding failures, including paper jams. However, the mechanism by which such contaminants affect frictional behavior has not yet been fully elucidated. The objective of this work is to clarify the influence of paper lint adhesion on both friction and wear mechanisms. The study demonstrates that the frictional characteristics cannot be accurately predicted solely by the optical measurement of paper lint accumulation, primarily because particle refinement caused by frictional interaction alters the effective contact state. Consequently, a friction-based evaluation approach is proposed as a more reliable method for quantifying paper lint adhesion and its effect on roller performance.

Introduction

Paper jams remain a persistent and costly maintenance issue for manufacturers of multifunction printers (MFPs) and copiers. Among the various mechanical and environmental factors contributing to paper-feeding failures, one of the most critical is the adhesion of paper lint — fine fibrous debris or filler particles detached from the surface of paper sheets during repeated transport. The complexity of this issue arises from two main challenges: the diversity of paper stock compositions in the global market, and the fact that lint-related effects typically manifest only after tens of thousands of feeding cycles rather than during early operation. These conditions make it extremely difficult to isolate the relative contributions of paper composition and roller material degradation.

When a particular paper brand is suspected to cause paper jams due to lint generation, reproducing the problem experimentally presents significant difficulties. It is often challenging to procure the exact lot of the paper used by the end user, to maintain consistent paper properties under varying humidity and temperature, and to reproduce the surface conditions of rollers after long-term use. Therefore, conventional evaluation methods — which feed tens of thousands of sheets under controlled environmental conditions using actual printers — are costly, time-intensive, and impractical for routine quality evaluation.

Against this background, there has been an increasing demand in Japan to develop standardized methods for evaluating paper lint behavior and its influence on friction using laboratory-scale apparatus. A particularly promising direction involves the measurement of frictional characteristics between paper and rubber rollers while accounting for lint adhesion. The Japan Business Machine and Information System Industries Association (JBMIA) has proposed such a method in its JBMS-88 standard[1], which defines a friction-based approach to evaluating the amount of paper lint adhering to roller surfaces. The present study aims to provide a tribological foundation for this standard by experimentally clarifying how the frictional properties of rubber rollers change as paper lint accumulates during feeding (Fig. 1).

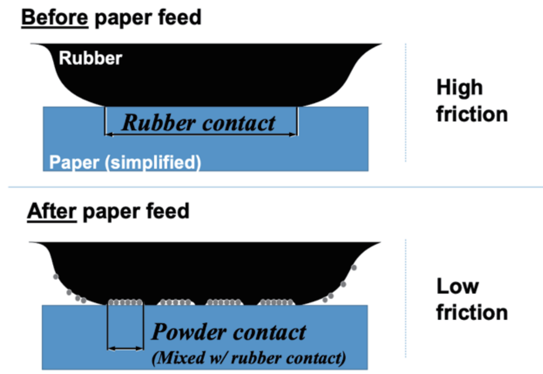

Figure 1. Schematic representation of the real contact area between rubber and paper under two conditions: before paper feeding (upper) and after paper feeding (lower). The illustration depicts the transition from a high-friction state, attributed to the clean rubber surface, to a low-friction state resulting from paper lint adhesion following repeated paper transport.

Experimental Method

A. Overview

The present experiments were designed to isolate the effect of paper lint adhesion on the frictional response of rubber rollers. Friction tests were conducted after feeding controlled numbers of paper sheets through rollers installed in a commercial MFP. Both the friction coefficient and the degree of lint adhesion were measured using mechanical and spectroscopic techniques.

B. Friction Mechanism Considerations

In metallic contact systems, friction is typically governed by adhesive and plowing components associated with surface asperities. In contrast, for rubber materials, the dominant contributors are adhesive friction and hysteresis friction[2], the latter arising from the viscoelastic deformation of rubber asperities against a rough counterface. Separating these two components is non-trivial; however, under conditions where paper lint forms a thin film on the roller surface without significantly altering the large-scale roughness, the hysteresis component remains nearly constant. Consequently, variations in total friction can be attributed primarily to changes in the adhesive component induced by lint adhesion.

C. Test Setup and Conditions

The test rollers were fabricated from polyurethane rubber with a hardness of 32 (Shore A) and featured an embossed surface texture identical to that used in commercial feed rollers. The rollers were installed in a KONICA MINOLTA bizhub C554 MFP and used to feed sheets of copy paper. After a predefined number of feeding cycles, the rollers were removed and tested for frictional characteristics using a fixed-roller tribometer. The roller was immobilized to prevent rotation, and friction was measured between the roller surface and a paper specimen under a normal load of 2 N and a sliding velocity of 0.5 mm/s. All tests were conducted in a controlled environment with constant temperature and humidity. The same lot of paper was used throughout, and the number of fed sheets was intentionally limited to prevent significant shape changes in the roller surface.

D. Measurement of Lint Adhesion

To quantify the amount of paper lint adhered to the roller and paper surfaces, both optical and spectroscopic techniques were employed. Direct observation of the real contact area was performed using a scanning laser microscope equipped with a transparent glass interface, as schematically illustrated in Fig. 2. The regions with and without lint adhesion were differentiated based on differences in optical refractive index.

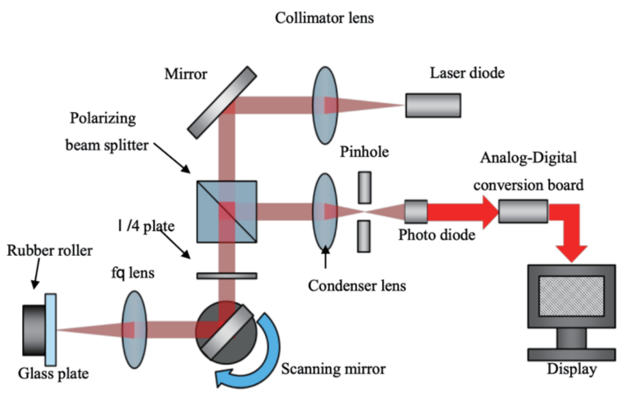

Figure 2. Schematic representation of the real contact area observation apparatus equipped with a scanning laser microscope system. By combining vertical motion stage (omitted in this figure) with laser scanning achieved through a scanning mirror and an fθ lens, the system enables comprehensive observation of the rubber surface through a transparent glass plate.

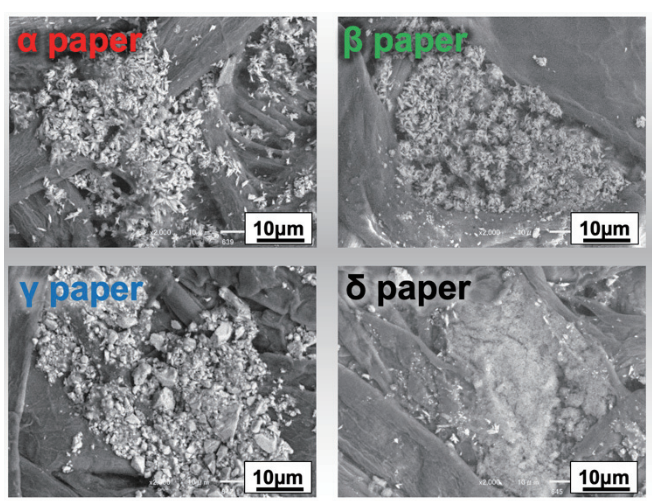

Figure 3. Scanning electron micrographs of the papers used in this study, designated as types α through δ. The surfaces of these papers exhibit calcium carbonate particles, either spindle-shaped or irregularly formed due to pulverization. Among these, particles insufficiently bonded by sizing are more prone to detachment from the paper surface and tend to adhere to the rubber roller during the feeding process.

In addition, the surface contamination was evaluated spectroscopically using an attenuated total reflectance Fourier transform infrared (ATR-FTIR) analysis[3]. The absorbance corresponding to calcium carbonate ($CaCO_3$) was used as an indicator of lint adhesion, since $CaCO_3$ is a primary filler constituent in copy papers. The measured absorbance was normalized by the intensity obtained from a thick layer of pure $CaCO_3$ to minimize particle-size effects.

E. Paper and Powder Samples

Four commercial paper brands, designated paper α, β, γ and δ, were employed in the experiments. Scanning electron micrographs of their surfaces are shown in Fig. 3. To further examine the relationship between particle morphology and friction, three types of $CaCO_3$ powders — labeled A, B, and C — were also prepared (Fig. 4). Powders A and B consisted of smaller particles, with A exhibiting needle-like shapes and B irregular granular forms. Powder C comprised larger, randomly shaped particles. The effects of particle shape and size on frictional properties were compared systematically by using paper samples with those powders scattered on a dust-free paper sheets.

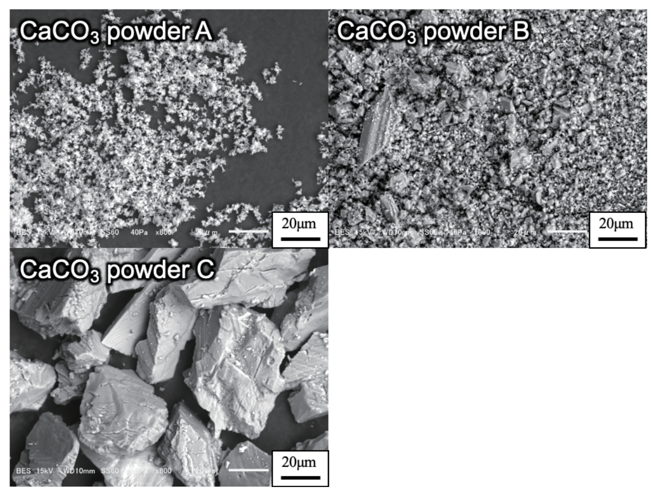

Figure 4. The powders used in this study are composed of calcium carbonate. Powders A and B possess fine particle sizes on the order of a few micrometers; powder A corresponds to light calcium carbonate, while powders B and C represent heavy calcium carbonate. Powder C has a relatively large particle size of several tens of micrometers.

Results

A. Relationship Between Paper Type and Lint Adhesion

Figure 5 shows the decrease in the powder-free real contact area as a function of the number of sheets fed for paper α, β, γ and paper δ. Visual inspection revealed that the amount of lint adhering to the roller was significantly greater for paper α. The reduction in clean contact area increased rapidly after the tenth feeding for paper α, whereas it increased gradually for paper δ. Beyond approximately 20 feedings, a curve for paper α saturated to a normalized value of unity, indicating that nearly the entire contact area was covered with lint. These results suggest that paper α generates and transfers paper lint more readily than paper δ.

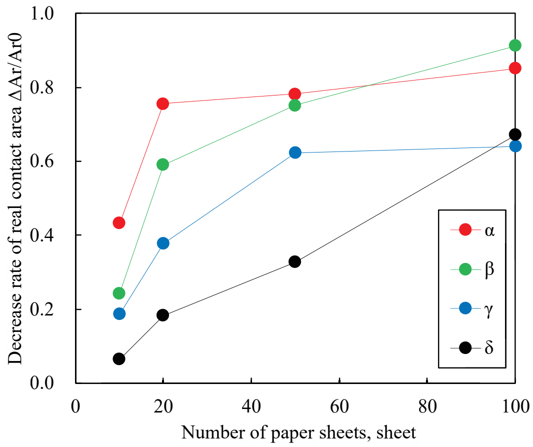

Figure 5. Relationship between the decrease ratio of the real contact area between the rubber and the glass surfaces and the number of paper sheets fed. The real contact area decreases as paper lint adheres to the rubber surface during paper feeding; therefore, the vertical axis can also be interpreted as the inverse indicator of the paper-lint adhesion ratio.

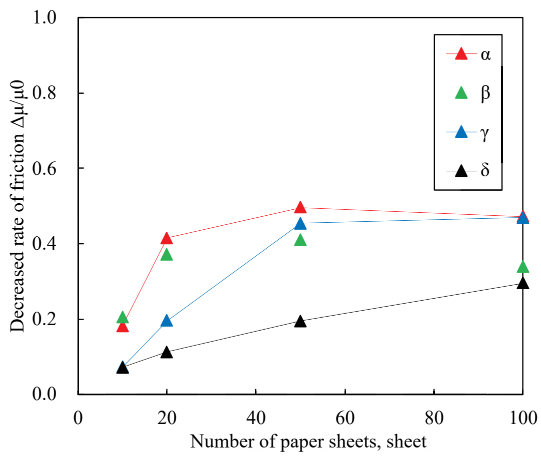

Figure 6. Relationship between the decrease ratio of the frictional force between the rubber and the glass surfaces and the number of paper sheets fed.

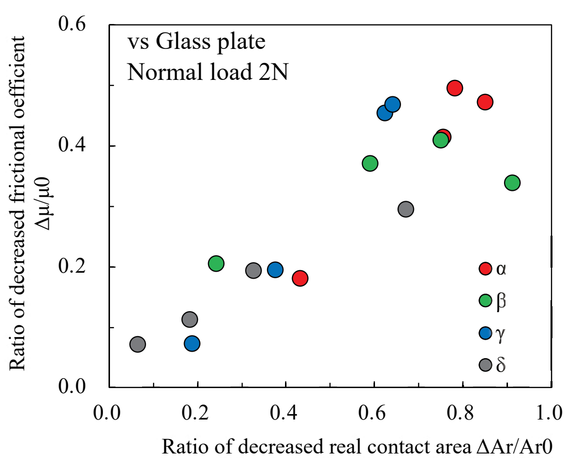

Figure 7. Relationship between the decrease ratio of the frictional force and real contact area

B. Correlation Between Contact Area and Frictional Force

Figure 6 presents the relationship between the decrease in the powder-free contact area and the corresponding reduction in frictional force. The slope of the correlation for paper α is noticeably steeper than that for paper δ. This indicates that as lint adhesion progresses, the friction coefficient of the roller decreases more rapidly for paper α. In the case of paper δ, a slower decline is observed, followed by a more pronounced decrease once the contact area approaches full coverage. This behavior implies that secondary effects, such as fine particle formation during repeated feeding, may further reduce friction at later stages. trend similar to that shown in Fig. 6 is observed, indicating that the frictional force varies in accordance with the degree of paper-lint adhesion. Figure 7 shows the clear relationship between friction and real contact area.

C. Effect of Artificially Applied Calcium Carbonate Powder

The relationship between the friction coefficient and the amount of artificially applied $CaCO_3$ powder on clean paper (dust-free paper) surfaces is shown in Fig. 7. For all powder types, the friction coefficient exhibited an approximately linear decrease with increasing measured $CaCO_3$ absorbance, confirming that powder coverage proportionally reduces interfacial friction. The comparison between powders A and B revealed minimal differences despite their distinct shapes, suggesting that particle shape alone exerts little influence. However, a clear difference emerged between powders B and C, which shared similar shapes but differed in particle size.

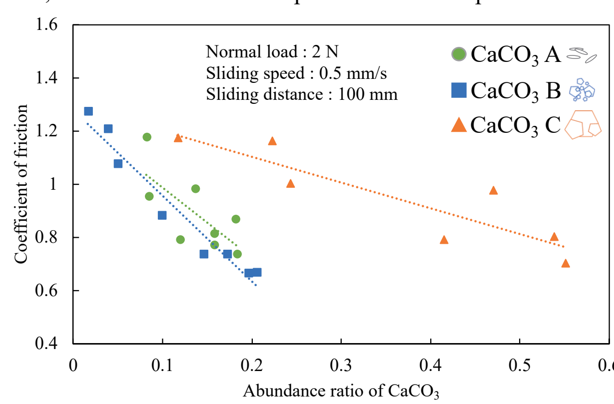

Figure 7. Relationship between the coefficient of friction and abundance ration of $CaCO_3$ powder on clean paper

D. Correlation Between Degree of frictional reduction and Cost of Paper

Figure 8 presents the relationship between paper cost and the degree of frictional coefficient reduction, as defined by the JBMS-88 standard. The vertical axis represents an index that quantitatively expresses the influence of paper lint on friction, where lower (negative) values indicate a higher tendency for paper lint to adhere to transport rollers, thereby increasing the likelihood of performance degradation.

The paper samples analyzed in this study were selected to represent a comprehensive range of brands and grades distributed not only in Japan but also across global markets, ensuring broad coverage of commercially available products. The results reveal that paper price does not necessarily correlate with the frictional stability or the resistance of the paper to lint-induced performance decline.

This suggests that, while the cost of paper is often associated with improvements in physical properties such as opacity, surface smoothness, and print quality, these attributes do not directly govern tribological behavior. Instead, factors such as filler composition, sizing quality, and surface treatment play more dominant roles in determining the frictional response of paper during feeding operations.

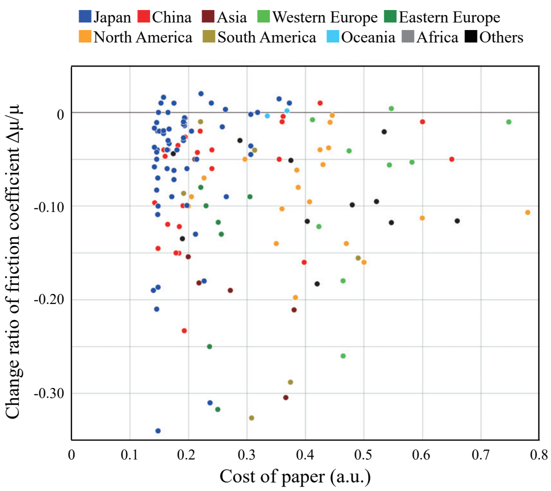

Figure 8. Relationship between the rate of change in the friction coefficient, measured in accordance with JBMS-88, and the cost of paper. The investigation includes a wide range of paper brands, encompassing both domestic and international products available in the global market. Negative values on the vertical axis indicate a higher tendency for paper lint to adhere to transport rollers, resulting in potential performance degradation during paper feeding.

Discussion

The experimental results confirm that paper lint significantly affects the contact mechanics and frictional performance of rubber rollers. The primary mechanisms can be interpreted as follows:

1. Dependence on paper composition and filler properties: Papers containing finer $CaCO_3$ fillers tend to release more detachable particles during feeding, leading to greater lint accumulation on the roller surface.
2. Effect of particle size on adhesion: Larger particles adhere less readily due to reduced van der Waals and electrostatic forces. Consequently, they contribute less to friction reduction. However, repeated feeding cycles can pulverize these larger particles, increasing the proportion of fine debris and gradually lowering the friction coefficient.
3. Non-linear relationship between optical lint measurements and friction: Frictional degradation does not always correspond directly to the optically measured adhesion rate of paper lint. The dynamic refinement and redistribution of particles under shear alter both the real contact area and adhesion friction in ways not captured by static optical inspection.
4. Implications for roller design and evaluation: These findings support the rationale of friction-based measurement standards such as JBMS-88, which explicitly account for tribological factors. Evaluations based solely on visual or optical lint quantification cannot fully predict frictional changes responsible for paper jams.

The results also highlight the importance of considering mechanical refinement of paper lint over extended use. Even when large particles initially produce minimal adhesion, continuous rolling and sliding actions fragment them into smaller particulates capable of filling micro-asperities and further decreasing the coefficient of friction.

Overall, the study underscores that the frictional characteristics of rubber rollers contaminated by paper lint depend not only on the amount of adhered debris but also on the evolving morphology of the particulate layer. Predictive models of roller performance must therefore incorporate tribo-mechanical interactions between particles, paper fibers, and viscoelastic rubber surfaces.

Conclusion

This study examined the influence of paper lint adhesion on the frictional properties of rubber rollers used in multifunction printers. The principal conclusions are summarized as follows:

1. The amount and morphology of paper lint adhering to the roller surface significantly affect the frictional characteristics between paper and rubber.
2. Particle size refinement caused by frictional wear must be considered when evaluating long-term frictional stability.
3. Frictional behavior cannot be accurately predicted solely from optical or non-contact lint measurements, as these methods neglect the dynamic effects of particle fragmentation.
4. The friction-based evaluation method specified in JBMS-88 provides a physically meaningful framework for assessing the tribological impact of paper lint on roller performance.
5. Furthermore, while paper cost often reflects enhancements in physical properties such as opacity, surface smoothness, and print quality, these attributes do not necessarily correlate with tribological performance. Instead, frictional behavior is more strongly influenced by material factors such as filler composition, sizing quality, and surface treatment.

These results provide a foundation for improving the design and maintenance of paper-feeding mechanisms in MFPs and other sheet-handling devices, enabling more accurate prediction and mitigation of paper jams due to lint contamination.

References

[1] Japan Business Machine and Information System Industries Association (JBMIA), Standard on Paper Lint Evaluation Method by Measuring Friction Force (JBMS-88), Tokyo, Japan, 2021. Available: https://hyojunka.jbmia.or.jp/pwg/jbms.html

[2] D. F. Moore, The Friction and Lubrication of Elastomers, Pergamon Press, 1972.

[3] B. Smith, Infrared Spectral Interpretation: A Systematic Approach, CRC Press, 1998

Author Biography

Yosuke Tsukiyama received his BS in engineering from Nagoya University (2005) and his PhD in mechanical engineering from Nagoya University (2010). After a post-doctoral research experience for one year, he has worked in the Institute of Science and Technology at Niigata University in Niigata, Japan. His professional interest is in Tribology (friction and lubrication) and has focused on the rubber friction and paper lint adhesion issues.

Title: Low-Pulsation Liquid Pumps and Their Applications

Nobuhiko Hosobata; KNF Japan; Tokyo, Japan

Abstract

Pump pulsation has long been a major issue affecting print quality in inkjet printers. Diaphragm pumps inherently generate pulsation, so users have traditionally installed external suppression mechanisms as a countermeasure. Recently, demand for recirculating printheads has increased, making pulsation suppression an even more critical challenge. KNF explored whether the pump itself could reduce pulsation without relying on the user. This led to the development of the FP series we are introducing.

Introduction

First, allow me to introduce our company, KNF.
KNF is a company headquartered in Germany. Founded in 1946, it develops, manufactures, and sells diaphragm pumps. It operates globally, primarily in Europe, with 3 development sites, 4 manufacturing sites, and 12 sales offices. Our primary markets are medical devices and inkjet printers. We also have a proven track record in various other applications, including analytical instruments, environmental equipment, semiconductors, and energy. Our product range includes gas pumps, liquid pumps, process pumps, and lab pumps. Gas pumps and liquid pumps are designed for equipment integration, process pumps for factory installations, and lab pumps for research and development in fields like drug discovery and chemistry. KNF has developed a modular system to facilitate customization. This modular system involves preparing components in advance, allowing specifications to be altered by changing the component configuration. It requires no initial investment and enables us to easily provide custom pumps starting from a single unit. KNF excels at consultative sales, offering proposals to help customers realize their desired systems. Over 90% of the pumps we provide are custom pumps. The specifications in Table1 represent the range KNF can accommodate.

Pumps	Flow rate L/min	Suction hieght/ Ultimate vacuum	Pressure head
Liquid	Max. 12	1.5 – 6 mWg	10 – 60, 160 mWg
Gas ※	Max. 240	0.5 – 800 mbar abs.	Max. 12 barg

Table1: Specification range

FP series

Next, KNF introduces the newly developed FP Series of low-pulsation liquid pumps for inkjet applications. As mentioned earlier, pump pulsation is a major issue in inkjet printers. Our company also sells the FPD pulsation damper as a product for conventional methods. However, it has not gained widespread adoption. The reason is that it has a narrow range of conditions it can suppress and cannot be customized, making it insufficient to fully meet the diverse requirements user's demand. The FP series pump was developed to solve this problem. It achieves low pulsation within the pump itself and employs a modular system, enabling customization.

Structurally, they can be divided into two types: multi-diaphragm type (Figure1) and damper-integrated type. The multi-diaphragm type (Fifure2) incorporates five diaphragms. Each diaphragm moves with staggered timing at equal intervals, counteracting the pulsation generated during suction and discharge to reduce pulsation. Theoretically, two or more diaphragms can cancel pulsation. However, in practice, achieving zero pulsation under ideal conditions is impossible due to factors like component interference and assembly tolerances. KNF selected five diaphragms based on the balance between pulsation reduction effectiveness and cost. The damper-integrated type reduces pulsation using dampers installed on both the suction and discharge sides. While the damper-integrated type may appear similar to conventional pump-and-damper combinations, its design is entirely different. Details are confidential, but the flow path, valve system, damper structure, and all other elements are designed to minimize pulsation generation. Consequently, it achieves not only low pulsation but also low vibration, low noise, reduced shear force on the liquid, improved linearity during flow rate changes, and reduced susceptibility to cavitation.

Figure1: Multi-diaphragm type

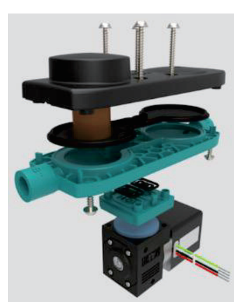

Figure2: Damper-integrated type

Five product types are available, each with standard discharge pressure-resistant and high discharge pressure-resistant variants.

Key specifications are shown in Table 2. Flow rate can be adjusted by changing the motor rotation speed, enabling adaptation to desired flow rates up to a maximum of 4.6 L/min. The high discharge pressure-resistant type is used when equipment enlargement necessitates transporting fluid over greater distances, or when the load from components (filters, valves, degassing filters, etc.) becomes excessive.

Characteristics

First, the primary pulsation characteristic has been significantly reduced compared to conventional pumps. Please refer to Graph 1. Particularly at low flow rates, such as FP7/1.7 and FP25/1.25, the peak-to-peak pulsation is less than 2 kPa. At this level, fluid can be delivered directly to a recirculating head. Pulsation is measured 20 cm downstream from the pump outlet, using rigid tubing to prevent attenuation. In practice, the distance to the head is longer, so further attenuation is expected, resulting in virtually pulsation-free operation. The pulsation of the three higher-flow pumps is not as low as the low-flow types. This is likely due to variations in components, including the diaphragm, and assembly tolerances, preventing assembly to an ideal state where pulsation is fully canceled. At this level, we consider it more suitable for ink supply rather than feeding a recirculating head. This is because pulsation during ink supply can adversely affect the ink circulation path.

Specifications		FP 7/1.7	FP 25/1.25	FP 70/1.70	FP 150/1.150	FP 400/1.400
Flow rate	ml/min	7 - 70	25 - 250	70 - 700	150 - 1500	460 - 4600
Pressure head	mWg	10 / 60	10 / 60	20 / 60	20 / 60	10 / 60
Pulsation	kPa	< 2	< 3	< 15	< 20	< 15

Table2: Specifications of FP series

The second characteristic is low vibration and low noise. Particularly, the multi-diaphragm type produces noise below 50 dB and vibration so slight it is barely perceptible unless touched. Since the risk of resonance with the equipment housing is low, this offers a significant advantage from the perspective of equipment integration. The multi-diaphragm type has a structure completely different from existing diaphragm pumps. Existing pumps convert motor rotation into linear motion perpendicular to the motor shaft via an eccentric rod, and this motion generates vibration and noise. However, the multi-diaphragm type moves the diaphragm horizontally relative to the motor shaft, eliminating lateral forces on the pump. This achieves noise levels below 50 dB. Vibration is barely perceptible unless touched by hand. The low risk of resonance with the equipment enclosure offers a significant advantage from the perspective of equipment integration.

The damper-integrated type also exhibits lower vibration and noise levels than existing pumps. While its basic structure is identical to existing types, the fluid inside the pump is rectified, ensuring fluid pressure is transmitted almost entirely in the direction of travel and eliminating vertical forces. This also contributes to improved linearity during flow rate changes. With minimal flow fluctuations caused by turbulence, the flow rate can be adjusted linearly from low to maximum flow.

Finally, pump lifetime. Based on our internal comparison, test results indicate it lasts approximately twice as long as conventional pumps with the same flow rate. KNF believes this is due to the design reducing pulsation, which in turn alleviates various mechanical loads.

The pump introduced was developed for inkjet applications, but it is now being considered for various uses. KNF cannot disclose details, so KNF will limit itself to listing the applications.

Various medical devices, robots, fuel cells, semiconductor manufacturing equipment, 3D printers, hydrogen power generation, food, beverages, drug discovery and new material development, space environment equipment, iPS cell culture, cultured meat production, printed circuit boards, solar panels, etc.

Summary

The FP7/1.7 and FP 25/1.25 are considered optimal for fluid delivery to recirculating heads, while other FP pumps are best suited for ink supply. Furthermore, the low vibration and low noise characteristics of multi-diaphragm types are useful in various applications, and demand for them is expected to increase in the future.

Biography

Nobuhiko Hosobata received her BS in applied physics Tokyo University of Agriculture & Technology (1983). Since, he worked on developing optical sensors at Copal, then served as a sales engineer for aircraft wiring at Tyco Electronics, then now holds the position of sales engineer at KNF Japan.

Measurement Technologies Supporting Color Management in the Growing Industrial Printing Industry

Genta Koori; Konica Minolta, Inc.; Tokyo/Japan

Abstract

In terms of the value of print production in Japan, paper media is on the decline, while non-paper media is on the rise in nowadays, responding to the industrial printing has become an urgent matter for printing industry. Based on the recognition that printing is an industrial product, we will introduce our latest spectrophotometers with some examples to promote unified color management based on the CIE/ISO standard light D65 and to support Refined CMF Design that have attracted attention in recent years.*

**An easy-to-understand way of referring to CMF (color, material, finish). In recent years, there has been a great deal of interest in CMF, including the use of recycled materials.*

1. Printing and Color Management for Non-Paper Media: An Increasing Trend

Japan's Ministry of Economy, Trade and Industry publishes production value statistics for the printing sector in seven categorizes: 1) Publishing Printing, 2) Commercial Printing, 3) Security Printing, 4) Office Printing, 5) Package Printing, 6) Building Materials Printing, and 7) Other Printing. Of these, 1) to 4) are mainly printing on paper media, while 5) to 7) are mainly printing and coating on non-paper media, which are expected to grow rapidly in the future. Looking at production value trends from 2015 to 2024, paper media will clearly decrease, while non-paper media will show a slight increase (see Figure 1).

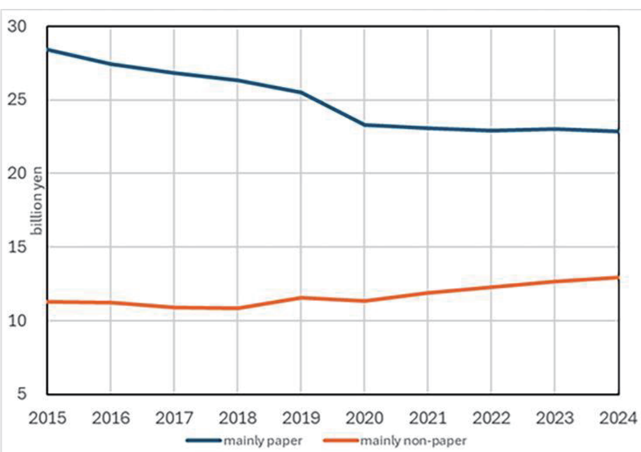

Figure 1. *Ministry of Economy, Trade and Industry: Trends in production value of paper and non-paper media from 2015 to 2024 (base: 4,300 printing)*

Here, non-paper media mainly refers to the industrial printing sector (packaging, decorative printed materials, printing on glossy surfaces such as building materials, flooring, wallpaper, tiles, resins, plastics, and metals). For color management in processes like gravure printing, diffused illumination integrated sphere instruments (compliant with ISO 7724/1, CIE No. 15 (2004), ASTM E1164 (SCI), DIN 5033 Teil 7, JIS Z 8722 Condition c) have been used for a long time. However, there are users who accurately utilize these instruments and those who do not. Moving forward, as we produce an increasing volume of non-paper printed materials, color management based solely on traditional paper media is insufficient for materials with diverse gloss levels due to differences in surface conditions.

2. Non-Paper Media and Instrument Light Reception Methods

As described above, non-paper media refers to substrates and colorants with a variety of glossy surfaces, and not only is 45°:0° illumination/reception method used for paper media, which has a lot of diffused light components and little gloss, unable to properly capture reflected light, but many of these media also require gloss management. Examples include:
a. Glossy substrates with surface treatments like varnish, wax, or lamination applied to labels, cardboard, etc.
b. Glossy substrates such as resins, films, and plastics
c. Colorants containing luminous materials like metallics or pearls that change color with viewing angle
d. Specular gloss substrates such as metal plating that reflect color components only in the specular direction
e. Substrates with minimal diffusions and high gloss, such as piano black or aluminum vapor deposition
Accurate measurement of these requires the use of diffused illumination integrated sphere instruments or multi-angle measuring instruments. Furthermore, achieving CMF Design —visually sophisticated ones that compel consumers to pick them up— requires evaluating not only color and gloss but also the appearance of the mirror surface. This necessitates measurement instruments that correspond to these numerical management indicators. We collectively refer to this product line as "Color & Appearance Measurement Instruments" and widely promote them as tools supporting color management for CMF Design industrial products.

3. Color & Appearance Numerical Management Supporting CMF-Design (Case Study: Color Management for Cosmetics, Outer Packaging, Display Stands, POPs, etc.)

Have readers of this article ever closely observed recent cosmetics sales floors? From department stores and electric stores to multi-brand shops, drugstores, and even convenience stores, cosmetics products can now be found everywhere, reflecting the broadening user base. In these spaces, outer packaging, display stands, POPs, etc. and more all blend seamlessly with the cosmetics themselves, creating visually and olfactorily stimulating, truly glamorous environments designed to elaborate customer mood. Consequently, the production requirements for these expressive elements—outer packaging, display stands, POPs, etc.—demand realism with visual effects matching the actual product.

3.1 Harmony Between "The Product: Foundation" and " Outer Packaging, Display Stands, POPs, etc. Representing the Product"

Observing printing in the cosmetics industry, it's evident in actual retail spaces that outer packaging, display stands, POPs, etc. are developed with the upstream product in mind. A commonly used example in foundation is the "interference pearl agent which color changes with film thickness." This interference pearl agent, which appears red at a certain film thickness, exhibits the effect of appearing red on a black base and white on a white base (see Figure 2).

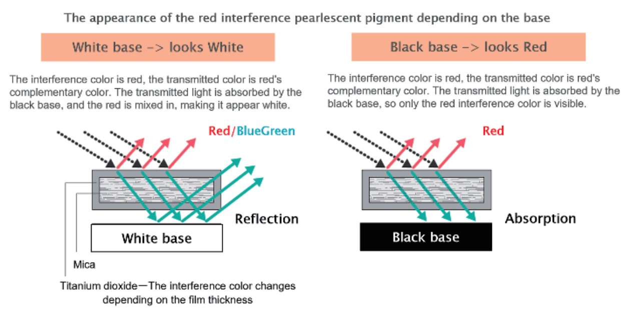

Figure 2. Differences in appearance of red interference pearlescent agent depending on the base

Products are developed that consider of these characteristics, and the outer boxes, display stands, POP displays, etc. also follow suit, pursuing product realism and displaying elaborate designs that use patterns, metallic luster, piano black, and other textures that increase purchasing desire. We propose the use of the following specific management indicators as color & appearance numerical indicators that support the reproducibility of these CMF designs.

[Colorimetric Values (SCI/SCE)]

For color measurement of glossy substrates as described in Section 2a./b., SCE (de: 8°) method, which excludes specular reflection, is used for color evaluation closer to visual inspection at angles where specular light is absent. SCI (di:8°) method, which includes specular reflection, is used for evaluating the inherent color of the material itself, regardless of surface condition. Additionally, for measuring materials like metallic colors as described in Section 2d, where color components reflect only in the specular direction, SCI (di:8°) method is used. By selecting the measurement method appropriate for the sample's surface condition in this way, optimal numerical evaluation can be achieved for each (see Figure 3).

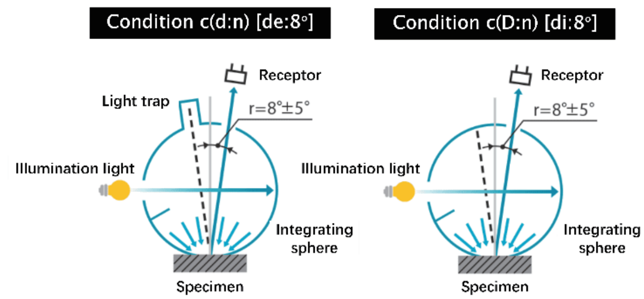

Figure 3. Diffused illumination integrating sphere system SCE (de: 8°) and SCI (di: 8°)

[FF Index]

For substrates exhibiting high brightness near the specular reflection angle (-15°, 15°) or those characterized by distinct "shadow effects" in non-illuminated areas, the FF (Flip-Flop) index—derived from measurements at the highlight (15°) and shade (110°) directions—has become increasingly effective.

As described in Section 2c, metallic flake agents and other luminous materials are oriented in nearly the same direction but with some variation, causing specular reflection to occur at various angles. Consequently, when observed in the highlight direction, the reflected light from the substrate surface and the light-reflective material within it mix, resulting in a significantly different appearance. When orientation is uniform and specular reflection increases, the FF value becomes larger. Conversely, when orientation is non-uniform and diffuse reflection increases, the FF value becomes smaller. (See Figure 4).

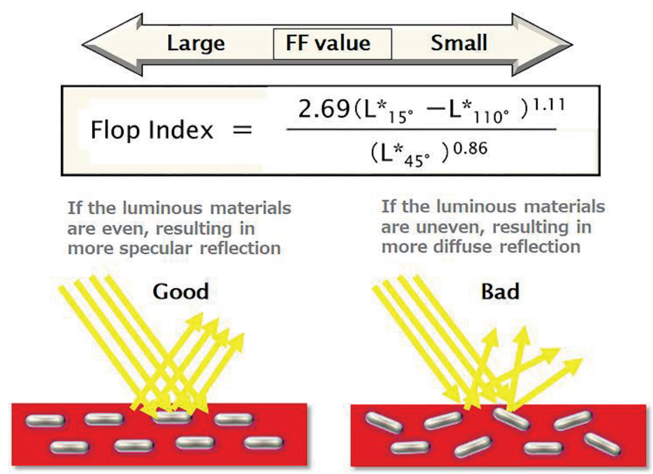

Figure 4. FF Index

[Angle Dependence]

Angle dependency refers to the characteristic where the perceived color and brilliance change depending on the viewing angle. As described in Section 2c, luminous materials like pearl pigments produce a pearlescent luster resembling a rainbow. This occurs because the combination of colors from light reflected off the luminous materials surface and the base changes as the viewing angle shifts. By utilizing this, by designing the film thickness to induce the "(amplified) interference" phenomenon at the appropriate thickness, the intended interference color can be created. When viewed in the shade direction, the transmitted light color of the pearlescent material is visible. When viewed in the highlight direction, the complementary color of the transmitted light of the pearlescent material is visible. As the pearlescent material thickness increases, the interference color of its transmitted light changes (blue ->green -> yellow -> red), while the interference color of the reflected light from the pearlescent material changes to the complementary color of the transmitted light (yellow -> red -> blue -> green) (see Figure 4).

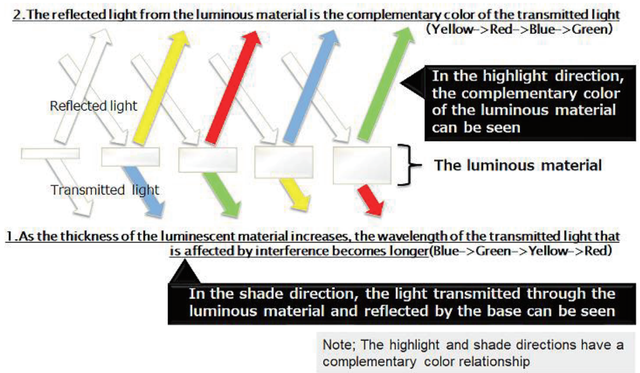

Figure 5. *Relationship between pearlescent agent film thickness and interference color*

[Gloss], [Haze (Cloudiness)], [Sharpness/DOI]

For evaluating specular gloss substrates or metallic finishes, 20°, 60°, and 85° gloss measurements are used to quantify specular reflectance intensity. However, Haze (Cloudiness) serves as an indicator for the perceived cloudiness of surface conditions—which gloss measurements cannot express—and the degree to which surrounding images appear clearly and undistorted, like in a mirror (see Photo 1). It is effective for evaluating materials like piano black and aluminum vapor deposition, as described in Section 2e. Furthermore, *Sharpness/DOI* captures and quantifies high clarity at narrower receiving angles, which cannot be expressed solely by gloss or reflective haze (see Photo 2). This allows the visual sense of brilliance to be quantified using management indicators appropriate for the measured object.

Photo 1. *Example of Haze measurement*

Picture 2. *Example of Sharpness/DOI measurement*

3.2 Issues for cosmetics color evaluation under different light source conditions

The color of any object requires three elements: light source, object, and vision. Among these, the difference in appearance caused by variations in light source is a critical variable that cannot be ignored. For example, a phenomenon called "metamerism" occurs where two samples that appear the same color under outdoor sunlight appear different under indoor LED lighting in a store. Therefore, during the research phase of industrial products or post-manufacturing quality evaluation, visual assessments typically involve using a dimmable light source box to switch between multiple lighting conditions and observe perceptual differences. For numerical evaluation using spectrophotometers, two or more light sources are selected, such as the D65 light source specified by CIE or JIS, or a fluorescent lamp F11 (see Figure 6), and differences in color measurement values are observed, and the product is manufactured while adjusting the color material mixture, etc.

This applies equally to all examples mentioned here—cosmetics, outer packaging, display stands, POPs, etc. Visual and numerical evaluations under multiple light sources, simulating the indoor/outdoor ambient lighting found in sales areas and actual usage scenarios, are essential. However, recent store lighting trends show a shift from fluorescent lamps to high-CRI LED lighting. Furthermore, many stores reportedly combine multiple LED lights with differing spectral distributions arbitrary for visual effective use. Consequently, manufacturers often cannot match the spectral distribution used in stores, making it increasingly difficult to predict how colors will appear at the point of sale during the product development stage.

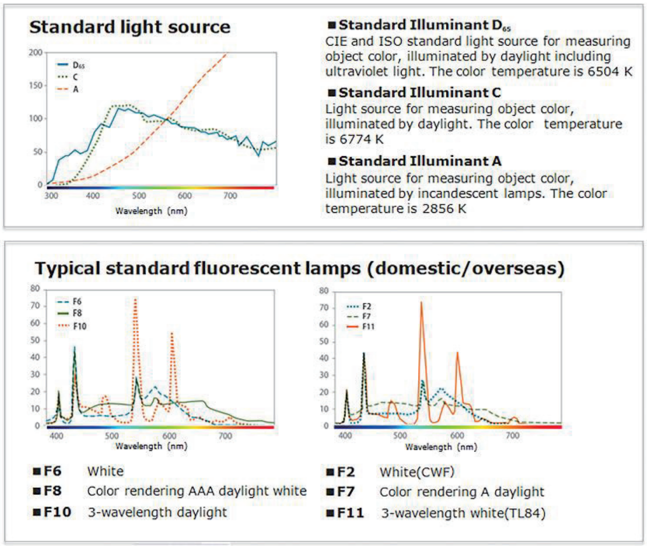

Figure 6. *D65 standard light source and typical fluorescent lamps*

4. Introduction to the Latest Integrated Sphere Spectrophotometer CM-17d, Multi-Angle Spectrophotometer CM-M6, and Appearance Analyzer Rhopoint IQ-S

The spectrophotometer CM-17d (see Photo 3), newly released in summer 2024, is the successor to the CM-700d spectrophotometer, which boasts numerous installations in development and production sites across all manufacturing industries worldwide. It maintains compatibility with measurement values from the vertical-type predecessor model capable of simultaneous SCE/SCI measurement using a diffuse illumination method integrating sphere type. It features an electronic viewfinder (see Photo 4) that facilitates positioning for small and curved samples, along with wireless LAN/Bluetooth communication capabilities. Other distinctive features are introduced below.

Picture 3. *integrated Sphere Spectrophotometer CM-17d*

Picture 4. *Electronic viewfinder*

4.1 Key Features of Integrated Sphere Spectrophotometer CM-17d

1) Incorporates "Observation Light Sources for LED Illumination Environments"

Newly incorporates LED-B1, LED-B2, LED-B3, LED-B4, LED-B5, LED-BH1, LED-RGB1, LED-V1, and LED-V2—new illuminants for various LED types introduced in CIE 015:2018. (See Figure 8) The spectral distributions of each LED light source differ significantly from standard light D65 and conventional fluorescent lamps. This enables color value evaluation closer to how colors appear under actual LED lighting in retail stores.

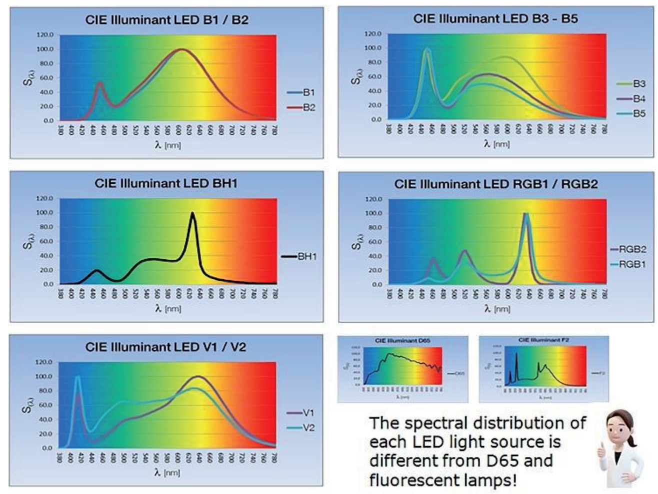

Figure 7. *New observation light source spectra for various LED types introduced in CIE 015:2018*

2) Incorporation of "User Illuminant Function"

This system measures the spectral distribution of the lighting in the location to be evaluated on-site using CL-500A spectroradiometer, and the light source spectrum data can be registered on the CM-17d unit as observation light source data via software (see Figure 8). This enables color value evaluation that closely matches the visual appearance under actual store lighting, even in retail environments where multiple LED lights with differing spectral distributions are combined for visual effect.

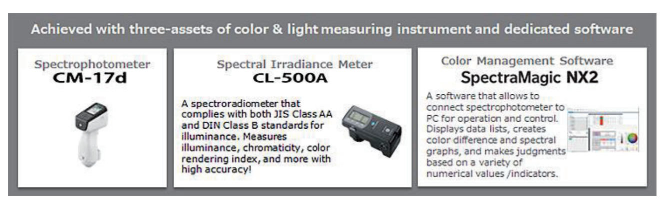

Figure 8. *User illumination function*

4.2 Key Features of Multi-Angle Spectrophotometer CM-M6

As described in Section 2c, cosmetics containing the luminous materials such as metallic and pearl pigments, as well as outer packaging, display stands, and POPs, etc. exhibit angle-dependent color characteristics where the perceived color changes significantly depending on the viewing angle. This makes accurate color evaluation difficult using the diffuse illumination method of CM-

17d described earlier. Multi-Angle Spectrophotometer CM-M6 (see Photo 5) incorporates an optical system with 1-direction illumination and 6-direction reception (45° illumination / -15°, 15°, 25°, 45°, 75°, 110° reception) (see Figure 9). This enables simultaneous acquisition of color measurement data for 6 angles in a single measurement and displays the FF value as well. Consequently, it allows evaluation of whether the intended angle dependency is achieved in the production of cosmetics containing metallic/pearl agents, outer packaging, display stands, and POPs, etc.

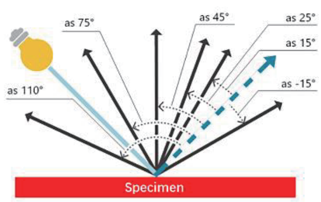

Picture 5. *Multi-angle spectrophotometer CM-M6*
Figure 9. *CM-M6 one-way lighting and six-way light reception*

4.3 Key Features of Appearance Analyzer Rhopoint IQ-S

Rhopoint IQ-S Appearance Analyzer (see Photo 6) enables measurements at 20°, 60°, and 85°, similar to conventional gloss meters, as well as appearance measurements using a photodiode array at 20° (see Figure 10). This enables evaluations previously unattainable with conventional gloss meters, using various indices of reflective properties and surface condition such as [Haze (Cloudiness)] and [Sharpness/DOI] for specular gloss substrates like piano black and aluminum vapor deposition, as described in Section 2e.

Picture 6. *Appearance analyzer Rhopoint IQ-S*

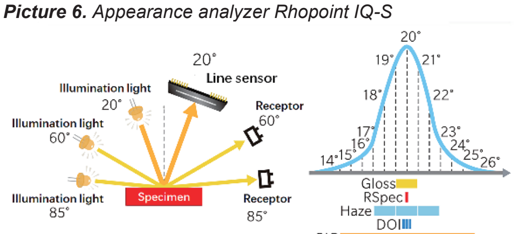

Figure 10. *Rhopoint IQ-S measurement principle*

As tools supporting CMF design strategies that make you want to pick them up, we strongly recommend combining and using these our "Color & Appearance" measurement instruments according to their intended applications. We envision these "Color & Appearance" measurement technologies becoming indispensable tools for creating differentiation in the production management of industrial printed materials for non-paper media, that is the field expected to grow significantly.

References

[1] Hiroshi Fukui, The Science of Beautiful Skin: Interesting Science, Nikkan Kogyo Shimbun, 2013.

[2] Konica Minolta, Inc., PRECISE COLOR COMMUNICATION: Color Control From Perception To Instrumentation, 2007

[3] Tomomi Setoguchi, "Maintaining the Traceability System with New CM-17d Product," Monthly Painting Technology," 2024

[4] Konica Minolta Japan, Inc., Sensing Business Division, "What About Cosmetic Colors Under High Color Rendering Index LED Lighting?" / "Application Examples in the Cosmetics Industry: Color and Light Measurement Instruments", 2025

[5] Konica Minolta Japan, Inc., "Hakaru Chikara" Web Magazine, 2025

Author Biography

Genta Koori graduated from Ritsumeikan University in Kyoto with a Bachelor of Business Administration in 1992. He has since worked in the Planning and Marketing Department at Konica Minolta HQs in Tokyo, focusing on product development and marketing for color & appearance measuring instruments. He is also a member of the G7 Promotion Committee of Japan Printing Academy.

The TriPAV: A High-Frequency Rheometer for Precision Inkjet Characterisation and Waveform Optimisation

Tri Tuladhar & Bart Hallmark, Trijet Limited, Cambridge, UK

Abstract

Inkjet printing involves the complex interaction of mechanical, acoustic, and fluidic phenomena operating on microsecond timescales and micrometre length scales. Within a printhead, inks experience pressure oscillations approaching 100 kHz and shear rates up to 10^6 s^{-1}*: these result from nanometre-scale deformations of the ink channel walls. These conditions impose viscoelastic stresses that are not captured by conventional rheometers, which are typically limited to oscillation frequencies below 100 Hz. Consequently, many inks that have apparently identical bulk rheology may exhibit very different jetting behaviours.*

The TriPAV High-Frequency Rheometer was developed to bridge this gap by characterising low-viscosity fluids under realistic inkjet operating conditions. TriPAV uses solid-state piezoelectric excitation to measure the linear viscoelastic properties (G', G'', η^**) of inks and functional fluids across frequencies from 1 Hz to 10 kHz—a frequency range much closer to those encountered during waveform actuation in Drop-on-Demand (DoD) and Continuous Inkjet (CIJ) systems. The instrument completes a full frequency sweep in under five minutes using <0.1 mL of sample and operates over 5–80 °C, enabling analysis of volatile or reactive inks, UV formulations, and solvent-based coatings.*

In its rapid step strain Printhead Mode, the TriPAV reproduces the acoustic excitation within a printhead channel. Controlled step-strain waveforms applied via a piezo actuator, and measured by a passive sensor, yield fluid response parameters—peak amplitude, peak time, and relaxation time—that correlate directly with waveform features such as drive voltage, pulse width, and wait time. Temperature-dependent tests (20–60 °C) further identify conditions that maximise pumping efficiency, meniscus stability, and droplet reliability.

Introduction

Inkjet technology requires precise control of droplet formation processes governed by the coupled effects of pressure, viscosity, surface tension, and viscoelasticity. Modern printheads operate at frequencies approaching 100 kHz, where the viscoelastic response of even low-viscosity inks influences filament stability, droplet detachment, and satellite formation. Conventional rotational or oscillatory rheometers, limited to <100 Hz, are unable to provide insight into ink behaviour under these conditions.

The TriPAV High-Frequency Rheometer, developed by Trijet Limited (Cambridge, UK), provides a quantitative link between ink formulation and jetting behaviour. Its unique design enables measurement of viscoelastic properties in the true operational range of industrial printheads. By combining high-frequency rheology and printhead-mode waveform simulation, the TriPAV offers predictive tools for ink formulation, waveform design, and quality assurance.

Experimental Methodology

Instrument Design

TriPAV operates as a solid-state, piezo-driven, squeeze-flow rheometer. A small volume of liquid (< 0.1 mL) is confined between two parallel plates separated by a 10–500 µm gap. The lower plate, coupled to an active piezoelectric element, is oscillated with nanometre amplitude (< 10 nm, 0.01–0.2 % strain). The upper plate carries a passive piezo sensor that records the transmitted stress response. Figure 1 shows the complete set of TriPAV equipment.

Using a lock-in amplifier, the system resolves both amplitude and phase shift between excitation and response, allowing calculation of the storage modulus (G′), loss modulus (G″), and complex viscosity (η)* over a 1 Hz–10 kHz frequency range.

Figure 1. *TriPAV equipment with lock-in amplifier, thermostat circulator, digital thermometer.*

Figure 2 highlights the usefulness of high-frequency data in distinguishing between seemingly identical inks [1]. The blue and black ceramic inks shown, both from the same supplier, exhibit similar bulk and low-frequency rheological behavior, yet display pronounced differences in elastic modulus (G') and complex viscosity at higher frequencies. Tests with a standard rheometer, spanning the frequency range shown in blue, would conclude that there is very little rheological difference between the two inks. TriPAV data, however, demonstrates that the blue ink has an elastic response ten times greater than the black ink on the timescale that becomes important for inkjet printing. This difference may lead to the blue ink not being fit for purpose.

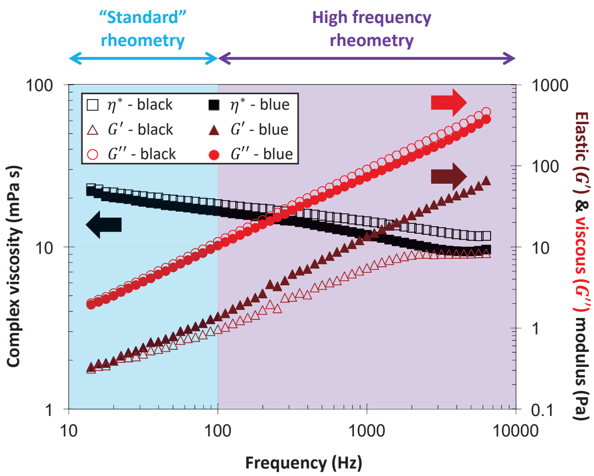

Figure 2. *PAV oscillatory linear viscoelastic data showing subtle differences between a set of ceramic blue and black inks from the same supplier at higher frequencies which otherwise had similar bulk properties.*

Printhead Mode (Waveform Simulation)

In Printhead Mode, the TriPAV mimics printhead actuation by applying a controlled square or step waveform (± 2 V) to simulate the piezo deformation within a printhead channel. The resulting fluid response—measured as voltage across the passive element—provides insight into the transient dynamics of the fluid.

Figure 3 shows a typical fluid response obtained from the TriPAV operating in step-strain printhead mode. Here, the blue curve is the applied waveform, consisting of a step change in voltage, and the brown curve is the inverted fluidic response .

The response curve parameters correspond to the:

- peak amplitude → effective pumping capacity (∝ 1/viscosity);
- peak time → acoustic transit time (related to the speed of sound and the channel length);
- relaxation time → meniscus damping and droplet stability.

These parameters can be directly translated into drive voltage, pulse width, and wait time for waveform design.

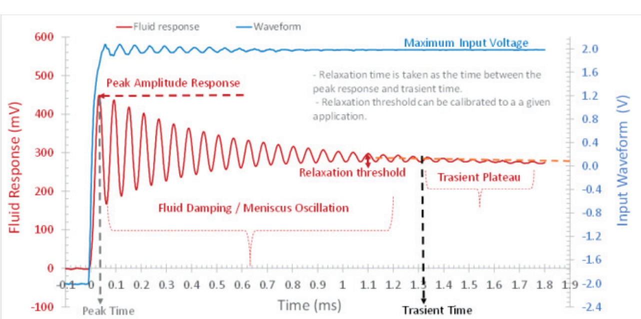

Figure 3. *Typical fluid response in TriPAV printhead-mode showing peak amplitude, peak time, and relaxation time.*

Operating Conditions

All experiments were conducted between 5–80 °C using a temperature-controlled circulator. Frequency sweeps required less than five minutes, while Printhead Mode temperature ramps (20–60 °C) were completed in under 30 minutes per sample.

Results and Discussion

Case Study 1 Showcasing TriPAV High Frequency Rheology of Aqueous CMYK Inks

A CYMK (cyan – magenta – yellow – key black) set of water-based inks for use in an inkjet printing press had been received from a supplier. Whilst the magenta, yellow and black inks printed as expected, the cyan ink did not. Conventional rheological testing, using steady shear and dynamic tests, could not detect any differences between the four inks.

Figure 4A shows a collage of rheological response for all four inks [2]. Here, the trends of complex viscosity, η*, as a function of frequency are shown as open squares and the trends of viscous modulus, G", as a function of frequency are shown as filled circles. Where it is present, the trend of elastic modulus, G', as a function of frequency is shown by filled triangles. The colour of each symbol denotes the ink type. While all four inks (C, M, Y, K) had similar low-frequency viscosities, only cyan displayed measurable elasticity (G′ > 0) at high frequencies (>1 kHz). This correlated with unstable jetting behaviour. Figure 4B shows the rheological response of the reformulated cyan ink.

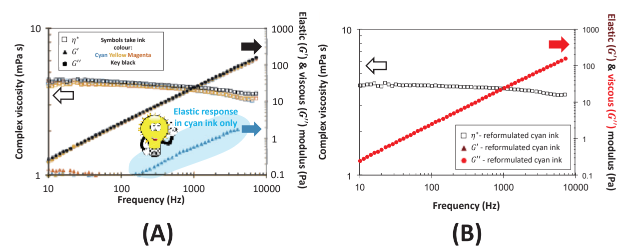

Figure 4. *TriPAV complex printhead-mode showing peak amplitude, peak time, and relaxation time.*

TriPAV testing demonstrated that a high frequency elastic response in the original cyan ink was responsible for the observed jettability problems.

Use of the TriPAV as part of ink the reformulation process allowed a replacement cyan ink to be designed that behaved identically to the remaining inks in the colour set.

Case Study 2 Showcasing TriPAV Printhead Mode Short Timescale Step Strain Data

In order to successfully jet an inkjet fluid, the fluid viscosity must lie within a range that is able to be jetted by the printhead. Whilst there are ways to design and operate a printhead such that it can be used with high viscosity fluids, fluid viscosity can also be manipulated to be compatible with existing print systems. One way in which this can be done is to use heat! Typically, fluid viscosity decreases with increasing temperature, which allows ink viscosity to be matched to printhead requirements.

The plots shown in Figure 5 demonstrate how the response to a step strain test differs for two inks, A and B, at three temperatures

[2]. The response voltage is plotted as a function of time on the primary y-axis in various shades of red, and the step change in driving voltage is shown on the secondary y-axis in blue.

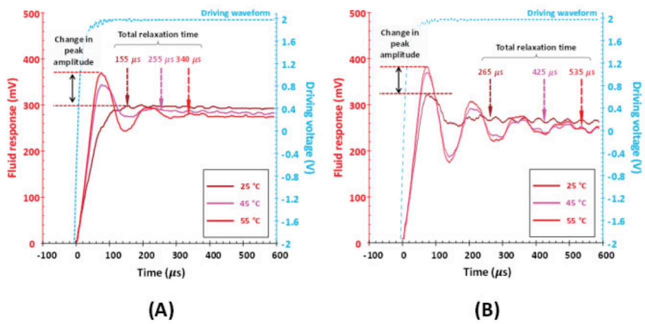

Figure 5. *Typical fluid response in TriPAV printhead-mode showing peak amplitude, peak time, and relaxation time (A) Ink A, and (B) Ink B.*

For ink (A) at 25°C, no oscillatory response can be seen. This infers that the energy transfer from the piezo actuator to the ink is poor and insufficient to result in jetting. As the ink temperature is increased, the amplitude of the first peak increases, indicating that more energy is being transferred to the liquid. These higher peak amplitudes correspond to conditions where jetting would occur in a printhead. It can also be seen that the hotter inks tend to "ring" for a longer period of time, with the oscillatory response damping out at 255 µs at 45°C and 340 µs at 55°C. These oscillations can be linked to the movement of the fluid meniscus within an inkjet nozzle. For reliable jetting, this movement is usually allowed to decay before another driving pulse is applied. The longer this decay time, the slower the printing process! The choice of temperature is a compromise between energy transfer to allow jetting and print speed. A similar set of trends can be seen for ink (B) except that the total relaxation time – the time required for oscillation to decay – is longer at every temperature.

Printhead mode step strain tests on the TriPAV can quickly identify the optimum jetting temperature for an inkjet fluid. The optimum temperature is a compromise between transferring enough energy to pump the fluid, and having a relaxation time short enough for the desired print speed.

Case Study 3- Optimising the Jetting Temperature of UV Inks

A yellow and a black UV-curable ink both had manufacturer's recommended jetting temperatures of 35°C. When these inks were trialled in a printing application, it became evident very quickly that there was a problem! At 35°C, the black ink failed to print and the print quality of the yellow ink was sub-optimal. A programme of investigation was started to understand why this was case and how to solve the problem.

Peak amplitude as a function of temperature from TriPAV step strain testing of both inks is shown in Figure 6A, with the total relaxation time for both inks as a function of temperature being shown in Figure 6B. The sequence of images in Figure 7 show droplet flight behaviour for both inks at three selected temperatures within the testing range.

The energy transfer to the inks, as evidenced by an essentially stable peak voltage, does not change significantly above 30°C. For the yellow ink, a change in the trend of relaxation time – indicating the onset of "ringing" - happens between 28°C and 31°C, with a similar change happening for the black ink between 41°C and 44°C. From the images, one can see that the onset of "ringing" corresponds to successful jetting. Temperatures above this onset temperature infer increasing meniscus oscillation, which can lead to misfiring and print quality problems.

TriPAV printhead mode tests (Figure 6A) quickly identified the optimal jetting temperature for both inks. A (time consuming) set of visualisation studies (Figure 7) confirm the choice of ink temperature.

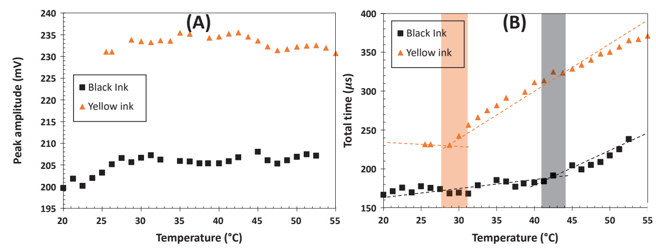

Figure 6. *TriPAV printhead mode data for UV yellow and UV black as a function of temperature showing (A) peak amplitude and (B) total time (peak time + relaxation time).*

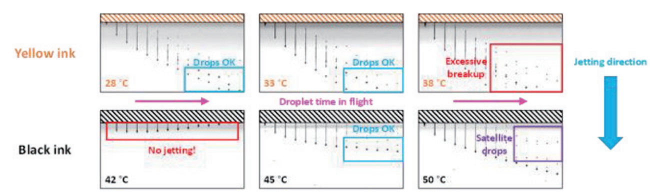

Figure 7. *In-flight jetting images of the UV yellow and black inks using a Ricoh Gen 5 printhead.*

Case Study 4- Jetting of High Viscosity Inks

Inkjet printing technology is being applied to an ever-wider range of applications, including additive manufacturing. This application provides a wealth of challenges and opportunities for the industry as fluids used for additive manufacturing can be orders of magnitude more viscous than traditional inks. Transferring a sufficient amount of energy from the printhead to the fluid for jetting to occur can be a significant challenge! Tailoring the formulation of an ink can make the difference between an ink that jets and one that does not.

Figure 8A shows the TriPAV complex rheology data for a jettable (closed symbols) and a non-jettable (open symbols) high viscosity fluid, and Figure 7(B) and (C) give TriPAV printhead mode step strain data for both fluids.

The complex viscosity for the jettable fluid is higher than that for the non-jettable fluid, but its formulation has been designed to produce an elastic response at the timescales relevant to jetting within a printhead ($G' \gg 0$ for $f > 2$ kHz). The effect of this high frequency elastic response is to enhance the energy transfer from the printhead to the fluid, resulting in high viscosity jettability.

TriPAV frequency sweep data combined with TriPAV printhead mode step strain data is a powerful tool to assist the development of inkjet fluids for use in challenging processes.

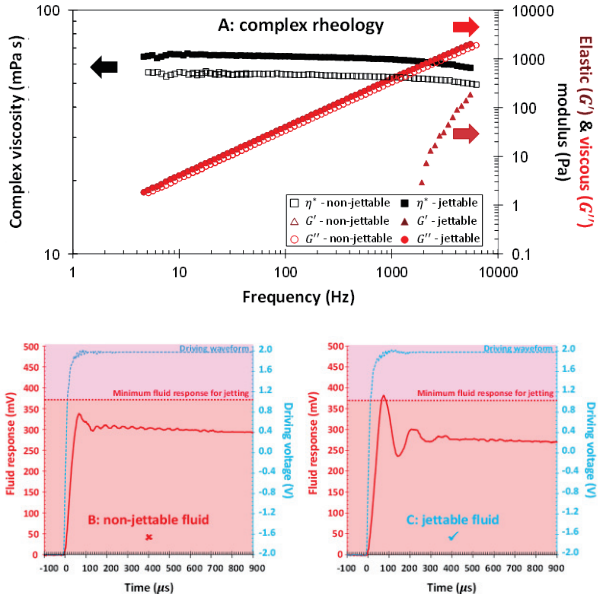

Figure 8. (A) TriPAV complex rheology of jettable and non-jettable ink, (B -C) TriPAV printhead mode step strain data of both fluids.

Conclusions

The TriPAV high-frequency rheometer introduces a new paradigm for understanding inkjet ink behaviour under realistic operating conditions. By extending rheology into the high-frequency regime relevant to inkjet printheads, the TriPAV provides a quantitative link between formulation, structure, viscoelastic response, and droplet dynamics.

The TriPAV printhead mode step-strain temperature sweep, which can be done in less than 30 minutes, supports real-time formulation screening and production QC, allowing early detection of formulation drift or additive incompatibility. This approach transforms waveform optimisation from empirical tuning to a quantitative, measurement-driven process.

Key outcomes include:

- Differentiation of inks with similar bulk rheology but different jetting outcomes;
- Predictive optimisation of waveform parameters (drive voltage, pulse width, wait time);
- Identification of optimum jetting temperature for each formulation;
- Reliable QC metrics for production environments.

The TriPAV's combined high-frequency and printhead-mode analysis thus accelerates ink development, improves process reliability, and supports growing industrial demand for predictive, data-driven inkjet characterisation.

Acknowledgements

The authors gratefully acknowledge validation support from iPrint, Switzerland, and the collaboration of industrial partners contributing ink samples for testing

References

[1] T R Tuladhar, "Metrology- Measurement of Complex Rheology and Jettability of Inkjet Inks" Chap. 22 in "Handbook of Industrial Inkjet Printing", edited by W. Zapka, pp 411-429, ISBN: 978-3-527-338320, Wiley-VCH, (2017).

[2] Extreme Rheology with the TriPAV rheometer, www.trijet.co.uk, 2025.

Author Biography

Dr. Tri Tuladhar holds a Ph.D. in Chemical Engineering from the University of Cambridge and bachelor's degree at RMIT University, Australia. With over 25 years of R&D experience in both academia and industry, he has specialised in the complex rheology of inkjet inks since 2005, pioneering methods that link fluid rheology to jetting performance.

As Founder and Head of Trijet Limited, Dr. Tuladhar leads advanced rheological characterisation and optimisation of inkjet inks, formulates specialty paints, glass enamels, and functional inks, and designs bespoke rheological tools. He also delivers workshops and training courses for industrial clients, sharing his expertise in ink formulation and jetting process optimisation.

Novel Additive Manufacturing Applications Enabled by Modular Integration of Ultra-High Viscosity Technology

Ramon Borrell; Quantica GmbH; Berlin, Germany

Abstract

Many industrial processes require the deposition of materials with very specific functional and physical properties, often rendering them incompatible with established digital printing technologies. Ultra-High Viscosity Inkjet has demonstrated a dramatic improvement in productivity, precision, and material efficiency, enabling additive manufacturing in many of these processes. Quantica's NovoJet™ printhead technology is being deployed in modular Print Engines that facilitate rapid adoption and integration into the production of fuel cells, electric motors, decorative products, and other high-volume, flexibly manufactured components.

Introduction

NovoJet™ is a novel piezo inkjet printhead technology that overcomes the limitations of conventional deposition techniques in productivity, precision, flexibility, and material compatibility, see Figure 1. It addresses material selection restrictions in functional and manufacturing applications by enabling the jetting of extremely high-viscosity fluids, significantly extending the conventional viscosity range considered feasible in inkjet printing. In the absence of widely recognised standards, Quantica defines ultra-high viscosity as viscosities above 100 mPa·s at jetting conditions. NovoJet™ provides a viable digital alternative to screen printing, pad printing, dispensing, spray, and slot-die coating. Customer trials have demonstrated its capability to deposit highly functional materials—including UV resins, adhesives, silicones, coatings, conductive pastes, and screen-printing pastes—onto diverse substrates and geometries with high precision.

***Figure 1**. NovoJet™ Printhead (Width: 30mm, Length: 190mm, Height 24 mm)*

Technology Overview

In October 2021, Quantica unveiled the NovoJet™ inkjet technology at the Print4Fab conference [1]. Four years later, that promise has materialised into a range of products approaching commercialisation, capable of improving real-world manufacturing applications. The printhead design has evolved significantly since 2021[3][4], becoming more suitable for initial commercial applications. A number of variants are planned for specialised uses.

The NovoJet™ printhead employs a novel actuation mechanism, enabling the jetting of ultra-high viscosity materials, including those with a high elastic component in their complex rheology and high particle loading. Unlike conventional piezo inkjet systems, the design operates in an extended range of Ohnesorge values, far exceeding one, with dynamics dominated by relatively large masses and forces rather than Helmholtz resonance. While this limits jetting frequency compared to acoustic actuation, it enables efficient momentum transfer from the actuator to ultra-high viscosity fluids.

The first commercial NovoJet™ printhead offers high-throughput, drop-on-demand deposition for materials with viscosities up to 250 mPa·s at the point of ejection, at frequencies up to 8 kHz, and with drop volumes between 200–600 pL depending on nozzle diameter. The measurement of viscoelastic properties of fluid in printheads is notoriously difficult, sometimes requiring smart approximations such as those described by Tuladhar [2].

The core of NovoJet™ lies in its unique actuator and fluid ejection mechanism, optimised for highly viscous, rheologically complex, and chemically demanding materials. The actuator uses PZT (lead zirconate titanate) piezo ceramic arranged in a tri-morph configuration, using d_{31} inverse piezoelectric effect to bend the actuator and transfer the resulting motion into large, highly controllable nozzle chamber deflection as shown in figure 2.

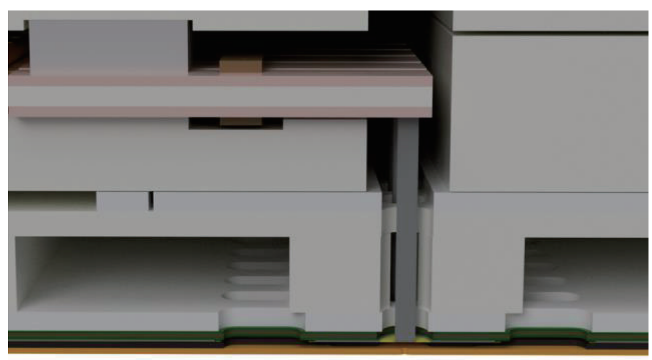

***Figure 2**. Segmented tri-morph actuator stacks with a connecting conductive crossbar and the plunger connected at the free-moving end.*

This configuration provides high blocking force and displacement, particularly beneficial for highly viscoelastic materials. Momentum is transferred via a plunger to a flexible membrane, creating pressurisation for ejecting viscous materials while maintaining a wide geometric cross-section for rapid material resupply during the back-stroke. The chamber geometry facilitates rapid refill even with highly viscous fluids, addressing material starvation issues. Displacements up 4 µm with high viscosity fluids and up to 6 µm with lower viscosities are achieved at 100V. Blocking forces up to 0.3 N meet the need for the viscosity ranges indicated above. Figure 3 shows membrane displacement response to a single pulse without cancellation at different voltages in empty chamber. Natural frequency of oscillation is 18kHz.

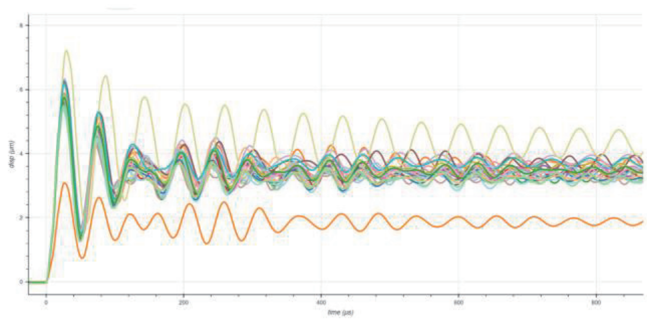

Figure 3. *Membrane deflection response in dry chamber at different voltages.*

The volumetric displacement approach necessitates specific design considerations. Large membrane surface areas limit nozzle density, resulting in a single row of nozzles spaced at 1.27 mm and a native resolution of 20 DPI. Large actuator displacements require wide chambers, high-voltage, and careful thermal management to ensure reliable, sustained jetting.

Detailed study of the factors influencing jetting show the detailed design of the membrane and how it is deformed during operation is a critical factor in enabling jetting of high viscosity materials, along with impact on printhead durability and thermal efficiency. Figure 4 shows a finite element model of deformation when high voltage is applied. Optimisation of geometries and materials to very fine detail has strong impact on operation and jetting capabilities. As know-how increases and design are refined, operational range is expected to significantly improve in future models.

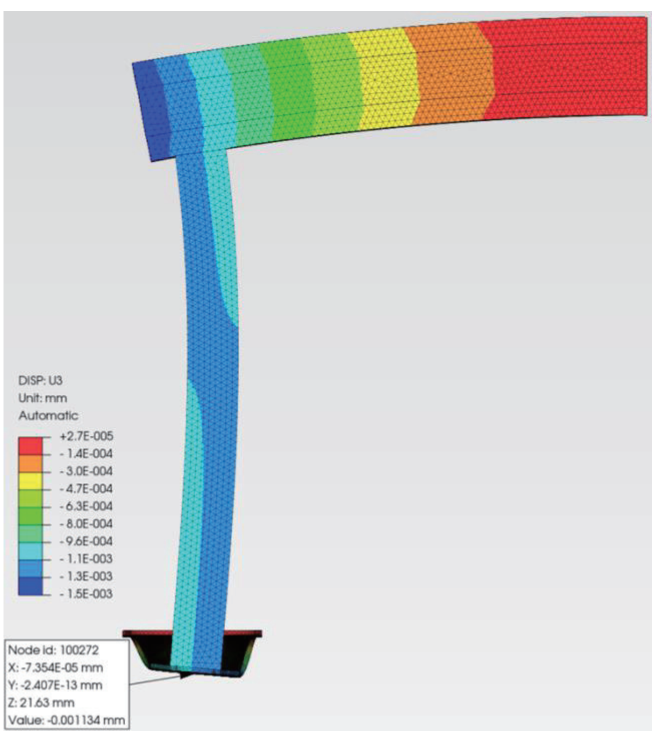

Figure 4*. FEA model of deformation of elements during actuation*

Operational parameters and control

Quantica's proprietary material management system, combined with printhead parameter controls, enables precise handling of fluid heating, back-pressurisation, and flow rate. Individual piezo elements can receive customised waveforms, allowing single- and multi-pulse control for enhanced drop uniformity across operational frequencies.

The system achieves stable ejection for viscosities up to 250 mPa·s, surface tensions from <30 to >72 mN/m, solids content up to 80% by weight, and particle sizes up to 9 µm (D90). Optimal performance requires tuning of displacement, actuator resting position, operating frequency, temperature, back-pressure, flow rate, voltage, and waveform design. Nozzle sizes from 40 µm to 90 µm have been successfully tested, with diameter critical for stable back-pressure window.

Chemically resistant materials—including alumina ceramic, polyimide (Kapton), PEEK, and inert epoxy adhesives—are used throughout the fluid path. The external material management system fully developed by Quantica for Novojet™ may be adapted with fluoropolymers or thermoplastics to optimise chemical compatibility and system cost.

Advantages

NovoJet™ allows jetting of fluids orders of magnitude more viscous than conventional inkjet printheads, handling approximately 250 mPa·s for shear-thinning fluids and 130 mPa·s for Newtonian fluids at operating temperature. Shear-thinning and thixotropic behaviours enable ejection of highly viscous, particle-loaded fluids, with speeds exceeding 7 m/s in some cases and stable jetting over distances far exceeding the typical 1–5 mm range.

Deposition rates reach up to 1.5 l/h, ejecting large drop volumes (up to 600 pl) at high frequencies (up to 8 kHz) across 96 nozzles. Printhead slanting or stacking enables single-pass printing in many applications. Drop volumes can be tuned via waveform adjustments, with 200–400 pL for 60 µm nozzles and 500–600 pL for 90 µm nozzles.

The fluidic circuit enables rapid refill and high-flow recirculation, handling fluids with up to 80% particle loading by weight (for example with Cu nanoparticles) and particles up to 9 µm D90, preventing sedimentation and agglomeration.

Applications

Quantica is expanding digital printing into high-value industrial sectors including, among many others, batteries, automotive, renewable energy, consumer electronics, medical devices, and semiconductors. Advanced use cases demand high viscosity handling, robust reliability, and unique material capabilities—areas where NovoJet™ offers a defensible advantage.

Adhesives for E-Motors

Precise, high-speed deposition replaces conventional dispensing, reducing material use and improving conformity to complex geometries. Manufacturers aim to integrate the deposition of adhesive inside the progressive punching die producing up to 3 parts per second. Space is very constrained and print speed of up to 2m/s may be necessary in order to not slow down production. The adoption of inkjet in this process will improve quality of emotors by reducing delamination and optimising the extension and location of the areas points of contact and insulation between the lamela, leading to more efficient operation. Cost may lower due to savings in material. Design freedom may lead to more efficient designs, including internal liquid cooling in more sophisticated models by ensuring the parts are completely sealed, which at this moment is not possible with a conventional manufacturing method.

Figure 5 shows a lamela for a rotor with adhesive printed using the prototype of the Print Engine.

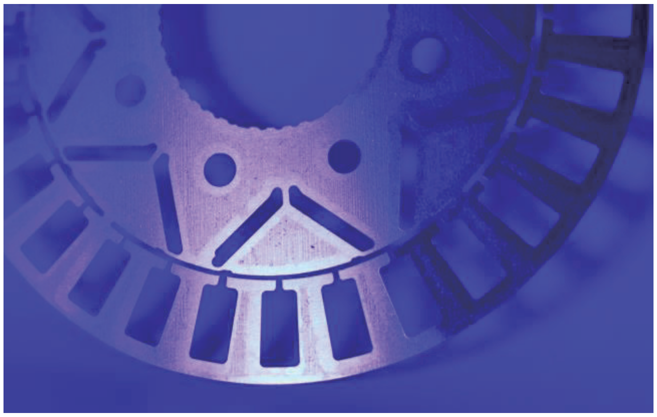

***Figure 5**. Temperature sensitive adhesive printed on e-motor rotor sample.*

Platinum Catalyst Jetting for Fuel Cells

High-particle-content inks with platinum catalyst materials can reduce total fuel cell production costs by at least 15% by avoiding waste produced by analog processes. Digital process enables deposition of exact quantities only at the right location. Adhesives and sealing have also successfully been printed for the assembly of cells.

Insulation Coatings for Li-Ion Batteries

Superior deposition quality reduces gas entrapment and material waste by up to 60% compared to spray methods, particularly on corners and edges where the desired thickness of the insulation layer can be guaranteed.

Other customer fluids

Over 20 customer fluids have been successfully evaluated for jettability on the initial commercial version of the Novojet™ printhead, with >80% demonstrating promising results. Common challenges include particle size distribution and excessive viscosity, requiring minor adjustments for jetting.

Scalability and Future Roadmap

NovoJet™'s design is highly scalable, allowing printheads of varying lengths and widths to be custome developed for specific applications. One such customer design is currently being evaluated in collaboration with a 3rd party.

Future models include multi-row printheads with up to 192–576 chambers and internal multi-material capabilities. Multi-nozzle per chamber configurations could raise productivity to 20 L/h per printhead. Improvements to actuator and chamber geometry show theoretically the capability to double both the blocking force and the membrane displacement, enabling jetting of even higher viscosity materials and lowering power consumption and thermal load.

Deployment: The Print Engine

Quantica's Print Engine integrates NovoJet™ technology into pilot and production lines, bridging expertise gaps in digital inkjet adoption. The key element is a modular print cell under development with integrated material management system and electronics specifically developed for Novojet™. It can scale in print and cross-print directions, delivering swath width, resolution, and productivity required for each industrial application.

A typical configuration for e-motor adhesive application uses 3×3 cells providing a 300 mm wide print area at 150×200 DPI, delivering 15 µm thick adhesive layer at average 1 m/s (equivalent to 80,000 parts per 8-hour shift). Beta versions for pilot line evaluation will be available in Q2 2026. Figure 6 shows a working prototype in a 6x2 cell configuration.

Figure 6. *Prototype Print Engine in a 150npi print comfiguration*

Future printheads with multiple rows and multiple nozzles per chamber will increase productivity and enable grammages up to 480 g/m² if required.

The dedicated electronics and SW will include individual nozzle tuning capability for extra control and precision.

Conclusion

NovoJet™ represents a major advancement in deposition technology, overcoming limitations of conventional inkjet and traditional analog methods. Its unique actuator design, volumetric displacement principle, and robust fluid handling enable high-throughput, precise jetting of ultra-high viscosity materials. This opens new possibilities in additive manufacturing, functional coatings, and industrial applications, enabling previously unattainable performance with UV resins, adhesives, silicones, coatings, conductive pastes, and screen-printing materials.

Author Biography

Ramon Borrell received MSc degrees in Industrial Engineering (1987) and Automotive Business (1993) from Universitat Politècnica de Catalunya, Barcelona. He held technical and management roles developing large-format inkjet printers at HP. In 2007 he was appointed R&D Director at Xaar plc, leading printhead development including the 5601 Thin-Film Piezo MEMS industrial printhead. In 2021 he joined Quantica GmbH as CTO and currently serves as Director of Product and Strategy. He is also Treasurer of IS&T.

References

[1] B. Hartkopp, M. Strobel, Quantica GmbH, Berlin, Germany; R. Borrell, Cambridge, UK. “Novel Piezo Inkjet Technology and Printhead Capable of Jetting Extreme Viscosity Fluids for Additive Manufacturing”, Proceedings of Printing for Fabrication 2021, Imaging Science and Technology Society.

[2] R. Tuladhar, Metrology – Measurement of Complex Rheology and Jettability of Inkjet Inks, Volume 2, Part VI, Chapter 28 in Inkjet Printing in Industry, edited by W. Zapka, Wiley-VCH, 2022, pp. 657–694.

[3] L. Färber, B. Hartkopp, Material Ejection System, Print Head, 3D Printer, and Method for Material Ejection, European Patent Application EP 3 825 100 A1, 2021.

[4] B. Hartkopp, D. Niedner, A. Garcia Gomez, Printhead, European Patent Application EP 4 497 599 A1, 2025.

Development of a Multi-Nozzle Hybrid Inkjet Printhead Enabling Droplet Ejection up to 200 cP Using Piezoelectric-Electrohydrodynamic Mechanism

Eunyoung Lee, Inho Na, Jongphil Choi, Youngjoon Han, Youngjun Jo, Chaerim Park, Juhyeon Park, Jaewoo Joung
Hyungdong Lee* and Jaeyong Choi *
ENJET Co.,LTD.; 45, Saneop-ro 92beon-gil, Gwonseon-gu, Suwon-si, Gyeonggi-do/Republic of Korea

Abstract

Inkjet printing is widely used due to its high precision in depositing ink at specific locations. However, it is limited to low-viscosity inks below 20 cP, restricting its compatibility with various functional materials. In contrast, electrohydrodynamic (EHD) printing allows jetting of inks with viscosities above 50 cP, but its short working distance (≤100 μm) and low throughput hinder large-scale application.

To overcome these limitations, we have developed an innovative hybrid inkjet printhead that integrates the benefits of both conventional piezoelectric and EHD printing mechanisms. Utilizing this advanced system, we conducted experiments on the ejection of 200 cP viscosity inks, a feat challenging for conventional piezoelectric-actuated systems.

The proposed hybrid inkjet printhead equipped with both piezoelectric actuators and EHD electrode to achieve a synergistic effect combining mechanical and electrical forces. The hybrid inkjet printhead enables stable ejection of high-viscosity inks (≤200cP) through 16 nozzles and 100 npi simultaneously. Also, this hybrid inkjet printhead can eject droplet volume range between 10 and 12 pL at a working distance exceeding 1 mm. Therefore, the ability to eject from multiple nozzles and high viscous ink concurrently enhances productivity, expanding the potential for applications across various industrial sectors.

Introduction

Inkjet printing systems, as digital and non-contact deposition platforms, have been widely adopted across various industrial sectors such as displays, semiconductor packaging, printed circuit boards (PCB), sensors, and biomedical devices due to their high printing speed, cost efficiency, and compatibility with a wide range of substrates [1-2]. In particular, in additive manufacturing and printed electronics, inkjet printing is gaining increasing attention as a key enabling technology for direct patterning without the need for complex masking or lithographic steps, thereby reducing process complexity while facilitating the fabrication of flexible electronic devices [3].

However, the most widely utilized drop-on-demand (DOD) inkjet systems based on piezoelectric actuation inherently suffer from rheological constraints, especially in terms of ink viscosity [4]. Commercial piezoelectric inkjet printheads are generally limited to fluids with viscosities below 20 cP, confining their operation to low-viscosity solvent-based inks. As a result, the precise patterning of high-viscosity functional materials—such as conductive adhesives, metal nanoparticle suspensions, and polymer-based bioinks—remains challenging [5-6].

In contrast, electrohydrodynamic (EHD) printing systems exploit electric field-induced stresses at the meniscus to eject liquids with viscosities exceeding 100 cP [7]. Moreover, EHD actuation can achieve sub-10 μm feature resolution, even below the physical nozzle diameter, making it a promising technology for ultrahigh-resolution patterning [8]. Nevertheless, EHD-based printing is constrained by its strong dependence on the applied electric field, resulting in restricted stand-off distances of only a few millimeters and relatively slow jetting speeds, which limit its applicability in high-throughput manufacturing. Furthermore, electrical interference between adjacent nozzles makes it difficult to scale EHD systems into multi-nozzle arrays, hindering their transition toward industrial continuous production [9].

Recent studies on hybrid printing strategies have demonstrated that applying an auxiliary electric field to a piezo-driven system can effectively suppress satellite formation in high-viscosity jetting. However, most of these demonstrations have been limited to single-nozzle configurations, and no scalable architecture capable of extending the concept to multi-channel arrays without nozzle-to-nozzle interference has been established to date [10].

Meanwhile, the demand for high-viscosity precision jetting is rapidly increasing in applications such as printed electronics, flexible packaging, micro-LED bonding, and hydrogel bio-fabrication. Consequently, hybrid inkjet systems that simultaneously leverage the high-speed stability of piezoelectric actuation and the high-viscosity jetting capability of EHD actuation are emerging as next-generation core technologies for digital additive manufacturing.

In this study, we propose a multi-nozzle hybrid inkjet Printhead (Model: EHDison-H16) that simultaneously employs piezoelectric pressure actuation and electric field assistance. We demonstrate that this approach enables stable ejection of inks with viscosities up to 200 cP. The proposed system effectively overcomes the viscosity limitations of conventional inkjet systems while maintaining compatibility with industrial multi-nozzle architectures, offering high scalability and practical applicability for future manufacturing platforms.

Furthermore, reliability evaluations are concurrently being conducted on the 512 nozzles large area printhead developed by ENJET. This printhead is designed to simultaneously achieve high-resolution and high-speed printing performance and is being assessed under actual industrial process conditions in terms of stable operation, nozzle-to-nozzle uniformity, and long-term continuous jetting characteristics. Such parallel studies serve as an important step in demonstrating that the proposed hybrid actuation scheme can be stably applied not only to small-scale single-nozzle heads but also to large-area multi-nozzle printheads.

Printhead Design

16 Nozzles & 512 Nozzles Hybrid Head

The proposed hybrid printhead, named EHDison-H16, is developed and commercialized by ENJET Co., Ltd. The EHDison-H16 printhead features a linear array structure with 16 nozzles arranged at a pitch of 100 NPI (Nozzles Per Inch). Each nozzle is precisely fabricated using MEMS technology, minimizing crosstalk and ensuring uniform droplet formation across the array. The printhead employs a hybrid actuation mechanism that separates the roles of the Piezoelectric (Piezo) actuator and the Electrohydrodynamic (EHD) electrode. The Piezo actuator instantaneously increases the chamber pressure to form the initial meniscus at the nozzle outlet. Once the meniscus is established, a high voltage is applied to the EHD electrode located at the nozzle gate, elongating the meniscus and enabling stable jetting even with high-viscosity inks. The EHD electrode is positioned near the nozzle exit and generates a strong electric field when high voltage is applied. The nozzle and EHD electrode are electrically insulated, allowing independent control of the electric field strength without interfering with the piezoelectric actuation. A Driver-Per-Nozzle (DPN) control circuit is implemented, enabling each nozzle to be independently driven by a customized piezo waveform. This allows optimization of jetting conditions for both high- and low-viscosity inks. The head also integrates a built-in heating structure, with a temperature sensor installed inside the ink chamber. The ink temperature can be adjusted up to 50 °C, enabling viscosity control and improving jetting stability. Unlike conventional cartridge-type systems, the EHDison-H16 adopts a refillable ink supply structure, which supports long-term continuous operation and repeated experiments with various functional materials.

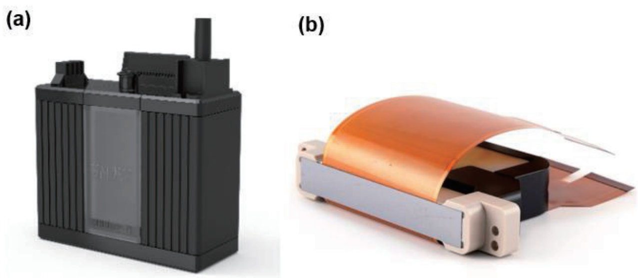

Figure 1. *(a) EHDison-H16, (b) 512 Nozzles Head*

The 512-nozzle (512Nz) large-area printhead is currently undergoing long-term reliability evaluation. It features a linear array of 512 nozzles with a pitch of 200 NPI (Nozzles Per Inch). A degasser is integrated into the system, which effectively removes bubbles from the ink and reduces bubble inflow into the head, thereby enabling stable and continuous jetting. The printhead is designed to simultaneously achieve high resolution, large-area coverage, and high-speed printing performance, and is being evaluated under actual industrial process conditions in terms of stable operation, nozzle-to-nozzle uniformity, and long-term continuous jetting characteristics.

EHDison-H16 Mechanism

The EHDison-H16 printhead integrates Piezoelectric (Piezo) and Electrohydrodynamic (EHD) actuation mechanisms within a single hybrid platform. Structural optimization of the actuator was performed using Finite Element Method (FEM) analysis. A comprehensive multiphysics simulation was conducted using the COMSOL Multiphysics® module, which included electrostatics, solid mechanics, and fluid dynamics. The simulation process was divided into multiple stages to accurately capture the droplet formation mechanism. Based on the simulated jetting behavior, the nozzle geometry and chamber dimensions were optimized to achieve stable droplet ejection. Similarly, the EHD electrode was optimized through detailed parametric analysis using coupled electrostatic–fluid simulations. The effects of electrode spacing, height offset, and electric field distribution were analyzed to determine the optimal configuration that enhances electric field uniformity and minimizes fluidic disturbance. The fabrication process employed Micro-Electro-Mechanical Systems (MEMS) technology. Three wafers—the chamber wafer, nozzle wafer, and EHD electrode wafer—were individually processed and subsequently bonded to form the final head assembly. A custom-designed FPCB and nozzle surface layout were developed to match the electrical and mechanical interfaces of the fabricated head. The housing structure was carefully designed to ensure that the Piezo and EHD electrodes operate independently without electrical or mechanical interference. The jetting performance of the EHDison-H16 was evaluated using a drop-watcher visualization system. Experimental results showed that the droplet velocity increased by up to 70% when the EHD voltage was applied in conjunction with Piezo actuation, compared to Piezo-only operation.

During hybrid operation, a unipolar trapezoidal waveform was applied to the Piezo actuator to generate pressure within the chamber and form a meniscus at the nozzle orifice. Once the meniscus was established, a synchronized EHD electric field was applied, which elongated the meniscus and enabled stable droplet ejection even for high-viscosity inks. Unlike the continuous cone-jet mode observed in pure EHD systems, the hybrid EHDison-H16 platform allows flexible operation in selective ejection mode, enabling Piezo-only, EHD-only, or simultaneous hybrid actuation depending on the ink properties and process requirements.

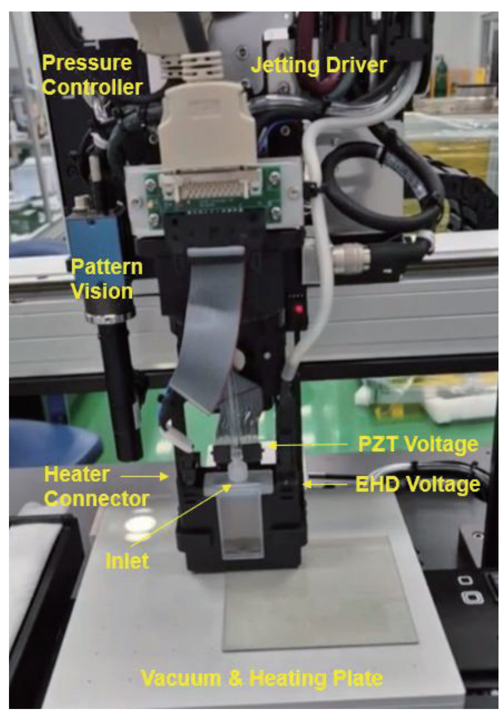

Figure 2. *EHDison-H16 Printer for R&D Printing*

Experimental Setup

To evaluate the jetting performance of the EHDison-H16 hybrid printhead, standard reference solvents covering a wide viscosity range from 4 cP to 200 cP were prepared in-house.

The rheological and physicochemical properties of the inks were characterized using in-house measurement equipment. Viscosity was measured with a CAS CL-1 viscometer, surface tension with a SITA DynoTester+, electrical conductivity with a Mettler Toledo SevenDirect SD30, and dielectric constant with an 871 Liquid Dielectric Constant Meter (Sanyo Trading Co., Ltd.).

Droplet formation and jetting behavior were visualized using a CCD (Charge-Coupled Device) camera system, which enabled real-time observation of droplet volume, ejection angle, and velocity. Sequential imaging and time-resolved velocity measurements were also employed to analyze droplet dynamics under various operating conditions.

Results and Discussion

Jetting of Viscosity Variable Standard Solvents

The jetting characteristics of viscosity-standard solvents were analyzed using the EHDison-H16 hybrid printhead. The results demonstrate that the hybrid actuation (Piezo + EHD) enables stable droplet formation even for inks with high viscosity (up to 200 cP), whereas the Piezo-only mode failed to eject beyond 30 cP.

The jetting behavior of viscosity-controlled standard solvents in the range of 4 cP to 200 cP was observed using a Drop-watcher system (see Figure 3). Stable droplet ejection was achieved using only the piezo actuator up to a viscosity of 30 cP. However, for inks exceeding 50 cP, piezo actuation alone was insufficient to generate droplets, and an auxiliary EHD voltage was applied. The applied waveform conditions were adjusted depending on viscosity. The piezo waveform included rising, dwell and falling times in the microsecond range, with voltage amplitude sufficient for stable actuation. For higher viscosities, an additional EHD waveform with extended dwell time and higher amplitude was used to optimize ejection.

The average droplet velocity across the viscosity range was measured to be approximately 2.5–3 m/s, and the average droplet volume was 10 pL. Furthermore, the jetting performance was evaluated at increasing actuation frequencies to verify stable droplet ejection without any anomalies in the printhead. A high-speed camera was employed to accurately observe droplet formation, and stable ejection was confirmed up to a frequency of 30 kHz (see Figure 4).

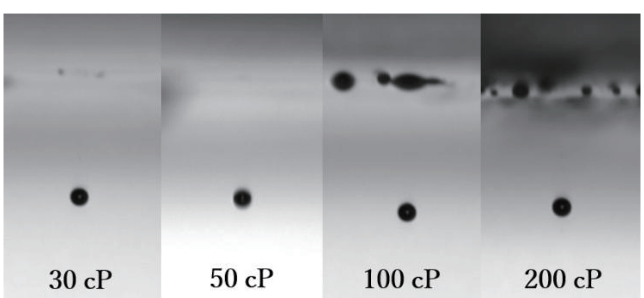

Figure 3. *Jetting Performance by Ink Viscosity*

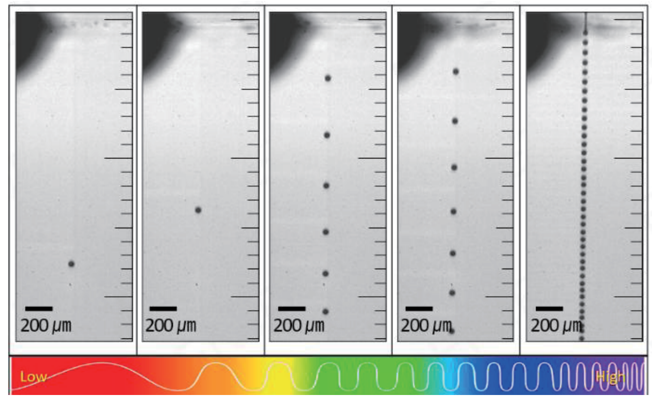

Figure 4. *Droplet Ejection Results by Frequency*

Inkjet printing of the ENJET logo and electrode patterns was performed on hydrophobically coated substrates using inks of varying viscosities. The substrates exhibited a Di-water contact angle of 100–110°, and the diameter of individual droplets was measured to be approximately 30 µm. Printing with multi-nozzle operation produced uniform patterns without satellite droplets, demonstrating precise and consistent droplet deposition. These results indicate that high-resolution and uniform printing can be achieved across a range of ink viscosities (see Figure 5, 6).

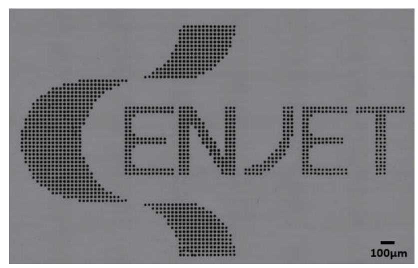

Figure 5. *ENJET Logo Printing Image*

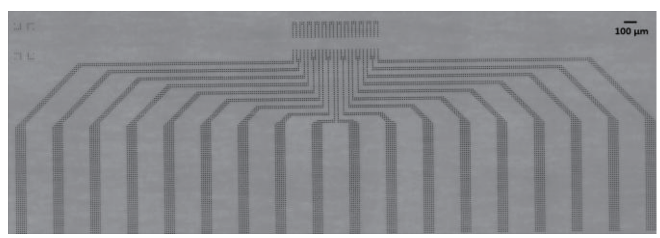

Figure 6. *Electrode Pattern Printed at 600 dpi*

512 Nozzles Printhead Jetting Test

To evaluate high-speed jetting performance, the 512Nz printhead was used to dispense the same viscosity-controlled standard solvents. The actuation frequency was increased up to 30 kHz, and nozzle uniformity and stability were monitored using a CCD camera. Figure 7 and 8 shows representative droplet images at 20 kHz and 30 kHz. All nozzles ejected droplets consistently, maintaining uniform droplet size and velocity across the array. These results demonstrate that the 512Nz printhead can achieve high-throughput printing while preserving droplet uniformity for viscosity-controlled solvents.

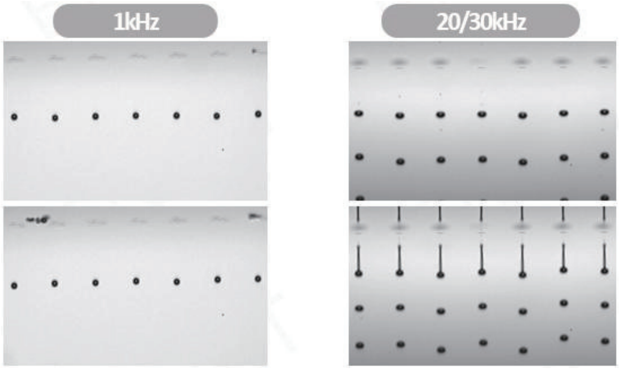

Figure 7. *512Nz printhead droplet ejection at 20 kHz and 30 kHz*

	Volume[pl]	Speed[m/s]
Average	10.72	2.89
Standard Deviation	0.63	0.27

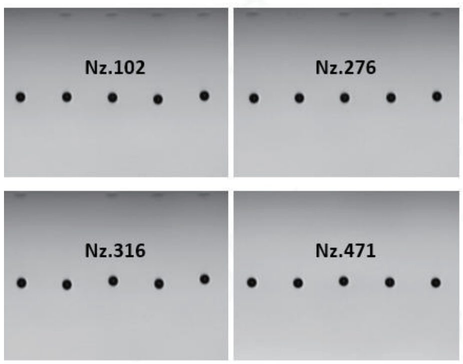

Figure 8. *Droplet velocity uniformity of the 512Nz printhead*

Conclusion

In this study, we successfully developed and evaluated a multi-nozzle hybrid inkjet printhead, the EHDison-H16, capable of jetting a wide range of ink viscosities from 4 cP to 200 cP. The hybrid actuation strategy, combining piezoelectric pressure actuation with electrohydrodynamic assistance, enabled stable droplet formation across all tested viscosities. Comprehensive jetting and printing experiments demonstrated that the printhead can reliably handle viscosity-controlled functional inks. Continuous droplet ejection tests confirmed long-term nozzle reliability, and practical printing experiments on substrates such as PCB, PET, and glass verified precise droplet placement and high-quality pattern formation.

These results highlight the versatility and robustness of the EHDison-H16 hybrid printhead in addressing the limitations of conventional piezoelectric and EHD-only systems. Moreover, the platform shows potential for scalability and high-speed operation with larger multi-nozzle arrays, such as the 512Nz printhead, which is currently undergoing long-term reliability evaluation.

Overall, the EHDison-H16 platform provides a scalable and industrially applicable solution for next-generation digital printing technologies, bridging the gap between laboratory research and practical manufacturing environments.

Acknowledgments

This study was supported by the Industrial Strategic Technology Development Program funded by the Ministry of Trade, Industry and Energy, South Korea (Grant 20026376: Development of an Electrohydrodynamic 128-Nozzle Printhead for 100-Femtoliter Droplet Generation and High-Viscosity Inks over 500 cP)

References

[1] J. Perelaer, “One-step inkjet printing of conductive silver tracks on polymer substrates” Adv. Mater., 2009.

[2] SD Hoath, “Fundamentals of inkjet printing: the science of inkjet and droplets” Fundamentals of inkjet printing., 2016.

[3] EB Secor, “Principles of aerosol jet printing” Flex. Print. Electron., 2018.

[4] B Derby, “Inkejt printing of Functional and Structural Materials: Fluid Property Requirements, Feature Stability, and Resolution” Annu. Rev. Mater. Res., 2010.

[5] S Magdassi, “The chemistry of inkjet inks” The chemistry of inkjet inks., 2010.

[6] J Park, “Flexible Transparent Conductive Films with High Performance and Reliability Using Hybrid Structures of Continuous Metal Nanofiber Networks for Flexible Optoelectronics” ACS Appl. Mater. Interfaces., 2016.

[7] JS Park, “Improvements in the device characteristics of amorphous indium gallium zinc oxide thin-film transistors by Ar plasma treatment” Appl. Phys. Lett., 2007.

[8] E Kang, “Digitally tunable physicochemical coding of material composition and topography in continuous microfibers” nature materials., 2011.

[9] JM Li, “Fabrication of 1D nanochannels on thermoplastic substrates using microchannel compression” Microsystem Technologies., 2013.

[10] OA Basaran, “Nonstandard Inkjets” Annual review of fluid mechanics., 2013.

[11] EB Secor, “Principles of aerosol jet printing” Flex. Print. Electron., 2018.

Author Biography

Jaeyong Choi received his BS in electronic and electrical engineering from the Sungkyunkwan University (2006) and his PhD in electronic, electrical and computer engineering from Sungkyunkwan University (2018). Since then, he has worked in Research and Technology Division at ENJET in Suwon, Republic of Korea. His work has focused on the development of EHD inkjet head and system.

Hyungdong Lee received his BS in mechanical engineering from the Sungkyunkwan University (2013) and his PhD in mechanical engineering from Sungkyunkwan University (2018). Since then, he has worked in Research and Technology Division at ENJET in Suwon, Republic of Korea. His work has focused on the development of EHD inkjet head and system.

Text-to-Image Generation AI Tools for 2.5D Prints: Preliminary Observations

Altynay Kadyrova [1] *and Marius Pedersen* [2]
[1] **Department of Computer Science, KIMEP University, Almaty, Kazakhstan**
[2] **Department of Computer Science, Norwegian University of Science and Technology, Gjøvik, Norway**

Abstract

Artificial Intelligence (AI) is being incorporated into almost every field as it can make procedures efficient. The printing industry for material appearance reproduction might sometimes require considerable time to fabricate final products. One of the technologies for realistic and natural-looking material reproduction is called 2.5D printing. To reduce intermediate printing stages, thereby making them more eco-friendly, time-efficient, and cost-efficient, well-known AI tools can be explored in the 2.5D printing field. In this way, customers can be presented with the digital versions of their 2.5D prints before proceeding to the (final) printing. To our knowledge, this is the first study that explores the potential of AI tools with regard to 2.5D prints. We test some of the well-known commercial text-to-image generation AI tools. The study is preliminary in order to obtain some initial observations on potential of AI tools to be able to generate realistic and natural-looking 2.5D prints.

Introduction

2.5D printing is an innovative technique that bridges the gap between traditional 2D printing and full 3D printing. Unlike standard 2D printing, which applies ink or toner in a single flat layer, 2.5D printing adds depth and texture to the printed surface, creating a relief-like effect. This is achieved by layering materials in a controlled manner to produce raised surfaces, giving the illusion of three-dimensionality. This technology is widely used in industries such as packaging, interior design, art reproduction, and electronics, where tactile and visual enhancements are valuable. For example, 2.5D printing can replicate the texture of oil paintings, simulate wood grain or embossed surfaces.

2.5D printing is demanded for material reproduction. However, digitization is not a straightforward process. Because of extra dimension (i.e., elevation), 2.5D prints' appearance might significantly vary from angle to angle. In general, there are various attributes that can be difficult to reproduce in the printing process. Therefore, it is desirable to have template sample prints to show to customers to make a decision about their choice on the prints' features. As a result, we propose to use current state-of-the-art Artificial Intelligence (AI) image generation models in 2.5D printing to visualize the prints before the final production stage.

There are a variety of commercial AI tools available which are based on or integrated with different AI models (e.g., diffusion models, Imagen). They can generate images through text prompts or reference images and videos. We dedicate this study to considering text-to-image generation models because 2.5D reference images for a diverse content might not be available. As a result, it is convenient to obtain 2.5D images from generative models based on text prompts. We test some of the current well-known AI tools and then assess the visual quality and naturalness of the generated 2.5D print images to gather relevant observations.

Related Works

The prompts can be considered as instructions from the users so that the models can generate diverse and unique outputs [1]. The simplest approach is to formulate them manually [2]. Generating images based on text prompts can become the result of a series of trial and error attempts [3] and it can be challenging for users [4]. Although models can work with complex prompts, understanding the logic of models' responses is still an unexplored area [2].

The prompts need to follow a certain format, for example, using prompt modifiers (i.e., keywords, key phrases) for efficiency purposes [5]. Oppenlaender [5] proposed a taxonomy of prompt modifiers that was based on an ethnographic study. Wang et al. [4] found that shorter prompts of around 6 to 12 tokens are the most demanded. However, some prompts might work well in one model, but might not generate similar quality images when the same prompt is applied to other models.

There exist many text-to-image generation models. Some of the well-known ones are DALL-E [6], latent diffusion model [7], and DM-GAN [8], to name a few. It is worth to mention that images with high aesthetic quality can be acquired by text-to-image generation models [9].

Ramesh et al. [6] explored a simple approach for text-to-image generation (DALL-E) based on an autoregressive transformer. They trained a 12-billion parameter autoregressive transformer on a 250 million image-text pairs. The Contrastive Language-Image Pre-training (CLIP) is a scalable method introduced by OpenAI for learning from natural language supervision [10]. During pre-training, CLIP learns to do a wide range of tasks (e.g., geo-localization, action recognition) and it can surpass ImageNet model. The pretrained contrastive model was used to rerank the samples from the transformer. They found that the scale can improve the generalization.

Generative Adversarial Networks (GANs) are widely used to synthesize photo-realistic images based on text prompts. Dynamic Memory GAN (DM-GAN) incorporates dynamic memory module to deal with quality of initial images generated and memory writing gate that dynamically selects relevant words for the generated image [8].

The first large-scale text-to-image prompt dataset was created by Wang et al. [4] that contains 14 million images synthesized via Stable Diffusion and 1.8 million unique prompts defined by real users. They created an interactive contour plot of their 1.8

million prompts' CLIP embeddings that shows popular topics of prompts. Based on their plot, it seems that prompts with 2.5D prints either do not present or they were not among the popular ones. In this light, we can assume that models of text-to-image generation tools might not be trained with 2.5D content.

Methodology

Our main research question was whether AI tools generate realistic 2.5D print images. In addition, we were interested in seeing if they generate images that match the given prompt text fully or if they can skip some of its parts. Consequently, another research question was about whether it is preferable to input longer or shorter prompts into AI tools with regard to reproducing natural-looking 2.5D prints.

Experiment 1

In Experiment 1, we were first interested in checking which AI tools can generate 2.5D prints that look realistic enough, especially in terms of elevation naturalness because elevation (i.e., height) is one of the most used distinct attributes in quality assessment of 2.5D prints [11]. Moreover, it plays a significant role in naturalness perception of 2.5D prints [12] and it is one of the perceptual attributes linked to the naturalness of 2.5D prints [13]. Additionally, elevation also affects the naturalness perception of 3D prints [14].

The prompts were formulated in a way to highlight different application areas of 2.5D printing, attributes (e.g., gloss, color), and lighting conditions. After an extensive trial-and-error process on the prompt texts, we came up with the following prompts for the tested tools:

Prompt 1: ”Generate a natural-looking 2.5D print tile depicting a text 2.5D in gold yellow, where 2.5D is slightly raised from the surface on a dark-brown wood background and with a matte finish captured from an oblique side angle, approximately 30 to 45 degrees above the horizontal plane. Lighting is natural.”

Prompt 2: ”Generate a natural-looking 2.5D print tile depicting a chamomile, where its petals are slightly raised from the surface on a turquoise background and with a bit glossy finish captured from an oblique side angle, approximately 30 to 45 degrees above the horizontal plane. Lighting is natural.”

Prompt 3: ”Generate a natural-looking 2.5D print tile depicting a spring tree. Slightly elevate leaves from the surface that should give a realistic appearance. Add a smooth texture to the print. The print is captured from an oblique side angle, approximately 30 to 45 degrees above the horizontal plane. Lighting is natural.”

Prompt 4: ”Generate a natural-looking 2.5D print tile depicting a part of purple decor wall with a rough texture that is slightly raised from the surface. The print is captured from an oblique side angle, approximately 30 to 45 degrees above the horizontal plane. Lighting is natural.”

The following commercial AI tools were tested due to their popularity (Table 1). Default settings were used in the tested tools. In Table 1, we provided model names that the tools use for text-to-image generation. It should be noted that the tested tools can be divided into groups based on their functionalities such as purely AI tools (Gemini, ChatGPT), platforms integrated with AI tools (Envato, Pixlr), and both AI tools and platforms (DreamStudio, OpenArt, Ideogram). We used the term AI tools for all of them hereafter in the article.

The height map generation ability of AI tools (ChatGPT, Gemini, Ideogram) was also considered and ChatGPT seems to be able to do it whereas Gemini seems to be unable to generate it. Ideogram seems to be able to generate it but does not follow the instructions properly in the prompt. We used the free version of all tools in this study and this might be a limitation that the full capacity of the tested tools was not used. Therefore, the height map generation part can be explored in the future work.

Table 1: AI tools tested and their model information.

AI Tools	Models
Gemini by Google [15]	Imagen 4
Envato [16]	ImageGen but doesn't publicly state which models are used for ImageGen
Dream Studio by Stability AI [17]	Stable Diffusion family of models
Ideogram [18]	Ideogram 3.0
ChatGPT by OpenAI [19]	DALL-E 3 (DALL-E integrated with GPT-4o)
Pixlr [20]	doesn't publicly state
OpenArt [21]	Flux Kontext

Experiment 2

Based on the results of Experiment 1, we selected Imagen-based model (Gemini) and DALL-E integrated with GPT-4o (ChatGPT) that showed good results to further explore the effect of the detail level in the prompts. The reason for this is our assumption that different levels of detail in the prompt might generate better results. Ideogram was not included as it was inconvenient to work with it in a free version.

Liu and Chilton [3] tested their hypothesis on the permutations of words of prompts. Their research question was whether different re-phrasings of a prompt using the same keywords will provide considerably different generations. They found that there were no statistically significant differences in the quality of the generation between their tested permutations. Based on this, they proposed a guideline that suggests focusing on subject and style keywords rather than connecting words (i.e., punctuation, function words, words for ordering). As a result, we do not consider a case with re-phrasings of the same prompt in different combinations.

From Experiment 1, we observed that tools can add some creativity to open-ended prompts (such as the leaves of a spring tree). As a result, we focus on specific prompts due to the nature of our application (2.5D prints). Despite testing prompts with more tokens (words), we still use simple sentences rather than complex ones to reduce over-complicated prompts.

We did not provide contextual information explaining what is 2.5D print or 2.5D printing in Experiment 1 because we assumed that the tools might have that information and/or they can build an understanding what is 2.5D print based on the descriptions we provided in the prompts (e.g., petals are slightly raised from the surface, slightly elevate leaves from the surface). In Experiment 2, we would like to add clarity on this and, therefore, we test cases with and without providing a well-defined context. This can help to minimize misinterpretation of prompts by the tools.

As a result, we tested the following prompt combinations in terms of context and the number of tokens and images were generated in this order: no context and fewer tokens (further case A), context and fewer tokens (further case B), no context and more tokens (further case C), context and more tokens (further case D).

Similarly to Experiment 1, the prompts were designed manually and the final versions were acquired based on trial and error. In total, we had 6 prompts $\times$ 4 cases $\times$ 2 tools that gives 48 images. One of the prompts for case D is as follows: *2.5D printing adds height to a 2D print and it becomes a 2.5D print. Generate a realistic 2.5D print tile showing a yellow-red autumn palmate compound leaf where the leaflets are slightly raised from the surface with sharp edges. Petiole is located at the bottom. The background is a light brown earthy color. Remove shadows, increase contrast locally, and add texture. Capture from an oblique side angle, approximately 30 to 45 degrees above the horizontal plane to see the surface with tactile elements. The base print is still flat with specific elements raised from the surface.* The first sentence is a contextual information. In cases A and C, we removed the first sentence only. The part highlighted in blue shows how we designed prompts for cases A and B with fewer tokens. Table 2 shows the minimum and maximum number of words in 4 cases for 6 prompts. The main topics for our prompts were about a yellow-red autumn palmate compound leaf, a blue road sign for compulsory right turn, a green braille tactile sign, an impasto style painting of cyan-colored lake surrounded by sky and clouds, reddish-grey cobblestones with radial patterns, and a pink purple butterfly.

Table 2: The range of words in each case.

Prompts	Minimum	Maximum
Case A	11	19
Case B	25	33
Case C	70	82
Case D	84	96

We did not consider 3D object quality metrics as they might not fully assess all features of objects [22]. 2D image quality metrics were tested as they can assess 2.5D prints under limited conditions [23]. And we applied Naturalness Image Quality Evaluator (NIQE) [24], Joint Objective Image Naturalness evaluaTor (JOINT) [25], and Perceptual Sharpness Index (PSI) [26] to the 2D images with 2.5D content.

Results and Discussion

In this section, we present the results for both experiments.

Experiment 1 results

Based on the generated images obtained (Figures 1, 2, 3, 4), it is visible that the Imagen-based model (Gemini) and DALL-E integrated with GPT-4o (ChatGPT) provided better results in terms of the naturalness and realism aspects of 2.5D prints upon visual examination. Although some blurriness is present for some prompts, it is also present in the generated images by other tools (e.g., Dream Studio, Envato, Ideogram). These two models also showed one of the challenges of 2.5D printing, which relates to the color of the elevation and the edge color of the objects. Naturally, elevated height should have the color of the object but the background color can be used for the height during height map processing of 2.5D prints. One of the methods that can solve this is to perform morphological operations on grey-scale height map images of the prints [27].

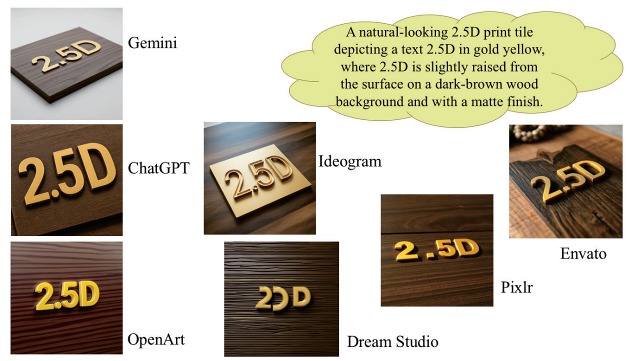

Figure 1. Generated images by different AI tools [15, 16, 17, 18, 19, 20, 21] based on given prompt about text 2.5D in gold yellow. The prompt in the Figure was shortened for illustration purposes. The full text can be found in the Methodology section.

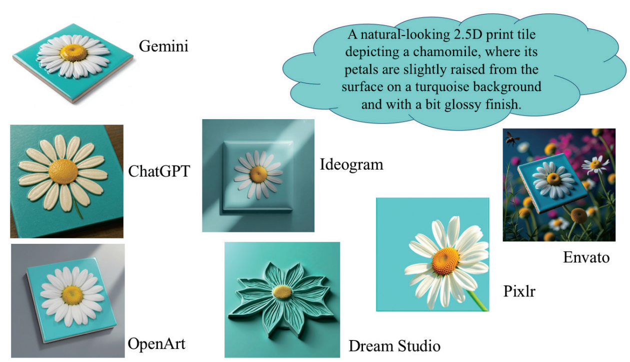

Figure 2. Generated images by different AI tools [15, 16, 17, 18, 19, 20, 21] based on given prompt about a chamomile. The prompt in the Figure was shortened for illustration purposes. The full text can be found in the Methodology section.

Ideogram also generated realistic enough 2.5D prints, though for prompt 2, the elevated parts (petals) are invisible at the angle it captured the image. Ideogram 3.0 is the latest model that is known for its stunning photorealism and text rendering quality with consideration of precise lighting and colors [28]. Among all the tested tools, Ideogram's generated images seem to have natural lighting that was requested in the prompts.

OpenArt's Flux Kontext model can generate realistic-looking 2.5D print (e.g., prompt 1). However, it can occasionally follow instructions incorrectly without taking notice of the prompt

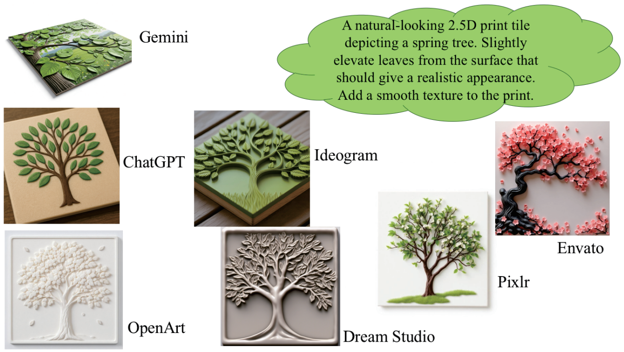

Figure 3. *Generated images by different AI tools [15, 16, 17, 18, 19, 20, 21] based on given prompt about a spring tree. The prompt in the Figure was shortened for illustration purposes. The full text can be found in the Methodology section.*

details [29]. The examples can be disregarding capture angle request (prompts 3 and 4) and the elevated features of 2.5D prints (prompts 2 and 4). In addition, the generated image for prompt 3 is too white for a spring tree.

The lower performance in terms of realistic appearance for 2.5D prints was shown by a stable diffusion model (Dream Studio) and models of Envato and Pixlr for some of the prompts. For example, DreamStudio was unable to properly generate prompt 1 about 2.5D text in gold yellow as well as prompt 3. Peong et al. [30] reported that generative models based on diffusion models might be insufficient when it comes to synthesizing typographic texts. It was also mentioned by Ramesh et al. [31] that their model (which is based on diffusion models) seems to struggle to generate coherent text. Both Envato and Pixlr generated less realistic looking 2.5D prints for prompts 2 and 3.

Figure 4. *Generated images by different AI tools [15, 16, 17, 18, 19, 20, 21] based on given prompt about a purple decor wall part. The prompt in the Figure was shortened for illustration purposes. The full text can be found in the Methodology section.*

Figure 5 presents the performance of the AI tools with regard to the naturalness of elevation in the generated 2.5D print images. In other words, we visually assessed whether the generated images of 2.5D prints look realistically. ChatGPT, Gemini, and Ideogram generated more images with natural elevation. In this assessment, the quality of match between the prompts' texts and the details in the generated images was not considered.

Overall, we can say that all the tools performed well in terms

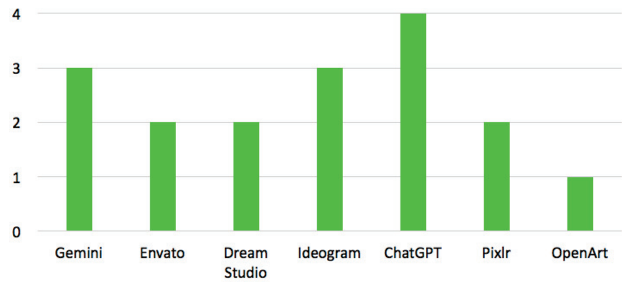

Figure 5. *AI tools' performance in terms of elevation naturalness of 2.5D prints in the generated images. The visual subjective assessment was done by the authors. Y-axis here represents just a number of prompts, not their order.*

of degree of matching between prompts' texts and details in the generated images, though there exist some mismatches by the tools in one or more prompts. For instance, when a bit glossy finish was requested, generated images were too glossy or with matte finish, or no gloss at all. Similarly, when a matte finish was requested, some gloss was present in the images. Also, some generated images looked like 2D or 3D instead of 2.5D. This could be due to the angle at which the images were captured, although the prompt was designed in a way that tools should capture them at a angle where the elevation of 2.5D prints could be visible and perceivable. Because of it, perhaps, it seemed that there was a space not filled with a color between the elevated part and the background in prompt 2 by Envato, Idegoram, and OpenArt, and in prompt 3 by Gemini.

Some tools' models seemed to add extra creativity such as in prompt 1 by Ideogram, in prompt 2 by Dream Studio, adding an extra object (e.g., in prompt 1 by Envato) or enclose print with background into another colorful background (e.g., prompt 2 by Envato), or adding shades of a requested color (in prompt 4 by Envato). Some tools generated spring tree differently (pink leaves by Envato, grey by Dream Studio, white by OpenArt). This indicates that the prompts should be very precise for accurate reproductions.

As a result, we further tested some of the tools for detail level in prompts and how it affects the generation of 2.5D print images from the naturalness aspect.

Experiment 2 results

The Type-Token Ratio (TTR) was used to check if the prompts contain fewer repetition of words (tokens) and thus more diversity. The higher the value, the more unique words the prompt contains. The calculated TTR values [1] are given in Table 3. We can see that our prompts are very diverse in case A followed by cases B and C, whereas case D has fewer unique words because it contains contextual information and more details, and it is possible that some words are repetitive.

Text-image similarity was assessed using the CLIP score (model: OpenAI's ViT-B/32 Transformer [2]) for cases A and B because the length of our prompts for cases C and D was too long for the model's text sequence length. The CLIP score was acquired for each prompt between their case texts and the generated

[1] https://pypi.org/project/lexical-diversity/
[2] https://huggingface.co/openai/clip-vit-base-patch32

Table 3: The TTR values in each case for 6 prompts.

	Case A	Case B	Case C	Case D
Prompt 1	0.92	0.70	0.72	0.66
Prompt 2	0.93	0.72	0.71	0.67
Prompt 3	0.92	0.69	0.71	0.65
Prompt 4	0.95	0.73	0.72	0.66
Prompt 5	1.0	0.73	0.73	0.66
Prompt 6	0.91	0.68	0.74	0.67

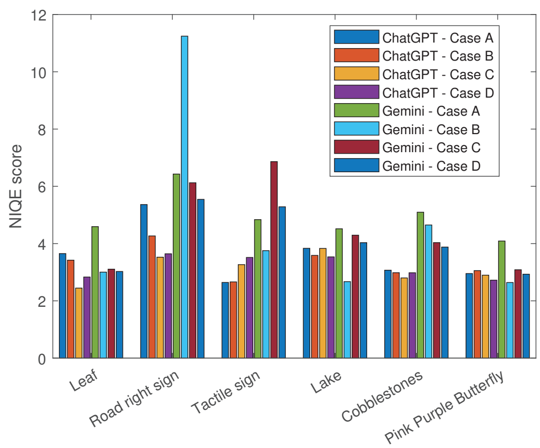

Figure 6. *NIQE scores, where lower score indicates higher perceived quality.*

images by two tools (Gemini, ChatGPT). Because we considered cases A and B, we can observe the effect of presence of contextual information when fewer tokens were used in the prompts. Both tools showed agreement that the generated image and its prompt have more similarity when there is no contextual information. The minimum and maximum differences in the CLIP score between cases A and B among all prompts were 0.1 and 7.7 by Gemini, accordingly. By ChatGPT, the minimum and maximum differences were 0.7 and 4.3, accordingly. Exception was one of the prompts (an impasto style painting of a lake) with a minor difference that contextual information presence gives more similarity than without it between text and generated image by Gemini.

To assess the results objectively, we applied our selected metrics to the generated images. Figure 6 shows the results of the NIQE. A lower score indicates higher perceptual quality. The presence of more tokens in the prompt (cases C, D) provided higher perceptional quality by ChatGPT in 4/6 generated images. For cases C and D, the PSI metric was applied to the generated images to assess sharpness because all prompts contained it. By comparing results of the PSI for cases C and D, ChatGPT generated images as instructed with sharp or smooth edges, unlike Gemini. Figure 7 shows the naturalness scores by the JOINT. In case D, ChatGPT generated more natural images than Gemini.

To sum up, we can observe that purely AI tools seem to perform better than platforms integrated with AI tools or combined ones in producing realistic-looking 2.5D print images. Each of the tool has its own strengths and weaknesses, and some are better in some specific application. Nevertheless, our insight was that Imagen and DALL-E integrated with GPT-4o models-based AI tools

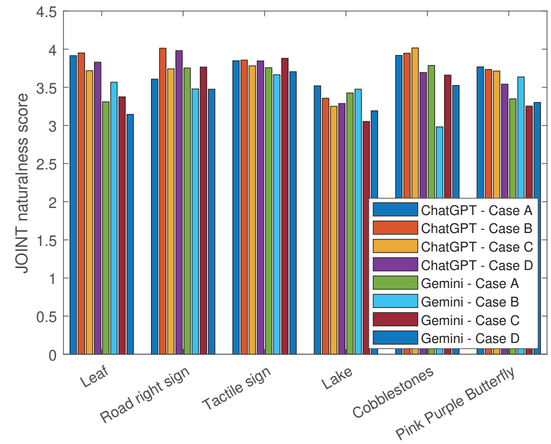

Figure 7. *JOINT naturalness scores, where higher score indicates more natural image.*

seem to show potential in generating natural-looking 2.5D print images that can highlight features (e.g., elevation, textures) of 2.5D prints and challenges (e.g., edge color) of 2.5D printing even though the insight was based on a limited number of prompts.

Conclusions

We explored some of the well-known AI tools for text-to-image generation. More specifically, we looked at how they perform in generating digital versions of 2.5D prints. Some preliminary observations were obtained.

First, AI models integrated into platforms seem to show a lower performance compared to those that are purely AI tools in generating 2.5D print images that look real to some extent. Second, AI tools seem to be unable to translate all text details in the prompts very accurately into the generated images. Some details might be just lost or the opposite ones might be displayed (e.g., matte to gloss finish). Third, precise texts for prompts should be used to avoid unnecessary details appearing in the generated images. Last but not least, ChatGPT showed promising results for realistic 2.5D print image generation when more tokens are used for a detailed prompt. Although the observations are derived from a small set of tested AI tools, they show their ability to generate and render 2.5D prints to some degree. These observations can be helpful when integrating AI tools in the 2.5D printing framework.

Prompts were designed manually, and automatic prompt generation can be used in the future to have more prompts and more images to detect statistical significant differences between effect of context and level of detail. Additionally, AI models and tools can be tested for text-to-video and image-to-image generation. And a psychophysical experiment with generated 2.5D print images can be conducted to check the compatibility of human perception with AI.

Acknowledgments

Marius Pedersen is supported by the Research Council of Norway through the “Quality and Content” project (grant number 324663).

References

[1] Khoi Trinh, Joseph Spracklen, Raveen Wijewickrama, Bimal Viswanath, Murtuza Jadliwala, and Anindya Maiti. Promptly yours? a human subject study on prompt inference in ai-generated art. *arXiv preprint arXiv:2410.08406*, 2024.

[2] Jiaqi Wang, Zhengliang Liu, Lin Zhao, Zihao Wu, Chong Ma, Sigang Yu, Haixing Dai, Qiushi Yang, Yiheng Liu, Songyao Zhang, et al. Review of large vision models and visual prompt engineering. *Meta-Radiology*, 1(3):100047, 2023.

[3] Vivian Liu and Lydia B Chilton. Design guidelines for prompt engineering text-to-image generative models. In *Proceedings of the 2022 CHI conference on human factors in computing systems*, pages 1–23, 2022.

[4] Zijie J Wang, Evan Montoya, David Munechika, Haoyang Yang, Benjamin Hoover, and Duen Horng Chau. Diffusiondb: A large-scale prompt gallery dataset for text-to-image generative models. *arXiv preprint arXiv:2210.14896*, 2022.

[5] Jonas Oppenlaender. A taxonomy of prompt modifiers for text-to-image generation. *Behaviour & Information Technology*, 43(15):3763–3776, 2024.

[6] Aditya Ramesh, Mikhail Pavlov, Gabriel Goh, Scott Gray, Chelsea Voss, Alec Radford, Mark Chen, and Ilya Sutskever. Zero-shot text-to-image generation. In *International conference on machine learning*, pages 8821–8831. Pmlr, 2021.

[7] Robin Rombach, Andreas Blattmann, Dominik Lorenz, Patrick Esser, and Björn Ommer. High-resolution image synthesis with latent diffusion models. In *Proceedings of the IEEE/CVF conference on computer vision and pattern recognition*, pages 10684–10695, 2022.

[8] Minfeng Zhu, Pingbo Pan, Wei Chen, and Yi Yang. Dm-gan: Dynamic memory generative adversarial networks for text-to-image synthesis. In *Proceedings of the IEEE/CVF conference on computer vision and pattern recognition*, pages 5802–5810, 2019.

[9] Jonas Oppenlaender. The creativity of text-to-image generation. In *Proceedings of the 25th international academic mindtrek conference*, pages 192–202, 2022.

[10] Alec Radford, Jong Wook Kim, Chris Hallacy, Aditya Ramesh, Gabriel Goh, Sandhini Agarwal, Girish Sastry, Amanda Askell, Pamela Mishkin, Jack Clark, et al. Learning transferable visual models from natural language supervision. In *International conference on machine learning*, pages 8748–8763. PmLR, 2021.

[11] Altynay Kadyrova, Vlado Kitanovski, and Marius Pedersen. A study on attributes for 2.5 d print quality assessment. In *Color and Imaging Conference*, volume 28, pages 19–24. Society for Imaging Science and Technology, 2020.

[12] Altynay Kadyrova, Marius Pedersen, and Stephen Westland. What elevation makes 2.5 d prints perceptually natural? *Materials*, 15(10):3573, 2022.

[13] Altynay Kadyrova, Marius Pedersen, and Stephen Westland. Effect of elevation and surface roughness on naturalness perception of 2.5 d decor prints. *Materials*, 15(9):3372, 2022.

[14] Raed Hlayhel, Simon Hviid Del Pin, Takahiko Horiuchi, Sony George, Jon Yngve Hardeberg, and Aditya Suneel Sole. Naturalness perception of 3d prints with highlighted features. *Journal of Perceptual Imaging*, 8:1–14, 2025.

[15] Google. Gemini. `https://gemini.google.com/`, 2025. Large multimodal model (Version 2.5 Flash).

[16] Envato. Envato ImageGen. `https://elements.envato.com/imagegen`, 2025. Image generation tool.

[17] Stability AI. DreamStudio. `https://dreamstudio.ai/`, 2025. Image generation tool (Stable Diffusion 3).

[18] Ideogram Inc. Ideogram. `https://ideogram.ai/`, 2025. Image generation tool (Ideogram 1.0).

[19] OpenAI. ChatGPT. `https://chat.openai.com/`, 2025. Large language model (GPT-4).

[20] Pixlr. Pixlr AI Image Generator. `https://pixlr.com/ai/ai-image-generator/`, 2025. Image generation tool.

[21] OpenArt. OpenArt. `https://openart.ai/`, 2025. Image generation tool.

[22] Markus Sebastian Bakken Storeide, Sony George, Aditya Suneel Sole, and Jon Yngve Hardeberg. 3d object quality metrics and their differences: How can we evaluate quality of digitization? In *Archiving Conference*, volume 21, pages 81–87. Society for Imaging Science and Technology, 2024.

[23] Altynay Kadyrova, Vlado Kitanovski, and Marius Pedersen. Quality assessment of 2.5 d prints using 2d image quality metrics. *Applied Sciences*, 11(16):7470, 2021.

[24] Anish Mittal, Rajiv Soundararajan, and Alan C Bovik. Making a “completely blind” image quality analyzer. *IEEE Signal processing letters*, 20(3):209–212, 2012.

[25] Zijian Chen, Wei Sun, Haoning Wu, Zicheng Zhang, Jun Jia, Ru Huang, Xiongkuo Min, Guangtao Zhai, and Wenjun Zhang. Study of subjective and objective naturalness assessment of ai-generated images. *IEEE Transactions on Circuits and Systems for Video Technology*, 35(4):3573–3588, 2025.

[26] Christoph Feichtenhofer, Hannes Fassold, and Peter Schallauer. A perceptual image sharpness metric based on local edge gradient analysis. *IEEE Signal Processing Letters*, 20(4):379–382, 2013.

[27] Altynay Kadyrova. *Quality Assessment of 2.5 D Prints*. Doctoral theses at ntnu; 2023:16, Norwegian University of Science and Technology (NTNU), Trondheim, Norway, 2023. PhD thesis.

[28] Ideogram. Ideogram 3.0. `https://about.ideogram.ai/3.0`, March 2025. Accessed: 2025-08-10.

[29] Black Forest Labs, Stephen Batifol, Andreas Blattmann, Frederic Boesel, Saksham Consul, Cyril Diagne, Tim Dockhorn, Jack English, Zion English, Patrick Esser, et al. Flux. 1 kontext: Flow matching for in-context image generation and editing in latent space. *arXiv preprint arXiv:2506.15742*, 2025.

[30] KhayTze Peong, Seiichi Uchida, and Daichi Haraguchi. Typographic text generation with off-the-shelf diffusion model. In *International Conference on Document Analysis and Recognition*, pages 52–69. Springer, 2024.

[31] Aditya Ramesh, Prafulla Dhariwal, Alex Nichol, Casey Chu, and Mark Chen. Hierarchical text-conditional image generation with clip latents. *arXiv preprint arXiv:2204.06125*, 1(2):3, 2022.

The role of nozzle acoustic sensing in inkjet printing, an Artificial Intelligence perspective

Fernando Rodriguez Llorente. iPrint, HEIA-FR, HES-SO University of Applied Sciences and Arts Western Switzerland, CH-1700 Fribourg, Switzerland.

Abstract

The idea of using the piezoelectric element of an inkjet printhead as an acoustic sensor for inferring the status of the jetting nozzles is almost as old as inkjet itself. While piezoelectric inkjet printing devices have evolved considerably since the early days of inkjet printing, enabling the continuous development of novel inks, functional fluids, substrates, pre- and post- printing treatments, and facilitating the adoption of new material deposition processes across many industries, nozzle acoustic sensing has seen minimal adoption by the industry. With a few notable exceptions, the inkjet community has been reticent to adopt this aspect of the inkjet technology. The main reasons argued for not embracing this technology are its perceived inability to identify subtle failure modes (deviated nozzles) and the difficulties of machine operators to interpret and react to this novel type of information. In this paper we will argue that developments in Artificial Intelligence can help overcome these limitations. Agentic AI and Reinforcement Learning provide a conceptual framework and a technology capable of improving nozzle failure classifiers and defining and evaluating multiple automatic responses of the printing system to changing printing conditions, enabling a quasi-real-time optimization of the printing process.

Introduction

Inkjet drop jetting is a complex physical process which requires the correct nozzle geometry, an acoustic pressure actuation tuned to the resonant chamber geometry, a fluid with acoustic and rheological properties compatible with the microfluidic design of the printhead and the pressure actuator, a fluid delivery system capable of maintaining the correct flow through printhead and nozzle microchannel, and a pressure regulator to keep the correct meniscus pressure at the nozzle to avoid nozzle plate flooding or air ingress. The jetting and drop formation processes are non-linear processes, as non-linearity is needed to detach the jetted fluid from the main body of fluid in the printhead.

Given all the factors that affect the inkjet drop formation process, and given that the process is highly non-linear, it is somewhat remarkable that the process is highly repeatable over a small, but usable, parameter window. Once the key jetting parameters for an ink-printhead combination have been established, it is possible in many cases to maintain stable and repeatable jetting performance across tens of thousands of nozzles in multiple printheads of the same manufacturer model.

Although the process is highly repeatable, it is prone to problems. Maintaining all the process parameters within the correct operating window can be challenging for more complex inks. Long term jetting performance can be compromised by different physical mechanisms intrinsic to the jetting and drop formation process.

Small air bubbles can appear in the nozzle due to air ingress at the end of the jetting process or by low pressure flow regions causing bubble nucleation in the nozzle microchannel during the jetting process fluid motion (Figure 1).

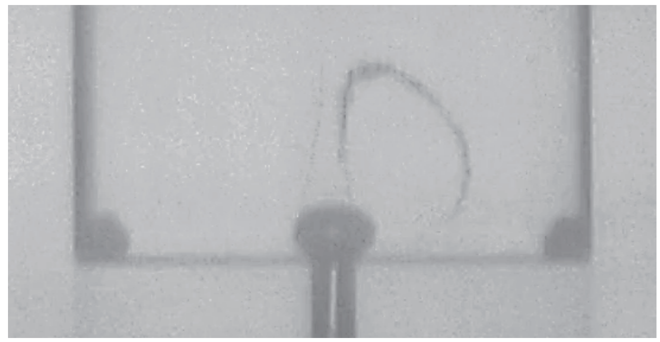

Figure 1. Air bubble formation by cavitation inside a glass nozzle. Air bubbles follow internal flow lines and aggregate into a bigger bubble on the nozzle corners (flow stagnation points).

Small femtolitre drops can be created at the end of the jetting process where the jet ligament detaches from the meniscus or when long jet ligament breaks into smaller satellite drops under the effect Rayleigh-Plateau instability. Because of their small size, the sub-picolitre drops are dominated by Stokes drag and Brownian motion, causing the sub-picolitre drops to lose their speed very rapidly and to move randomly close to the nozzle plate. As the gravitational force experience by such a small drop is weaker than the average force the experience though collisions with air molecules, many of the femtolitre drops make their way back to the nozzle plate. Over time, these drops will coalesce and create small, flooded regions in the nozzle plate. When these regions are close to a nozzle, they eventually cover the nozzle and interfere with the jetting process, causing nozzle malfunction (Figure 2).

Other external factors can affect the jetting process. Particles in the nozzle, whether carried by the ink, created by ink particle aggregation over time, or existing particles in the substrate and air between the printhead and the substrate, can partially or completely block a nozzle. Partial polymerization of UV inks on the nozzle and solid residues left in nozzle by water or solvent ink evaporation at idle printing time can also partially or completely block a nozzle. In either case, this will lead to nozzle malfunction in the form of a deviated or a non-jetting nozzle.

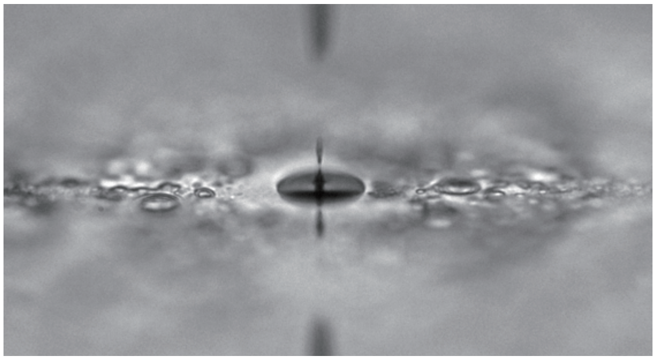

Figure 2. Drop coalescence on a nozzle plate with a degraded coating.

Three different approaches can be used to try to characterize most of the above problems with nozzle jetting: nozzle pattern print analysis, drop watcher imaging and acoustic nozzle sensing. In this paper we will address how to use acoustic nozzle sensing information to control the printing process with the objective of minimizing printing production downtime while maintaining printing image quality using Reinforcement Learning as the main systems modeling and control framework.

Nozzle acoustic sensing

The capability of a piezoelectric crystal to convert electrical energy into mechanical energy is the underlying principle of piezo-based inkjet technology. The piezo actuator creates a pressure pulse that acts onto the ink and forces the ink to be jet out of the nozzle to form a drop while it is flying towards a substrate. This physical process is reversible, enabling the measurement of pressure from acoustic waves within the inkjet nozzle as they act on the piezo.

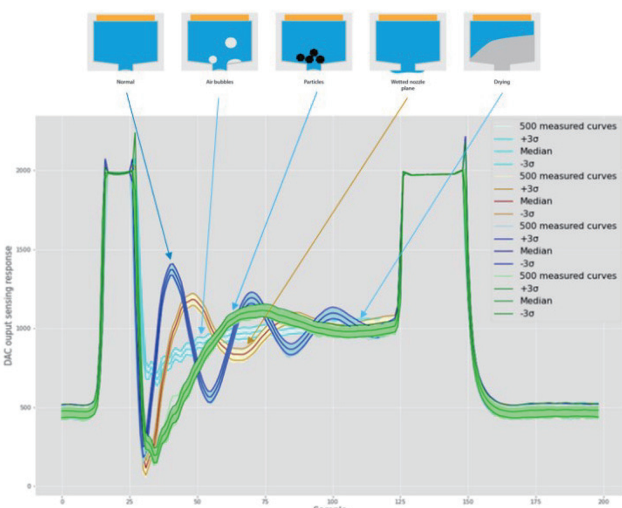

Figure 3. Acoustic sensing signals of different nozzle malfunctions: normal jetting, air bubbles, particles in nozzle, nozzle flooding and nozzle air ingress.

These pressure waves not only respond to the actuation process but also reflect the conditions of the fluid, the nozzle and nozzle microchannel (Figure 3). Consequently, they offer valuable means to detect various issues and assess the properties of the fluidic system.

The piezoelectric effect couples the electrical and mechanical part of the printhead due to its reversibility. The electrical side involves notably the output impedance of the printing waveform amplifier, cable and ASIC parasitics, and the capacitance of the piezo actuator. The mechanical part encompasses the properties of the actuator, the vibrating diaphragm, and the response of the fluidic system.

Overview of Reinforcement Learning

Reinforcement Learning is a subset of Machine Learning and Artificial Intelligence that addresses the problem of achieving a goal in an uncertain environment. RL is a form of algorithmic learning by interaction with the environment, with an explicit objective of achieving a goal. It is different from Supervised Learning, where pairs of system inputs and outputs are used to train a learning agent, and it is also different from Unsupervised Learning, where algorithms learn patterns using only unlabeled data as inputs.

While the better-known applications of Supervised and Unsupervised Learning are in the field of data classification, Reinforcement Learning (RL) is concerned with the continuous interaction between a system and its environment. RL makes a clear distinction between the actions taken by the system, the objectives the system wants to achieve and the response of the environment to actions taken by the system. In this sense, RL is closely related to optimal control, stochastic control, classical optimization and dynamic programming. The algorithms used in RL require an iterative exploration of the interactions between a system and its environment, where sequences of actions and responses are analyzed at each step and the knowledge gained from the interaction is used to determine the next action of the system to bring it closer to achieving its objective. This approach makes RL a natural framework for the study of optimal sequential decision making, a problem commonly encountered in the engineering of systems where complex interactions between machinery and physical process take place.

RL system view

RL can be described as a system consisting of an agent and an environment over which the agent acts (Figure 4). Tipically, the agent is implemented as a software application and the environment includes all the SW & HW of the system, and the actual environment with which the system interacts. The state of the environment is determined by some means (like a set of sensors) and this information is used by an agent to produce and action over the environment, which will change it. This change in the environment will bring the system closer or further away from the overall objective of the system behavior, increasing or decreasing the reward the agent gets for its actions. The function used to map the state of the system into an action is called a policy. A policy does not need to be a deterministic function or be known at the beginning of the learning process. In fact, finding a suitable policy for a system to be able to achieve its objective can be the main goal of a RL system.

A RL system works on the balance of exploration and exploitation strategies. Exploration is used understand the system, build models, determine policies, etc. The exploitation phase uses this knowledge to run the system as optimally as possible.

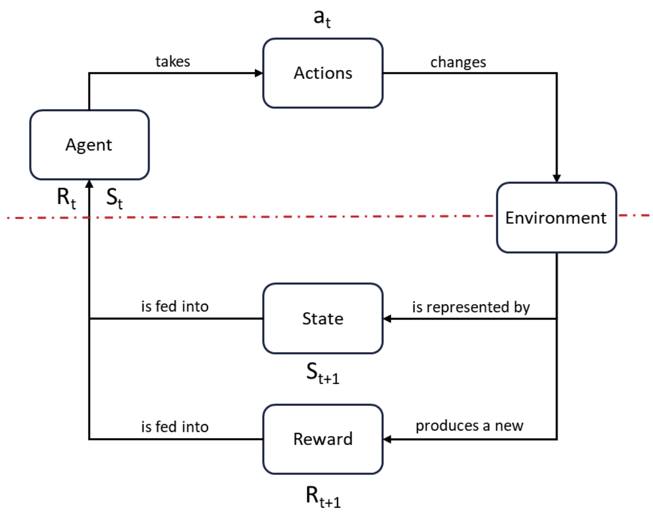

Figure 4. Block diagram of a Reinforcement Learning system.

A key element in the implementation of an RL system is the closeness of the agent's internal state representation of the environment, and the environment itself. When the environment is a control system with known dynamic model, RL optimization is very close to optimal control theory and stochastic control. When the environment is a system that can be described by a State Machine with known transitions between states, where the current state fully describes the system (a Markov process), RL can use optimization results from Dynamic Programing (the RL problem can be mapped to a known Markov Decision Process MDP where an optimal policy for achieving the objective can be found).

The above approach works well for systems which can be described as an MDP with fully observable states and computably manageable size for the combinatorial space of all possible states and actions the system can take. As we will see in the next section, this is not the case for an inkjet printing system subject to nozzle malfunction.

Limitations to nozzle state determination

The state of an inkjet nozzle cannot be easily mapped into a Markov process. The underlying physical processes that control the behavior of the nozzle during jetting process involve the interplay of fluids dynamics, acoustic wave propagation and electro-acoustic interaction between the piezo element and the fluid to be jetted. The physics of this process is notoriously difficult to model, especially when the causes of nozzle malfunction, e.g. partial nozzle blockage, break the cylindrical geometry assumed by many of the numerical simulation schemes that have been used to simulate the jetting process.

A second limitation comes from the difficulties encountered in sensing the state of the nozzle. The amount of physical information that is required to determine the time evolution of the jetting process, that is the initial conditions and boundary conditions needed to simulate the physical process, is simply impossible to acquire via sensor sampling in a real inkjet device. A different approach is needed.

One such a possible alternative approach is to use World Models, an approach which is currently being considered as a way to simplify the internal state representation of the RL agent. The idea behind this approach is to mimic the way humans are able to make successful interventions in industrial systems, or in other complex systems too, with a simplified understanding of the system states. Humans interact with the environment with simplified WM in their heads, where details of the environment state are simplified and abstracted to produce a simplified but very effective representation of the environment they are working on. Following this analogy, the exploration phase of RL could be equated to human learning, with the exploitation phase of RL could be equated to human expert control based on learned experience.

From an inkjet printing perspective two possible approaches to produce a WM of the printhead seem natural, one based on a description of the nozzle state based on a physical change in the nozzle (for instance blocked or not blocked), the other based on the effect of the nozzle state on the printed image (high quality images vs. low quality images with defects). For the first approach the acoustic sensing signal could be used, for the second one an image acquisition camera and image quality measuring software could be added to the system.

A framework for integrating nozzle sensing technology and Reinforcement Learning

In a typical inkjet printing system nozzle malfunction can go undetected for a very long time as most systems have limited access to the state of the jetting nozzles, even when camera-based inspection systems are used. Many camera-based systems do not have sufficient optical resolution to identify individual nozzle failures, or have the system intelligence needed to map printed dot errors into a specific malfunctioning nozzles in a printhead.

To help overcome this problem, iPrint has designed and developed an electronics system capable of measuring the acoustic nozzle signal during and after jetting. It has build a high resolution optical imaging system and developed a printing strategy that allow us to map printed dot errors to specific nozzles in the printhead. This system can be used to label the status of a nozzle based on its printed signature. The acoustic signals of a nozzle can then be labelled against the corresponding printed nozzle classification, a algorithmic process that allow us to label the acoustic signals against their jetting footprint.

Acoustic nozzle signals do not provide a perfect representation of the nozzle state. At best, we can use them to infer what is called in RL a *belief* of the underlying state of the nozzle. It is possible, at least in principle, to build an RL system where the status information is incomplete and is replaced by such a belief. As the state cannot be perfectly determined, it is necessary to move away from MDP based RL and to use an approach based on neural networks.

To complete the RL framework we need to add actions functions to specify the interaction with the inkjet printer environment and a reward function to quantify the impact of the actions on the environment relative of the RL objective. After putting these elements together, we can try to build a complete RL system, where we identify the different elements of the system defined as:

- **Agent**: printer controller.
- **Environment**: printer.
- **State**: (inferred from acoustic nozzle signal) straight-jetting, not-jetting, deviated jetting, intermittent jetting.
- **Action**: start-print, stop-print, continue-print, clean-nozzle, change-waveform, disable-nozzle, mask-nozzle-error, change-printhead.
- **Policy**: maps states into actions.

- **Reward**: time printing (+) vs. maintenance time (-).
- **Learning algorithm**: changes/adapts policies.

The reward function is designed to be compatible with the system objective: to maximize the amount of time the system is printing quality images. With this RL framework we can attempt to discover an optimal policy (policy-based learning algorithms) that maximizes the printing system reward to achieve our system design goal. The RL framework could also be used to infer a usable model of the environment (mostly the printhead nozzles) by combining policy-based and model-based learning algorithms. In this approach, neural networks (deep RL) are used to infer functions as there are no analytical results to help us build these functions (as is the case for MDP).

A potential mapping between nozzle states and printing output states is also interesting to find optimal printing strategies for systems where only images obtained with a camera are used to determine the state of the printer. Normally we would expect straight-jetting nozzles to produce high quality printing and malfunctioning nozzle to produce low quality printing. If the nozzle state is not a binary function, it might be possible to detect nozzle gradation before it has an image quality impact.

Building an environment for nozzle sensing and Reinforcement Learning integration

To help us collect all the data needed to train our deep RL neural networks, we are building an automated printing system with acoustic sensing technology and printed nozzle patter image acquisition and nozzle classifier. The printing system also incorporates a printhead cleaning station, and all actions in our RL framework can be performed automatically, apart from exchanging a printhead (Figure 5).

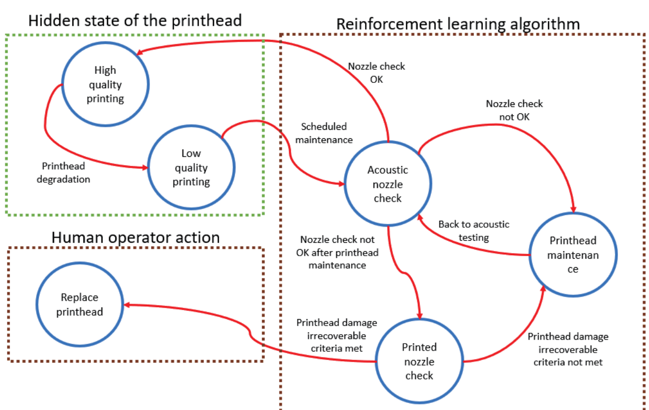

Figure 5. Reinforcement Learning based printing system controller.

As a comparison, we show in Figure 6 a conventional printing system the press operator takes action to improve image quality based on personal experience or pre-fixed maintenance schedules, and no real information regarding the hidden state of the printhead.

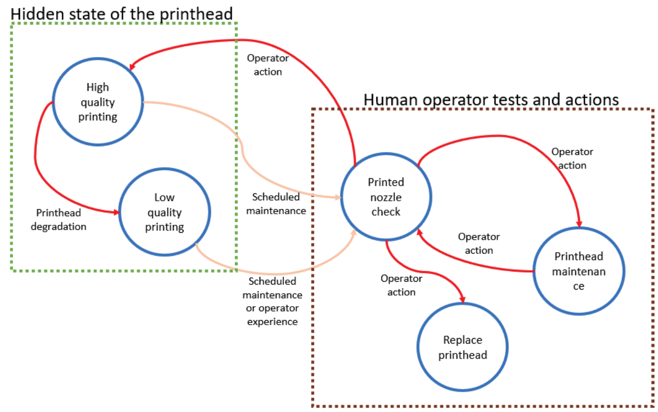

Figure 6. Human operator-based printing system control.

Once this system is completed, we hope to be able to evaluate different printer maintenance strategies and be able to compare them. Ultimately, we hope that strategies that improve existing fixed maintenance schedules can be found.

Conclusion

Many factors affect the image quality of an inkjet based printhead. One of the most difficult factors to identify is the malfunctioning of jetting nozzles in the printhead, as their state is difficult or impossible to observe directly ahead of their effect starting to cause a considerable loss in printed image quality.

In this paper we explore the use of acoustics nozzle signal analysis in conjunction with Reinforcement Learning as an effective tool to create useful belief representations of the status of the nozzle, and how to use nozzle beliefs representations to optimize the printing process with the overall goal of minimizing printer maintenance downtime while maintaining a high image quality output. In order to test our ideas, we are building a printing system which incorporates acoustic nozzle sensing technology, a high-resolution in-line image camera acquisition, a printhead maintenance station and nozzle plate camera. This will provide us with a system with very high nozzle state observability. This. In conjunction with an automated maintenance station will permit us to explore the different optimal maintenance strategies the RL system will generate, for both the exploration and exploitation phases of the RL process.

References

[1] J. Frits Dijksman, Design of Piezo Inkjet Print Heads,

[2] Kye-Si Kwon, “Methods for detecting air bubble in piezo inkjet dispensers,” Sensors and Actuators A: Physical, vol. 153, no. 1, pp. 50–56, 2009.Wiley-VCH Verlag GmbH, 2018.

[3] Byung-Hun Kim, Sang-Il Kim, Hyun-Ho Shin, Na-Rae Park, Hyun-Seok Lee, Chang-Soo Kang, Seung-Joo Shin, and Seong-Jin Kim, “A study of the jetting failure for self-detected piezoelectric inkjet printheads,” IEEE Sensors Journal, vol. 11, no. 12, pp. 3451–3456, 2011.

[4] Kye-Si Kwon, Yun-Sik Choi, Dae-Yong Lee, Jeong-Seon Kim, and Dae-Sung Kim, “Low-cost and high-speed monitoring system for a multi-nozzle piezo inkjet head,” Sensors and Actuators A: Physical, vol. 180, pp. 154– 165, 2012.

[5] R. S. Sutton, A. G Barto, Reinforcement Learning, The MIT Press, Cambridge, Massachusetts, 1998.

[6] A. Zai, B. Brown, Deep Reinforcement Learning in Action, Manning Publications Co., 2020.

Author Biography

Fernando Rodriguez Llorente received his MSc in physics from the University Complutense of Madrid (1993) and his PhD in applied physics from University Complutense of Madrid (1999). After his PhD, he worked in fiber optics telecommunications, ultrasound non-destruction testing, and engineering consultancy. Since 2012 he has been involved in inkjet printing, as VP of technology of Meteor Inkjet Ltd. and since 2023 in iPrint Institute (HES-SO), as senior inkjet systems engineer.

Next-generation Intelligent Media Sensor System: Automating Operations and Enhancing Productivity through Paper Type Identification

Takahiro Tsujimoto; Konica Minolta, Inc.; Toyokawa, Aichi/Japan

Abstract

When copying or printing, the user sets the paper into the paper feed section and gives the operation start command, and the paper is fed and transported, and an image is formed on the paper. Stable paper transport and image quality are closely related to paper characteristics, and detailed control is required for each paper. Wrong paper can cause JAM (poor paper delivery) and poor image quality (customer dissatisfaction). Konica Minolta develops a wide range of electrophotographic products from office printing (OP) to production printing (PP). Currently, although there are differences in the content between OP and PP, we have prepared paper setting items that can be set by customers related to "basis weight" and "paper type", which are closely related to printing performance.

Konica Minolta has introduced new technologies to bizhub new i-series to prevent paper jams and image quality degradation caused by improper operation or settings of MFPs. Based on "paper property sensing technology" generated from Konica Minolta's optical and ultrasonic technology assets, an "automatic identification algorithm" has been built by combining various optical characteristic judgment results, which accurately identifies paper and automatically performs the optimal printing settings. An improved intelligent media sensor system has been featured in the latest products for office and production printing, reducing paper setup effort and time. Specifically, the new i-series has succeeded in improving detection accuracy by increasing the variety of wavelengths of light source LEDs from three to six and has expanded the number of detectable paper types from about a few dozen to about 1,000. By combining the vast amount of field data with the detection results, it has been possible to successfully handle a wider variety of paper types used worldwide, contributing to further productivity gains. The intelligent media sensor system also constantly detects changes in paper characteristics during printing, preventing jams and reducing user annoyance, as well as reducing the burden on administrators. Konica Minolta's invisible technology improves operational efficiency.

Introduction

In the electrophotographic process, toner image on the photoreceptor is transferred to the conveyed paper surface and fixed to the paper with heat and pressure during fixation. In this process, paper characteristics greatly affect the through-paper performance and image formation process conditions, and detailed control is required based on paper characteristic information. Each printer development company has prepared paper setting items related to "basis weight" and "paper type", which are deeply related to printing performance, although the content is different from each other, and requires customers to operate them appropriately.

Basis weight is the most basic specification value that indicates the characteristics of paper, and the weight per square meter of paper is expressed in units (g/㎡). There is a wide variety of paper types used in the world. The paper used for electrophotography can also be classified into multiple types, and can be broadly divided into two types: uncoated paper and coated paper. Uncoated paper (plain paper) is generally used in office printing, and is also called thin paper, plain paper, cardboard, recycled paper, and colored paper depending on the basis weight and material. Coated paper is a paper with a resin coating on the surface of uncoated paper, and the surface is smooth and shiny. Due to the difference in gloss, it is classified into gloss paper and matte paper, and is mainly used in catalogs and photo books.

It is absolutely important to correctly recognize the type of paper and the basis weight and set the appropriate printing conditions. Konica Minolta has equipped the first generation of bizhub i series with an intelligent media sensor system for the first time, and has provided further advancements for the next generation of bizhub i series. The in-line intelligent media sensor system for office printing introduced in this article is installed in the following products.

First-generation media sensor system: [1][2]

bizhub C750i/C650i/C550i/C450i
IM-102 (option for bizhub C360i/C300i/C250i)

Next-generation media sensor system:[3]

bizhub C751i/C651i/C551i/C451i
IM-103 (option for bizhub C361i/C301i/C251i)

Technology Goals

Background of technology selection:

In office printing, it is necessary for the customers to select paper type such as thin paper, plain paper, cardboard, recycled paper, colored paper and envelopes linked to the basis weight table. However, it is difficult for them to judge it from the label on the packaging, and in some cases, they may not even recognize the necessity for a selection operation. According to our field data analysis, 12.5% of the defects that occur in the market were related to paper setting errors.

To overcome this situation, we have developed a basis weight determination system and an en

velope detection system that do not require the user to select the type of paper. By automatically matching the detection results to the current basis weight table, it is expected to reduce the operation time for printing and eliminate JAM and image quality defects caused by non-conformity in paper type selection.

Selected items:

Basis weight is an important item that represents paper characteristics, and the developed basis weight sensing system is to be used in common with OP (office printing) and PP (production printing).

In this article, we will introduce the basis weight sensing system developed based on Konica Minolta's core optical technology, as well as the basis weight conversion and paper type discrimination algorithm.

Basis Weight Determination

When selecting the sensors that make up the basis weight determination system, they need to be contactless detectable in order not to damage the paper. Non-contact measurement methods were considered using ultrasound and light transmission. As a result of comparing the characteristics of each method, it was found that ultrasound is greatly affected by humidity and temperature, so we adopted a measurement method using the transmittance of light that can be stably measured.

Optical detection of basis weight:

We found that there is a wavelength suitable for measuring the basis weight by the transmittance of light. Figure 1 summarizes the correlation coefficients between transmittance and basis weight at each wavelength tested on approximately 1,000 major paper brands. The paper types surveyed here were selected in collaboration with paper marketing companies from paper brands used around the world, and are considered to fully reflect the current market conditions. In the range of visible light, the correlation was low because the transmittance profile changed due to the difference in the components contained to adjust the color of the paper when the paper manufacturer and brand were different. In addition, since the correlation between transmittance and basis weight differs depending on the paper type, we chose to combine two wavelengths, blue B and near-infrared IR.

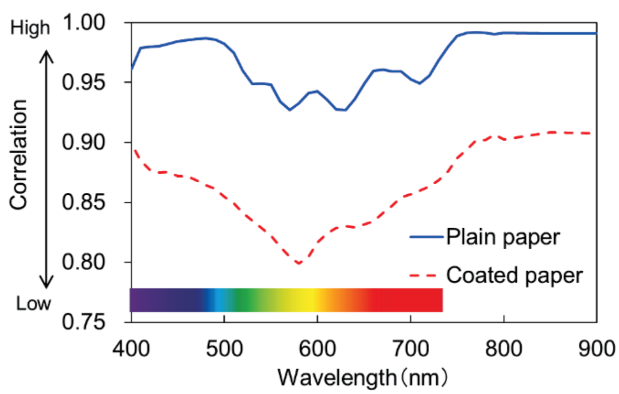

Figure 1. *Correlation between transmittance and basis weight at each wavelength.*[1]

Basis weight conversion formula:

First-generation media sensor system

Since the trend of transmittance and basis weight differs depending on the paper type, it is necessary to select the optimal weight conversion formula for each paper type. Figure 2 shows the basis weight measurements distribution based on the combination of transmittance and reflectance of multiple wavelengths, classified in paper types. From the figure, it can be seen that the transmittance of blue through the coated paper tends to be lower due to the influence of the components of the surface layer. Therefore, plain paper and coated paper can be classified by the difference in transmittance between near-infrared and blue wavelengths. In addition, recycled paper contains wastepaper components, which can be classified as reducing the reflectivity of green from the surface of the paper.

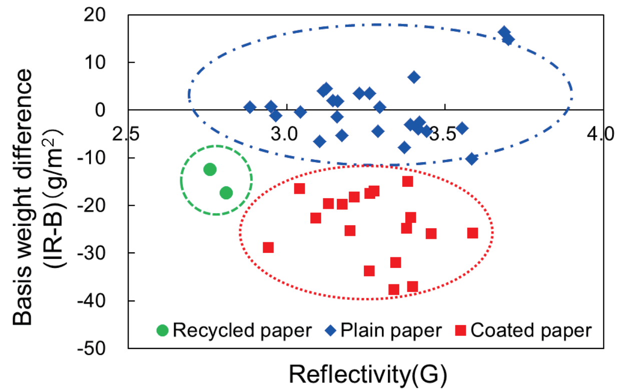

Figure 2. *Classification of measured values of basis weights by paper type based on combinations of transmittance and reflectance of multiple wavelengths.*[1],[2]

Using the above characteristics, the optimal basis weight conversion formula is selected in the following flow to calculate the basis weight.:
Step 1: Identify recycled paper from reflectivity G.
Step 2: Determine whether it is coated paper or plain paper (non-coated paper) from the basis weight difference IR-B, and select the basis weight conversion formula.

Next-generation media sensor system

Since the relationship between the basis weight and the combination of transmittance and reflectance is different for paper types with different optical properties even though they are the same paper type classification, we have devised an algorithm that can be applied for more variety of paper types. Transmitted and reflected light at wavelengths that are dependent on paper characteristics are detected, and paper types are determined by combining optical characteristic judgments. After the paper type is determined, an algorithm was introduced to calculate the amount of basis weight for the determined paper type (Table 1). By selecting a highly correlated

Table 1. Example of a definition table for basis weight conversion formulas based on multiple optical property judgment results.[3]

Optical characteristic judgment result				Paper type identification	Basis weight conversion formula
Sens. A	Sens. B	Sens. C	Sens. D		
○	○	○	○	Plain paper	Plain paper formula 1
○	○	○	×	Plain paper	Plain paper formula 2
○	○	×	○	Coated paper	Coated paper formula 1
○	○	×	×	Coated paper	Coated paper formula 2
○	×	○	○	Recycled paper	Recycled paper formula 1
×	○	○	○	Color Paper	Color paper formula 1
…	…	…	…	…	…
…	…	…	…	…	…

Legend: ○ indicates that the criteria are met, × indicates that the criteria are not met.

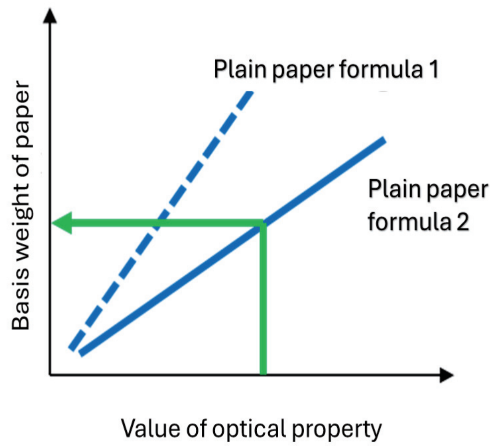

Figure 3. Example of basis weight definition from a conversion formula selected by the improved paper type identification algorithm.[3]

conversion formula for each paper type, it is possible to accurately detect the weight of each paper type (Figure 3).

The combination of multiple LEDs and PD (Photodiode) that make up the system are arranged along the paper path to detect transmitted and reflected light, respectively. By optimally arranging LEDs and PD to minimize detection variations due to paper position fluctuations, it is possible to detect paper characteristics while passing through paper.

Basis weight sensing configuration:

First-generation media sensor system

Figure 4 shows the configuration of the first-generation media sensor system for the sensing of the basis weight. Three types of LEDs (Light Emitting Diode) were placed. PD (Photodiode) placed on opposite sides of the paper detects the transmitted light of IR and B and calculates the transmittance of each. The reflectivity is calculated by detecting the light G reflected by the green LED on the paper surface.

Next-generation media sensor system

The next-generation media sensor system featured six types of LEDs (Light Emitting Diodes). The transmittance is calculated by detecting the transmitted light of IR and B with a PD (Photodiode) placed on the opposite side of the paper. The reflectivity of each is calculated by the reflected light of IR (near-infrared), UV (ultraviolet), V (violet), and R (red) on the paper surface.

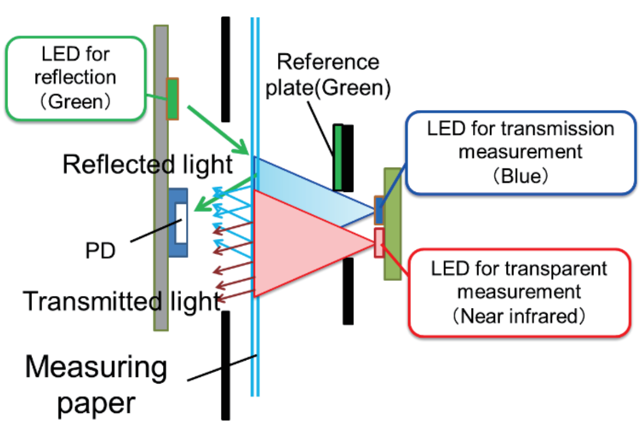

Figure 4. Basis weight sensing configuration of the first-generation media sensor system.[1],[2]

Ultrasonic sensor configuration

Next-generation media sensor system

Figure 5 shows a diagram of ultrasonic sensor configuration for envelope identification. In office printing, the application of printing on envelopes is relatively high. The system automatically detects envelopes so that they can also be optimally printed for envelopes. Envelope identification takes advantage of the attenuation of ultrasonic waves through the interface of the various media layers of acoustic impedance. The weakening of the strength of the ultrasonic signal through the air layer in the envelope can determine that it is an envelope (first application in the MFP industry). Automated envelope-specific printing settings reduce machine downtime for frequent envelope printing, increasing operational productivity.

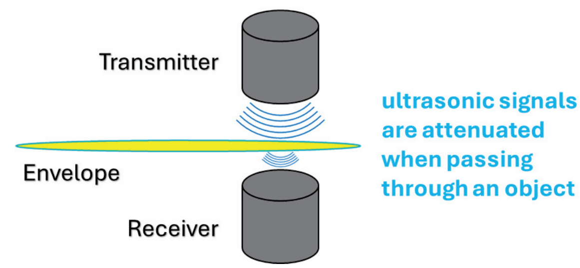

Figure 5. Diagram of ultrasonic sensor configuration for envelope identification.[3]

Circuit configuration:

First-generation media sensor system

Figure 6 shows the circuit configuration of the optical detection of basis weight. In the light-emission circuit, each LED intensity is adjusted with PWM-duty to ensure that the light receiving output is constant when not feeding paper. The light reception circuit has the function of switching the gain of the amplification circuit (AMP) depending on whether paper exists or not, and even if the signal of light received from paper is small, it amplifies the signal to a predetermined voltage and inputs it into the basis weight conversion circuit to accurately measure the transmittance/reflectivity of the paper and guarantees the accuracy of the basis weight conversion.

Next-generation media sensor system

This section provides an overview of the hardware configuration and control of the optical sensing for basis weight

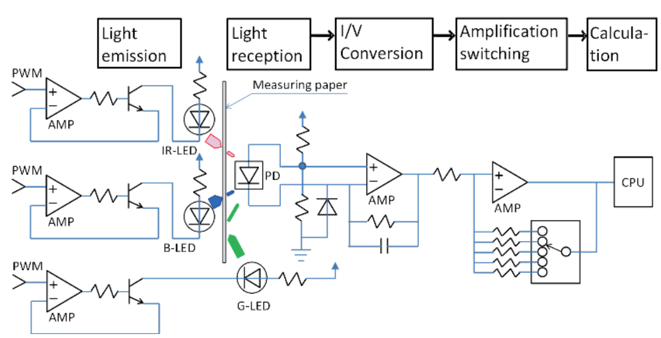

Figure 6. Detection circuit diagram implementing LED light intensity adjustment and light reception signal amplification switching.[1]

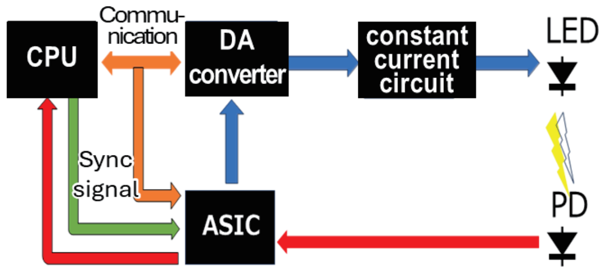

Figure 7. Optical sensing circuit diagram for basis weight determination applied to the next-generation media sensing system.[3]

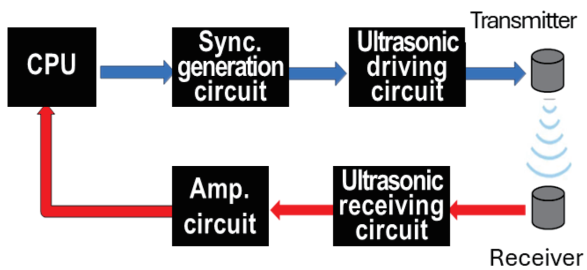

Figure 8. Ultrasonic sensing circuit diagram for envelope identification applied to the next-generation media sensing system.[3]

determination and ultrasonic sensing for envelope identification. In optical sensing (Figure 7), the analog value is instructed to the DA conversion element through communication from the CPU that controls calculations, the gain of the constant current circuit is set, and the drive current is switched by a synchronization signal to light up the LED. In ultrasonic sensing (Figure 8), the ultrasonic drive signal is transmitted from the CPU for control calculation to the ultrasonic drive circuit via a synchronous generation circuit, and the received ultrasonic signal is amplified by an amplification circuit to read the received value.

Product Implementation

Figure 9 illustrates the requirements for installing a sensor system in a product. The loading requirements are described in the following two paragraphs;

1. Identify the paper coming from all paper feeders (port 1, 2, 3, 4 and manual).
2. Paper should be detectable without stopping the paper in order to detect the signals multiple times and average them.

Due to the wide conveying path and the paper fluttering, the problem that the paper angle when passing through the sensor was different depending on the paper feed port has arisen during the study. Therefore, by providing paper positioning wheels (roller) in the basis weight sensing section, the paper path has been narrowed and the posture during transportation has been stabilized. In addition, by reducing the angle difference when the sensor passes through and placing the position of the basis weight sensing above the center of the roller, the angle fluctuation at the detection position has been reduced and the accuracy of paper judgment was improved.

Figure 10 shows the screen for setting the paper of the feed cassette on the operation panel. Automatic detection of paper type for each paper feed cassette is enabled by default. By eliminating the need for customers to intentionally select paper, we have realized a man-machine interface that eliminates configuration errors. For customers who do not know the paper type, the information from the automatic paper type detection is reflected on the paper setting screen, eliminating the need for investigation time for unknown paper.

We compared the paper jam ratio with a media sensor system (multiplied by the coefficient of market JAM incidence) and that without a media sensor system (including the user's misconfigured paper selection) (Figure 11). The survey results are from the first generation of media sensor systems. From the statistical data for one year in FY2022, it can be seen that machines equipped with media sensor systems have about half less paper jams compared to conventional machines, which are left to the user to select paper, contributing to reducing user downtime. We expect further effects from the next-generation media sensor system with an expanded number of supported paper types.

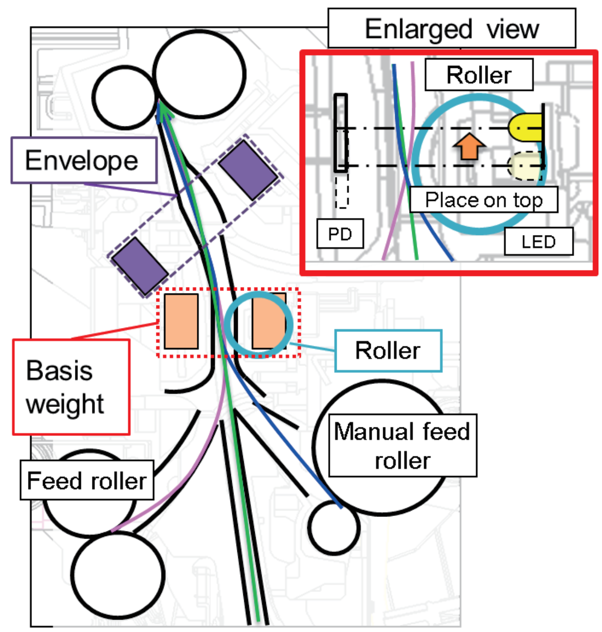

Figure 9. Placement of Basis weight sensing/ Envelope sensing / Rollers and transport guides in the paper transport path.[1]

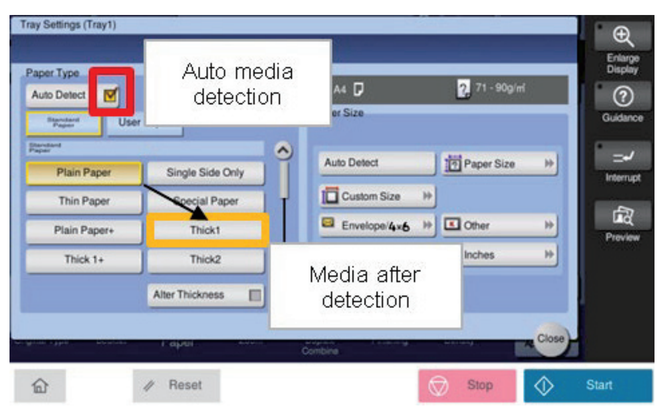

Figure 10. Automatic media detection is enabled by default on the control panel. After detection, the detected paper is automatically displayed.[1]

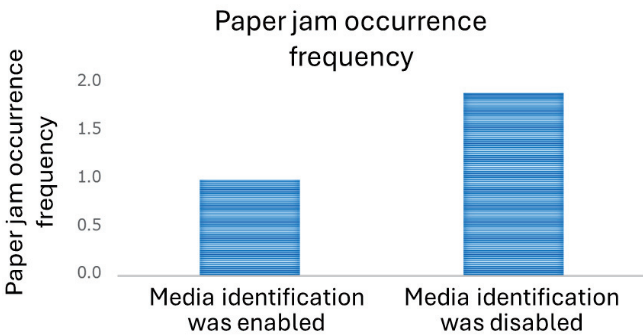

Figure 11. Comparison of the incidence of paper jams caused by incorrect paper type settings between models with equivalent specifications but equipped with a media sensor and conventional models without one (analysis results for the JP region in 2022).[3]

Summary

We expect that this product development will improve the operability of customers, reduce operation time, and reduce problems related to paper setting. In office printing, the customer's paper setting is no longer required, and the operation time is reduced by more than ten seconds compared to the past, and it is now possible to judge the characteristics of a wide variety of paper types. In the future, by correlating and analyzing the paper type detection results collected from this product series in the market with the product's operation history information, we will verify the effect of improving operability and lead to further workflow improvement proposals for customers. In addition, we aim to expand the number of compatible paper types by improving our sensing technology and revising the estimation algorithm.

References

[1] K. Yoshimura et. al., “Development of Intelligent Media Sensor”, Konica Minolta Technology Report vol. 17, pp. 34 -40, 2020 [in Japanese]

[2] Konica Minolta, Inc., “Printing paper automatic determination technology”, https://research.konicaminolta.com/en/technology/tech_details/printsetting/ (accessed 2025.10.08)

[3] T. Tsujimoto, “Automating operations and improving productivity with paper type detection technology using an intelligent media sensor”, Proceedings of the 2nd ISJ Technical Seminar in 2024 (160th in total), pp. 37-51, 2025 [in Japanese]

Author Biography

In 1991, Takahiro Tsujimoto joined Minolta Camera Co., Ltd. (now Konica Minolta, Inc.) and was in charge of the development and design of control panels. Until 2001, he belonged to the advanced technology development team and contributed to technological innovation. After that, he worked in the A4 printer model development team until 2009, working to improve product performance. Currently, he is a member of A3 MFP development team and is involved in the development of various advanced technologies such as high-precision drive, energy-saving fixing technology, motor PID control technology, and media sensor development.

Exploring the Future Potential of Artificial Intelligence for Printing

Marius Pedersen; Colourlab, Department of Computer Science, Norwegian University of Science and Technology

Abstract

Artificial Intelligence (AI) is likely to impact the printing industry by introducing capabilities that extend far beyond current automation and optimization practices. Recent advances in machine learning and deep learning have enabled novel approaches to print quality inspection, defect detection, predictive maintenance, and process parameter optimization. We will first review relevant works that apply AI in diverse areas of printing, ranging from computer vision–based systems for real-time defect recognition to data-driven methods for process control in emerging technologies such as additive manufacturing printing. Building on this foundation, we will further explore the potential role of AI in shaping the future of printing. In particular, we emphasize the value of transferring and adapting methodologies from adjacent research fields. For example, techniques from computer vision can be leveraged for fine-grained analysis of print quality; natural language processing offers opportunities for document understanding, automated layout generation, and intelligent handling of printed text archives; robotics contributes to the integration of AI-guided manipulation in hybrid print-manufacturing environments; and generative design provides pathways for AI-driven innovation in printable structures, materials, and layouts. Through this interdisciplinary perspective, we aim to highlight how AI can support not only efficiency and reliability, but also creativity, adaptability, and new forms of value creation in the printing industry.

Background

The printing industry, one of the drivers of technological innovation, is once again at the threshold of a paradigm shift. Although advances in automation, digital workflows, and industrial quality control have shaped its development over the past decades, the emergence of Artificial Intelligence (AI) promises an even more profound transformation. AI methods, particularly those enabled by recent progress in deep learning and large-scale computing, have demonstrated remarkable success in various domains such as computer vision [1], natural language processing [2], robotics [3], and generative design [4]. These capabilities are increasingly being adapted to tackle complex problems in the printing sector, ranging from print quality assurance and defect detection to predictive maintenance and even the design of entirely new printing processes.

Existing AI applications in printing have focused primarily on improvements in efficiency, throughput, and defect reduction. For example, convolutional neural networks have been applied to the detection of fine-grained defects in print lines [5], while reinforcement learning approaches have been proposed to optimize process parameters in additive manufacturing [6]. Similarly, machine vision–based inspection systems have started to replace manual quality checks [5, 7], allowing for high-speed and real-time monitoring. However, the full potential of AI in printing has yet to be fully uncovered. Beyond optimization and automation, AI can introduce new paradigms for creativity, adaptability, and interoperability between disciplines.

The transfer of methods from adjacent fields illustrates this potential. Computer vision techniques, for example, have been tailored to the challenges of print quality control [5] and color deviations [8]. Natural language processing methods can support tasks such as document understanding [9], layout generation [10], and digitization of historical printed archives [11]. Robotics research can provide AI-driven solutions for intelligent manipulation, enabling tasks such as adaptive print-path planning [12], while generative techniques can be leveraged to create novel design [13].

The purpose of this paper is three-fold.

- Provide a review of recent work applying AI in printing, including both traditional and emerging print technologies.
- Highlight opportunities for cross-pollination by examining transferable AI methodologies from other domains.
- Propose a forward-looking perspective on how AI might redefine the scope and possibilities of the printing industry.

By synthesizing existing research and envisioning future applications, this work aims to contribute to a broader understanding of AI's role in transforming printing. The rest of the paper is organized as follows: We will first go through some of the relevant publications related to the use of AI in printing, before we explore trends of AI in printing. Finally, we conclude.

Background

We will review the use of AI in the wider area of printing, ranging from traditional printing to additive printing such as 3d printing. We will first present the use of computer vision techniques in printing and then present work that use large language models. The goal is to give examples of work, not a complete overview of the existing literature.

Computer vision

Liu et al. [5] proposed a method for defect detection for inkjet printing labels. They use a modified YOLOv5 [14] network for this purpose, which helped to detect narrow and elongated defects common to this type of printing. This is an example where YoloV5, made for object detection and applied to the printing field.

Villalba-Diez et al. [15] applied deep learning in industrial print settings with the goal of automatic quality control process. They used a deep neural network that performed binary classification (ok and not ok). They achieved a high accuracy on their dataset.

Pandey et al. [16] focused on aerosol jet printing, and did systematic experiments varying printing parameters, then used different machine learning techniques to optimize parameters with the goal of improving print quality. Their results indicate that deep learning models can be used, and show robustness.

Zhang et al. [17] built a large dataset of printing defect images (coarse- and fine-grained), then used a convolutional neural network to classify defect types. Their results show that their model worked better than many standard transfer learning models.

Chen et al. [18] focused on detecting inkjet printing defects in production dates on food packaging (e.g., missing or damaged codes). They used computer vision and deep learning to automate the detection of these defects to improve throughput and reduce defective items.

Shen et al. [19] used a convolutional neural network architecture for automatic error compensation in 3D printing. Their proposed method tried to predict deformation, and then use this to compensate for the deformation. Their experiments showed that they could improve the accuracy with little need to increase the hardware cost.

Large language models

Jadhav et al. [7] proposed a framework that uses pre-trained large language models (LLMs) as agents to analyze images captured during prints, diagnose common Fused Deposition Modeling (FDM) failure modes (stringing, warping, layer adhesion, etc.), query the printer for parameters, and generate corrective actions, effectively closing a loop to autonomously correct prints. They also show comparisons to human expert engineers, and concludes that the proposed technique closely match human evaluations.

Jignasu et al. [20] evaluate multiple state-of-the-art LLMs on tasks involving G-code (the low-level instructions for printers): debugging, detecting/correcting common errors, and geometric transformations. They concluded that LLMs have reasonable proficiency in debugging, performing geometric transformations, and reasoning. However, there are critical limitations.

Pak and Farimani [21] fine-tuned LLMs on process-parameters on defect datasets to predict defect regimes (e.g., keyholing, lack of fusion, balling). Their results showed that LLMs can be competitive in mapping tabular process data to defect labels when trained appropriately.

Wang et al. [22] focused on documents and printed pages, where they used LLM reasoning to understand and generate visual documents (forms, invoices, printed pages). The results indicate that the proposed method could extract meaningful information from a wide range of visual documents in several different datasets.

Kadyrova and Pedersen [23] used well-known commercial text-to-image generation AI tools for making 2.5D prints. The study investigated whether these tools could generate realistic and natural-looking 2.5D prints. The experimental results indicate that they can, to a certain degree.

Zhu et al. [24] introduced a compact tokenization scheme to incorporate layout information into LLMs for document understanding and generation, while improving the handling of the page structure.

Optimization

Different techniques have also been applied for optimization, and many works can be found to optimize job scheduling. These mostly use techniques such as hybrid genetic algorithms [25] and neural networks [26].

Ataeefard and Tilebon [27] used machine learning to choose and predict the performance of a paper with the appropriate properties to achieve the maximum color gamut.

Velastegui and Pedersen [28] evaluated four different machine learning approaches that have been implemented to perform the color space transformation between CMYK and CIELAB color spaces. They explored support-vector regression, artificial neural networks, deep neural networks, and radial basis function. The results indicated that all methods obtained high transformation accuracy.

Trends

Generative AI and large language models

As already seen in the previous section, the use of LLMs have been used in printing. With the more widespread use and availability of such models, these will also be applied to various problems in printing. We see that they have been used to analyse prints [7, 21], helping to debug [20], understand and generate documents [22, 24]. Generative models have already been extensively used to automate layout design [29], and we will see more advanced models able to better handle difficult cases and with more creativity. AI based techniques can also analyze vast amounts of user data to create highly personalized print materials. There have been an increasing demand for personalized content, and by tailoring content and design to individual preferences, user satisfacation can increase. There have also been increase in research on how to optimize quality for an individual or a group of users [30], and this can be used to optimize quality for each user or each group. There is also work on how to generate print-ready art using AI tools [31].

LLMs have also been extensively used to generate captions [32] or summarize content [33], such techniques can also be applied to printing, such as to explain or describe the quality of the prints. This has already been done for general image quality [34].

The use of generate AI and LLMs will extend their impact in the printing fields, and we will likely see such tools being applied from an idea and design phase till the end of the printing chain.

Explainability

Explainable AI, with the goal of interpreting AI systems, has received greater interest and has been applied to a number of fields such as medical imaging [35] and autonomous driving [36]. There is an increasing demand for an explainable AI to understand how AI models make predictions. The explanation of the decision-making process in AI systems is critical for different fields, including printing. Different approaches for explainability have been proposed. We will likely see these being applied more commonly to the printing domain. Models that are intrinsic are interpretable by design, such as decision trees and rule-based methods. These have already been used in printing [37]. Post-hoc explainability refers to techniques used to interpret and explain the behavior of a machine learning model after it has been trained. There exist a number of methods for post-hoc explainability, as LIME [38] and Grad-CAM [39]. As an example, Grad-

CAM has been applied to 3D printing [40] and offset printing [41]. Other post-hoc techniques include counterfactual explanations [42], where one shows how small changes to the input could lead to a different prediction.

There is also a growing demand for transparency, fairness, and bias mitigation. This will drive the field, and result in more explainable methods. This is also driven by regulatory frameworks such as the EU AI Act [43].

Optimization

AI has been used successfully in optimization in different fields. Optimization has been done in printing since its inception. However, current and future AI techniques are likely to impact this field. We are likely to see improvements in being able to handle increased complexity and to do so in real-time. This will come from having access to more extensive datasets and more sophisticated architectures, and we are also likely to see techniques that are based on unsupervised learning without the need of large datasets. These will in turn allow for better assignment of resources, optimized setups and scheduling, as well as reduced turnaround time and reduction in waste. Such optimization is also likely to enable better personalization, where content is adjusted to each individual user or group.

We will also see AI-based techniques being applied to optimize and assessment print quality. Print quality assessment will likely follow traditional schemes as [44, 45, 46, 47], but with more advanced image quality metrics, for example, deep learning based metrics [48, 49].

Colour accuracy

There are also works on how AI techniques can help to increase color accuracy or increase gamut volume. An example is the work of Ataeefard and Tilebon [27] to select the paper with the highest gamut. Wang et al. [50] used neural networks to predict color accuracy and gamut expansion. Work has also been carried out to look at color space transformations [28].

Generative models, such as generative adverserial networks, are good at image colorization, and are likely to be used more extensively in, for example, automated color correction. We have also seen methods that allow for real-time color calibration and in-print adjustment, which can be adjusted to ensure color consistency. Defect detection to identify color inconsistencies and trigger corrective actions is likely to become more common, perhaps especially in 3D printing.

Open challenges

There are several open challenges that are likely to be driven by advancements in machine learning and various application areas. There will continue to be a trade-off between the size of models and the performance when compared to efficiency and energy. Further, one will need to ensure interpretability and fairness, without a cost in performance of usability. Robustness is also a key challenge, and models need to be robust to adversarial attacks and distribution shifts. Bias in the datasets will influence the model, and needs to be taken into consideration to ensure generalization. In deployment, regulatory, ethical, and privacy concerns become more central and will vary by region. We are also likely to face challenges on how to evaluate explainability or interpretability in a rigorous, standardized way.

The advances to come in order to solve these challenges can be useful also in the printing field, and one could try to ensure cross-pollination from adjacent fields.

Conclusion

Artificial intelligence is rapidly reshaping the printing industry, offering transformative capabilities that go far beyond traditional automation. Through the integration of machine learning and deep learning, printing systems are becoming more intelligent, adaptive, efficient, enabling real-time defect detection, predictive maintenance, and data-driven process optimization. Our review highlights how AI techniques from adjacent fields such as computer vision, natural language processing, robotics, and generative design are being successfully transferred and adapted to printing workflows.

Looking ahead, the convergence of these technologies opens new possibilities. As AI continues to evolve, its role in printing will not only enhance operational reliability and quality, but also foster innovation, personalization, and new forms of value creation. Embracing this interdisciplinary approach will be the key to unlocking the full potential of AI in the future of printing.

Acknowledgments

This work was supported by the project “Quality and Content: understanding the influence of content on subjective and objective image quality assessment” (grant number 324663) from the Research Council of Norway.

References

[1] Junyi Chai, Hao Zeng, Anming Li, and Eric WT Ngai. Deep learning in computer vision: A critical review of emerging techniques and application scenarios. *Machine Learning with Applications*, 6:100134, 2021.

[2] Lewis Tunstall, Leandro Von Werra, and Thomas Wolf. *Natural language processing with transformers*. ” O’Reilly Media, Inc.”, 2022.

[3] Josip Tomo Licardo, Mihael Domjan, and Tihomir Orehovački. Intelligent robotics—a systematic review of emerging technologies and trends. *Electronics*, 13(3):542, 2024.

[4] Damilola Onatayo, Adetayo Onososen, Abiola Oluwasogo Oyediran, Hafiz Oyediran, Victor Arowoiya, and Eniola Onatayo. Generative ai applications in architecture, engineering, and construction: trends, implications for practice, education & imperatives for upskilling—a review. *Architecture*, 4(4):877–902, 2024.

[5] Jie Liu, Zelong Cai, Kuanfang He, Chengqiang Huang, Xianxin Lin, Zhenyong Liu, Zhicong Li, and Minsheng Chen. An efficient printing defect detection based on yolov5-dcn-lsk. *Sensors*, 24(23):7429, 2024.

[6] Jihoon Chung, Bo Shen, Andrew Chung Chee Law, and Zhenyu James Kong. Reinforcement learning-based defect mitigation for quality assurance of additive manufacturing. *Journal of Manufacturing Systems*, 65:822–835, 2022.

[7] Yayati Jadhav, Peter Pak, and Amir Barati Farimani. Llm-3d print: large language models to monitor and control 3d printing. *arXiv preprint arXiv:2408.14307*, 2024.

[8] Hongwu Zhan, Yuhao Shou, Lidu Wen, Fang Xu, and Libin Zhang. Color detection of printing based on improved superpixel segmentation algorithm. *Scientific Reports*, 14(1):23449, 2024.

[9] Mohammad Minouei, Mohammad Reza Soheili, and Didier

Stricker. Embedding layout in text for document understanding using large language models. In *International Conference on Document Analysis and Recognition*, pages 280–293. Springer, 2024.

[10] Jian Chen, Ruiyi Zhang, Yufan Zhou, Jennifer Healey, Jiuxiang Gu, Zhiqiang Xu, and Changyou Chen. Textlap: Customizing language models for text-to-layout planning. *arXiv preprint arXiv:2410.12844*, 2024.

[11] Christian Schultze, Niklas Kerkfeld, Kara Kuebart, Princilia Weber, Moritz Wolter, and Felix Selgert. Chronicling germany: An annotated historical newspaper dataset. *arXiv preprint arXiv:2401.16845*, 2024.

[12] Yaxin Wang, Chun Zhao, Wenzheng Liu, and Shun Li. Path planning and real-time optimization of robotic arm 3d printing. *International Journal of Modeling, Simulation & Scientific Computing*, 16(3), 2025.

[13] Waad Almasri, Dimitri Bettebghor, Fakhreddine Ababsa, and Florence Danglade. Shape related constraints aware generation of mechanical designs through deep convolutional gan. *arXiv preprint arXiv:2010.11833*, 2020.

[14] Rahima Khanam and Muhammad Hussain. What is yolov5: A deep look into the internal features of the popular object detector. *arXiv preprint arXiv:2407.20892*, 2024.

[15] Javier Villalba-Diez, Daniel Schmidt, Roman Gevers, Joaquín Ordieres-Meré, Martin Buchwitz, and Wanja Wellbrock. Deep learning for industrial computer vision quality control in the printing industry 4.0. *Sensors*, 19(18):3987, 2019.

[16] Prashantkumar Pandey, Steffen Ziesche, and Gauranggiri Meghanathi. Improving performance of aerosol jet printing using machine learning-driven optimization. *Applied Research*, 3(5):e202300110, 2024.

[17] Erhu Zhang, Bo Li, Peilin Li, and Yajun Chen. A deep learning based printing defect classification method with imbalanced samples. *Symmetry*, 11(12):1440, 2019.

[18] Ning Chen, Hao Feng, Kangyi Wu, Yingquan Lin, and Lini Li. Research on food production date inkjet defect detection system based on deep learning. In *International Workshop of Advanced Manufacturing and Automation*, pages 18–24. Springer, 2022.

[19] Zhen Shen, Xiuqin Shang, Meihua Zhao, Xisong Dong, Gang Xiong, and Fei-Yue Wang. A learning-based framework for error compensation in 3d printing. *IEEE transactions on cybernetics*, 49(11):4042–4050, 2019.

[20] Anushrut Jignasu, Kelly Marshall, Baskar Ganapathysubramanian, Aditya Balu, Chinmay Hegde, and Adarsh Krishnamurthy. Towards foundational ai models for additive manufacturing: Language models for g-code debugging, manipulation, and comprehension. *arXiv preprint arXiv:2309.02465*, 2023.

[21] Peter Pak and Amir Barati Farimani. Additivellm: Large language models predict defects in additive manufacturing. *arXiv preprint arXiv:2501.17784*, 2025.

[22] Dongsheng Wang, Natraj Raman, Mathieu Sibue, Zhiqiang Ma, Petr Babkin, Simerjot Kaur, Yulong Pei, Armineh Nourbakhsh, and Xiaomo Liu. Docllm: A layout-aware generative language model for multimodal document understanding. *arXiv preprint arXiv:2401.00908*, 2023.

[23] Altynay Kadyrova and Marius Pedersen. Text-to-image generation ai tools for 2.5d prints: Preliminary observations. In *Advances in Printing Technologies*, 2025.

[24] Zhaoqing Zhu, Chuwei Luo, Zirui Shao, Feiyu Gao, Hangdi Xing, Qi Zheng, and Ji Zhang. A simple yet effective layout token in large language models for document understanding. In *Proceedings of the Computer Vision and Pattern Recognition Conference*, pages 14472–14482, 2025.

[25] Simin Huang, Linning Cai, and Xiaoyue Zhang. Parallel dedicated machine scheduling problem with sequence-dependent setups and a single server. *Computers & Industrial Engineering*, 58(1):165–174, 2010.

[26] Diana Bratić, Suzana Pasanec Preprotić, Denis Jurečić, and Marko Šapina. Bookbinding operational planning and scheduling optimization with deep learning algorithms. In *Proceedings-The Twelfth International Symposium GRID 2024 14-16. November 2024, Novi Sad*. University of Novi Sad, 2024.

[27] Maryam Ataeefard and Seyyed Mohamad Sadati Tilebon. Seeking a paper for digital printing with maximum gamut volume: a lesson from artificial intelligence. *Journal of Coatings Technology and Research*, 19(1):285–293, 2022.

[28] Ronny Velastegui and Marius Pedersen. Cmyk-cielab color space transformation using machine learning techniques. In *London Imaging Meeting*, volume 2021, pages 73–77. Society for Imaging Science and Technology, 2021.

[29] Xinru Zheng, Xiaotian Qiao, Ying Cao, and Rynson WH Lau. Content-aware generative modeling of graphic design layouts. *ACM Transactions on Graphics (TOG)*, 38(4):1–15, 2019.

[30] Olga Cherepkova, Seyed Ali Amirshahi, and Marius Pedersen. Individual contrast preferences in natural images. *Journal of Imaging*, 10(1):25, 2024.

[31] Noah Pursell and Anindya Maiti. Generating print-ready personalized ai art products from minimal user inputs. *arXiv preprint arXiv:2405.18247*, 2024.

[32] Haoran Wang, Yue Zhang, and Xiaosheng Yu. An overview of image caption generation methods. *Computational intelligence and neuroscience*, 2020(1):3062706, 2020.

[33] Yang Zhang, Hanlei Jin, Dan Meng, Jun Wang, and Jinghua Tan. A comprehensive survey on process-oriented automatic text summarization with exploration of llm-based methods. *arXiv preprint arXiv:2403.02901*, 2024.

[34] Zhihao Chen, Bin Hu, Chuang Niu, Tao Chen, Yuxin Li, Hongming Shan, and Ge Wang. Iqagpt: Image quality assessment with vision-language and chatgpt models. *arXiv preprint arXiv:2312.15663*, 2023.

[35] Anuja Vats, Marius Pedersen, and Ahmed Mohammed. Concept-based reasoning in medical imaging. *International Journal of Computer Assisted Radiology and Surgery*, 18(7):1335–1339, 2023.

[36] Sazid Nazat, Lingxi Li, and Mustafa Abdallah. Xai-ads: An explainable artificial intelligence framework for enhancing anomaly detection in autonomous driving systems. *Ieee Access*, 12:48583–48607, 2024.

[37] Konstantinos Balaskas, Georgios Zervakis, Kostas Siozios, Mehdi B Tahoori, and Jörg Henkel. Approximate decision trees for machine learning classification on tiny printed circuits. In *2022 23rd International Symposium on Quality Electronic Design (ISQED)*, pages 1–6. IEEE, 2022.

[38] Marco Tulio Ribeiro, Sameer Singh, and Carlos Guestrin. " why should i trust you?" explaining the predictions of any classifier. In *Proceedings of the 22nd ACM SIGKDD international conference on knowledge discovery and data mining*, pages 1135–1144, 2016.

[39] Ramprasaath R Selvaraju, Michael Cogswell, Abhishek Das, Ramakrishna Vedantam, Devi Parikh, and Dhruv Batra. Grad-cam: Visual explanations from deep networks via gradient-based local-

ization. In *Proceedings of the IEEE international conference on computer vision*, pages 618–626, 2017.

[40] Douglas AJ Brion and Sebastian W Pattinson. Generalisable 3d printing error detection and correction via multi-head neural networks. *Nature communications*, 13(1):4654, 2022.

[41] Anton Nailevich Gafurov, Thanh Huy Phung, Inyoung Kim, and Taik-Min Lee. Ai-assisted reliability assessment for gravure offset printing system. *Scientific Reports*, 12(1):2954, 2022.

[42] Riccardo Guidotti. Counterfactual explanations and how to find them: literature review and benchmarking. *Data Mining and Knowledge Discovery*, 38(5):2770–2824, 2024.

[43] EU Artificial Intelligence Act. The eu artificial intelligence act. *European Union*, 2024.

[44] Marius Pedersen, Yuanlin Zheng, and Jon Yngve Hardeberg. Evaluation of image quality metrics for color prints. In *Scandinavian Conference on Image Analysis*, pages 317–326. Springer, 2011.

[45] Marius Pedersen, Nicolas Bonnier, Jon Yngve Hardeberg, and Fritz Albregtsen. Attributes of image quality for color prints. *Journal of Electronic Imaging*, 19(1):011016–011016, 2010.

[46] Marius Pedersen. *Image quality metrics for the evaluation of printing workflows*. PhD thesis, University of Oslo, 2011.

[47] Altynay Kadyrova, Vlado Kitanovski, and Marius Pedersen. Quality assessment of 2.5 d prints using 2d image quality metrics. *Applied Sciences*, 11(16):7470, 2021.

[48] Vlad Hosu, Hanhe Lin, Tamas Sziranyi, and Dietmar Saupe. KonIQ-10k: An ecologically valid database for deep learning of blind image quality assessment. *IEEE Transactions on Image Processing*, 29:4041–4056, 2020.

[49] Seyed Ali Amirshahi, Marius Pedersen, and Azeddine Beghdadi. Reviving traditional image quality metrics using cnns. In *Color and Imaging Conference*, volume 26, pages 241–246. Society for Imaging Science and Technology, 2018.

[50] Po-Tong Wang, Chiu Wang Tseng, and Li-Der Fang. Physics-constrained deep learning for security ink colorimetry with attention-based spectral sensing. *Sensors (Basel, Switzerland)*, 25(1):128, 2024.

Author Biography

Marius Pedersen (1983) is a professor in Colour Imaging at the Department of Computer Science, Norwegian University of Science and Technology (NTNU). He is also deputy for Gjøvik for the Computer Science department. His research interests are in colour imaging, with applications to graphic arts, medical, security, and more.

Observation of Pore Formation in Binder Jetting with Granulated Ceramics Particles

Yohsuke Konishi, Kiichi Kamoda, Nobuhide Sekine, Shozo Sakura, Yukie Inoue, Satoshi Miyagawa

Abstract

Ricoh Company, Ltd. is developing a novel binder jetting method called particle homogenizing modeling (PHM), using ceramic granulated particles and ink containing ceramic nanoparticles. The existence of pores inside the built parts by this method has been reported. To reduce these pores, it is necessary to understand the mechanism behind their formation. This study presents the mechanism of pore formation in the PHM method obtained through in-situ observation of the powder surface with ink applied during building and CT analysis of the built parts. The results show that the pores are most likely formed by two phenomena that occur during building, especially when the ink is applied to the powder layer. Furthermore, image features were extracted from the powder bed observation images, and the relationship between build quality and image features was analyzed using machine learning to construct a quality prediction model.

Introduction

Ceramic materials possess excellent properties such as mechanical strength, high melting points, and superior corrosion resistance, and their application as structural materials is expanding in fields such as aerospace and automotive industry. On the other hand, ceramics are difficult to process, and compared to metals and polymers, conventional manufacturing methods impose restrictions on the shapes that can be produced. Therefore, additive manufacturing (AM) technology, which enables the fabrication of components with complex and freeform geometries, is attracting attention as a novel manufacturing method for ceramic parts.

Ricoh Company, Ltd. has developed a novel binder jetting technology called "Particle Homogenizing Method (PHM)," which utilizes ceramic granulated powder and ink which contains ceramic nanoparticles [1]. Figure. 1 illustrates the concept of the PHM method used in this study. This technology is characterized by the dissolution of the resin that forms the powder by the solvent in the ink, resulting in the breakdown of the powder. As a result, it enables the fabrication of dense and homogeneous green bodies. Furthermore, the amount of resin in the green bodies produced by this technology is smaller than that in green bodies fabricated by other AM technology, which offers the advantage of reducing deformation and cracking during the subsequent debinding and sintering processes.

However, it has been confirmed that pores with diameters of several tens of micrometers exist inside the green body fabricated using this technology [1]. In order to apply this technology to the manufacturing of structural components that require high reliability, it is necessary to improve the density of the green body, that is, to reduce the internal porosity. Elucidating the mechanism of pore formation is essential for reducing porosity, but analyzing the green

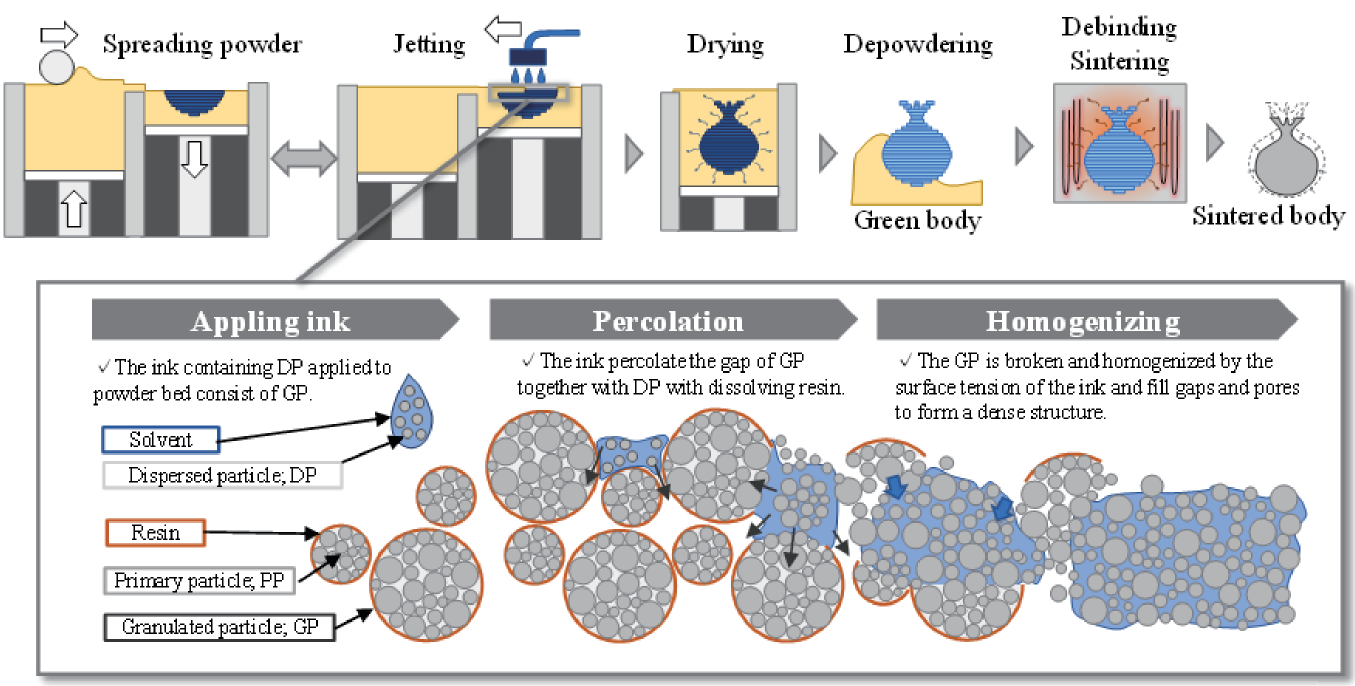

Figure 1. *Schematic illustration of Particle Homogenizing Modeling (PHM) process [1]*

body after pore formation makes it difficult to clarify the process leading to pore formation.

In this study, we conducted in-situ observation of the powder bed impacted by ink during the fabrication process (hereafter referred to as "powder bed"), as well as X-ray CT analysis of the green bodies. Through these approaches, we attempted to directly observe the pore formation process, and report on the pore formation behavior in the particle homogenizing modeling as inferred from the results.

Materials and Methods

In this study, alumina granulated powder and alumina-dispersed ink were prepared using the same method as described in Reference 1. Figure.2 shows SEM images of granulated powder. The powder was obtained by spray granulation of a slurry prepared by mixing and dispersing primary alumina particles with resin. The ink was produced by dispersing alumina particles, dispersant, and solvent together using a ball mill. The viscosity of the ink was adjusted to allow ejection from the inkjet head.

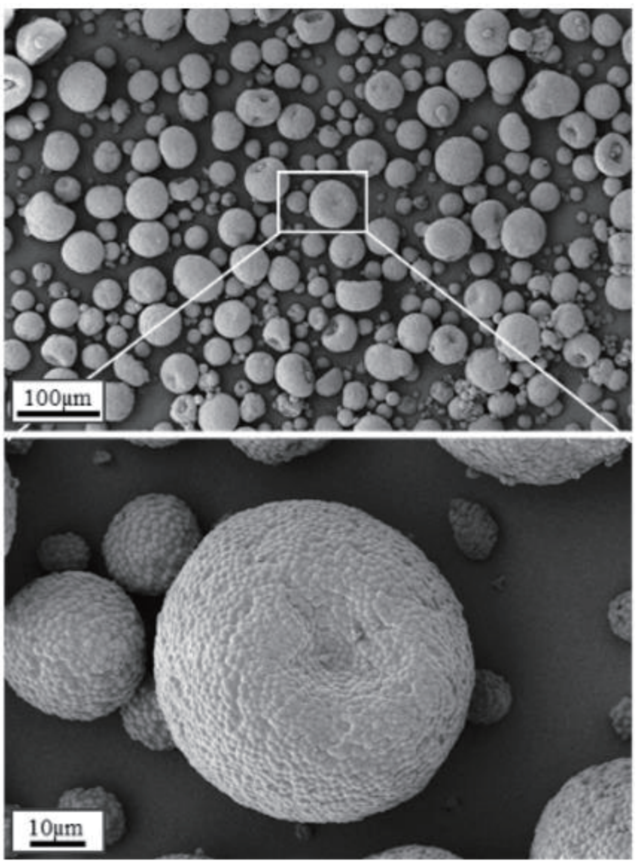

Figure 2. *SEM images of granulated particle*

Fabrication was performed using an in-house developed 3D printer. A schematic diagram of the apparatus is shown in Figure. 3. The system consists of a supply tank, build tank, and roller for forming a uniform powder layer; an inkjet head for applying ink onto the powder layer; and a powder bed heating unit. For the purpose of this study, a camera was installed directly above the build tank to enable microscale observation of the powder bed during the fabrication process.

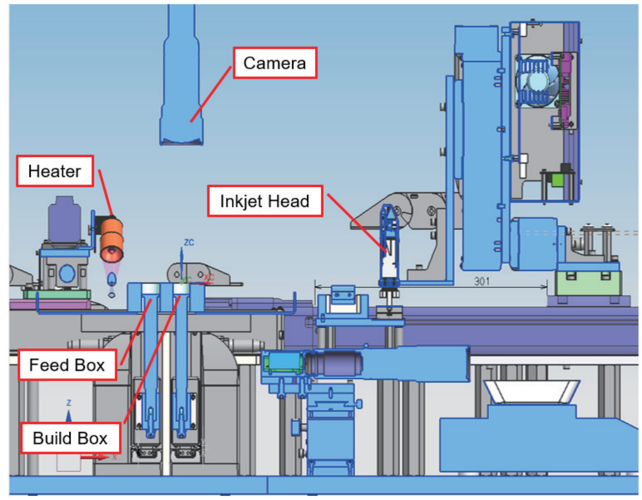

Figure 3. *3D Printer for Observation of Powder Surface with Ink Applied*

The printed bodies were formed by repeating the following steps: layering granulated powder with the roller, applying ink to the powder, and heating the powder bed with the heater. The dimensions of the printed bodies were set to 10.0 mm (length) × 10.0 mm (width) × 3.0 mm (height). The fabrication conditions, including layer pitch, scanning resolution, heater temperature, and relative ink saturation (Saturation), were adjusted during the process. It has been reported that the density of the green bodies closely related to the amount of ink deposited onto the powder bed [1]. Here, the amount of ink is defined as Saturation, which is the volumetric ratio of ink to the non-powder volume in the build box. In this study, the droplet size was varied by adjusting the head voltage multiplier, and Saturation was set to three levels for fabrication. The fabrication process was observed in situ, and after removal, the solvent in the printed bodies was dried to obtain green bodies.

Porosity analysis of the green bodies was performed using X-ray computed tomography (X-CT, µB4600, Matsudaira Precision Co., Ltd.). To enable comparison between powder bed photographs and CT images at the same location, a marker region without ink deposition was created within the green bodies. In the particle homogenization fabrication method, regions without ink deposition tend to remain as pores due to lack of homogenization, making it easy to identify the marker region in CT images.

Results

The surface area of the powder to which ink was applied with a certain amount of ink or more had gloss and to shrink horizontally both before and after heating. It has been revealed that differences in glossiness and surface irregularities caused by shrinkage depend on the amount of ink. The results of the comparison between the powder bed during fabrication and the internal pores of the green body are described below. Figure.3 shows a comparison between photographs of the powder bed during fabrication and CT images of the same location in the green body. The dashed lines in each image indicate the marker positions.

At a low ink amount (Saturation 52%), pronounced surface irregularities were observed on the powder bed. The powdered surface exhibits a mixture of glossy areas and areas that appear to be powder, giving the impression of significant unevenness. Then, CT analysis of the green body revealed the presence of irregularly shaped pores with diameters greater than 100 µm inside the green body, which resembled the surface irregularities of the powder bed. It is supposed these irregular pores are formed due to the unevenness of the powder surface during build process. However, there were cases where no pores were observed in the CT images, even when irregularities were present on the powder surface. At a high ink amount (Saturation 59%), quite a little pronounced surface irregularities were observed on the powder bed, but the behavior of small bubbles rising from the powder bed was confirmed. The CT images of the same location showed the presence of relatively small pores, several tens of micrometers in diameter, scattered throughout. These small pores were also characterized by their nearly spherical shape, in contrast to the pores observed at low ink amounts. At an intermediate ink amount (Saturation 56%), both the number of surface irregularities on the powder bed and the number of pores in the CT images were lower than those observed under the other conditions.

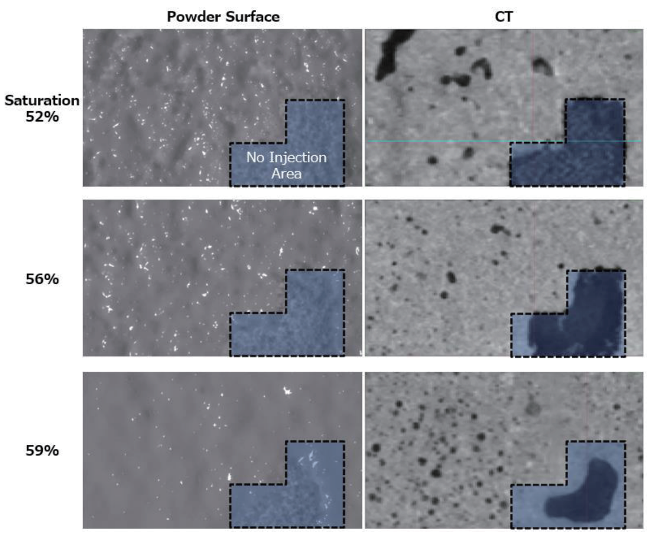

Figure 4. *Photos of Powder Surface Applied Ink and CT images for each Saturation*

Furthermore, observations revealed that the previously mentioned surface irregularities and bubbles on the powder bed occurred during the heating process in fabrication. Figure 5 shows photographs of the powder bed before and after heating. Before heating, no significant surface irregularities or bubbles were observed, and the powder bed exhibited no noticeable gloss. In contrast, after heating, surface irregularities and bubbles appeared throughout the powder bed, and gloss was also observed.

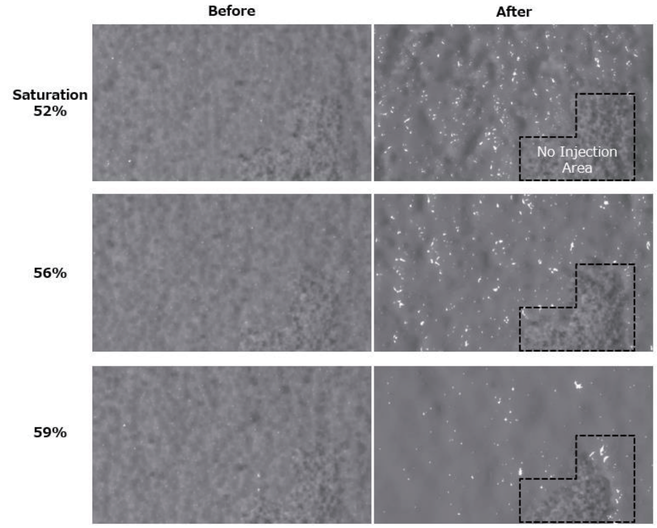

Figure 5. *Photographs of the powder bed before and after heating*

Discussion

Based on the above results, the pore formation behavior within the green bodies was considered to be classified mainly into two models.

The first model describes the case where, if the powder bed surface exhibits significant unevenness—such as during powder bed heating—the powder supplied during recoating does not sufficiently fill the concave regions, resulting in the formation of pores that remain within the green body. It has been reported that, in the particle homogenization fabrication method, insufficient homogenization due to a low amount of ink leads to the formation of pores larger than 100 µm, which is consistent with the behavior observed in this study [1].

The second model involves the hollow regions present inside the granulated powder particles; when these regions are surrounded by a large amount of ink, the hollow spaces remain as pores within the green body. In the granulated powder used in this study, hollow regions of several tens of micrometers were confirmed, which matches the observed pore sizes. Furthermore, the reason why pore formation is more pronounced when a large amount of ink is used remains unclear and is currently under investigation.

To reduce pores within the green body, it is necessary to avoid the two models described above. In other words, printing conditions and materials should be designed to produce a smooth surface and suppress bubble formation. This suggests the possibility of predicting fabrication quality based on qualitative information such as the powder bed state. Based on these considerations, we extracted image features from powder bed observation videos, analyzed the relationship between fabrication quality (relative density) and image features using machine learning, and attempted to construct a quality prediction model.

Figure. 4 shows the relationship between the predicted and measured values of relative density obtained from the constructed prediction model. The coefficient of determination (R^2), used as an evaluation metric, was calculated by cross-validation. The value of the coefficient of determination indicates a moderate correlation in general, demonstrating that build quality can be predicted from powder bed images. In the present prediction model, only planar information was used as input. However, it is expected that incorporating height-direction information will enable even more accurate predictions.

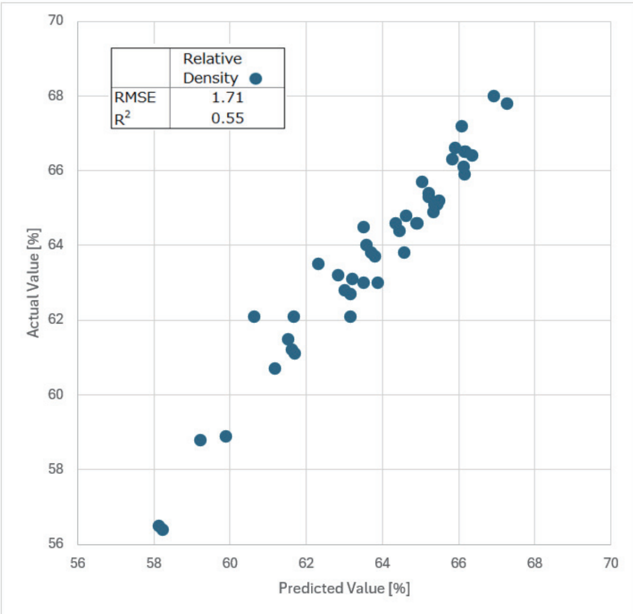

Figure 6. *Prediction Results and Accuracy for Relative Density*

Conclusions

In this study, we investigated the pore formation behavior in our original binder jetting technology, the Particle Homogenization Molding Method, by comparing in-situ observations of the powder bed impacted by ink during fabrication with CT images of the green bodies. As a result, it was suggested that internal pores in the green bodies are likely formed by two phenomena occurring during the fabrication process. Based on these findings, we plan to further improve the material and process conditions to achieve higher density and strength in future developments. In addition, the possibility of predicting fabrication quality from powder bed images was indicated. We will continue to refine the prediction algorithms and input information to construct more accurate prediction models. Ultimately, we aim to advance this technology, which is currently at the research stage, to a level where it can be applied to a wide range of fields, thereby contributing to the realization of a sustainable society.

References

[1] Kiichi Kamoda, Tadahiko Morinaga, Hiroki Hagiwara, Yohsuke Konishi, Nozomi Terai, Shota Hayakawa, and Insei Son "Ceramics Additive Manufacturing by Granulated Particle and Nanoparticle Containing Ink," *RICOH TECHNICAL REPORT*, vol. 45, pp. 122-131, 2023.

Author Biography

Yohsuke Konishi received his Bachelor of Science in Physics from Kobe University (2012) and his Master of Science in Physics from Kobe University (2014). Since then, I have been working in the technical division of Ricoh Company, Ltd., located in Kanagawa Prefecture, where I am engaged in device design and research and development of inkjet printers.

Development of metal decoration technology using on-demand thermal transfer printing

Masaya Takahashi, Kenta Suzuki, Masahito Watanabe, Hirotoshi Terao; Engineering Dept. S&C6, Alps Alpine Co., Ltd; Miyagi-Pref, Japan

Abstract

In recent years, in-car decorative elements have been developed with an eye towards autonomous driving, emphasizing comfort and coziness as key concepts. This includes a desire for interior materials to be more genuine, such as wood grain and metallic finishes, as well as designs that eliminate protruding switches in favor of seamlessness. Additionally, lighting systems like LEDs (light-emitting diodes) have been introduced, leading to a demand for more luxurious interiors. However, authentic materials are expensive and pose challenges for weight reduction and compatibility with static panels, leading to a search for alternative materials. While conventional decorative finishes typically use plating, which has a significant environmental impact, there is active development of alternative methods. One such alternative to plating is melt thermal transfer printing, which allows for high-gloss, luxurious printing with metallic inks, and can be combined with lighting systems for enhanced effects. Furthermore, there is the potential for non-conductive printing, which can be integrated with millimeter-wave or electrostatic sensors. Additionally, limitations on printing size that have been problematic in the past are now being addressed. This paper introduces the features of our on-demand metallic decorative printing using this melt thermal transfer printing technology.

1. Introduction

In recent years, with an eye toward autonomous driving in the automotive decoration sector, there has been a demand for interior materials that emphasize comfort and coziness, leaning towards genuine finishes such as wood grain and metallic finishes. Designs aim to eliminate protrusions like switches in pursuit of a seamless look, and lighting systems like LED (light emitting diode) have been introduced, resulting in a more luxurious interior space. However, real materials are costly and pose challenges concerning weight reduction and compatibility with electrostatic panels, leading to the need for alternative materials. Traditional metallic decoration techniques predominantly use plating; however, because of the significant environmental impact, there is active development of alternative methods. Notably, processes like in-mold decoration and film insert molding for vapor-deposited films have attracted attention due to their high design quality and ease of adding functionality. Decoration film methods include techniques like painting, silk screening, and gravure printing, but our company utilizes the melt thermal transfer printing method. This time, we will introduce our on-demand metallic decoration printing using this melt thermal transfer printing.

In melt thermal transfer printing, ink is melted and transferred from an ink ribbon film by applying heat and pressure with a thermal head. Since neither vacuum nor wet processes are required, this is a one-stop printing process and an environmentally friendly printing technology that does not produce hazardous waste. Since metallic materials can be made into ink ribbons, metal printing can be performed on-demand.

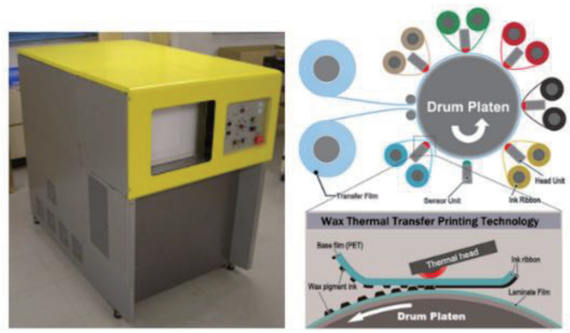

Figure 1. *Printer appearance and internal diagram.*

Figure 1 shows the external appearance of the thermal transfer printer and Internal diagram. This printer can print on film by the roll-to-roll method, and 6 colors can be overprinted in one run. Multi-color printing is possible by running multiple times. This printer can be used to create a variety of metallic decorations.

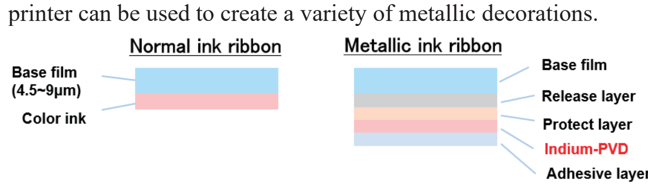

Figure 2*. Layer structure of ink ribbon.*

Figure 2 shows the structure of color ink and metallic ink. Metallic inks can be printed in the same way as color inks, and by combining them with color inks, it is possible to print metallic colors and complex designs such as patterns on metal.

2. Features of metal-like printing by Alps Alpine

This introduces our metallic printing sample displayed at 3DECOtech held at Tokyo Big Sight in January 2025. (**Figure 3**)

Figure 3. *3DECOtech exhibition in January 2025.*

2.1 Luxurious metallic luster

The metal ink ribbons used by our company are made from aluminum (Al), tin (Sn), and indium (In) materials. The gloss level of metal printing exceeds 100%, allowing for a high metallic feel in appearance. (**Figure 4**)

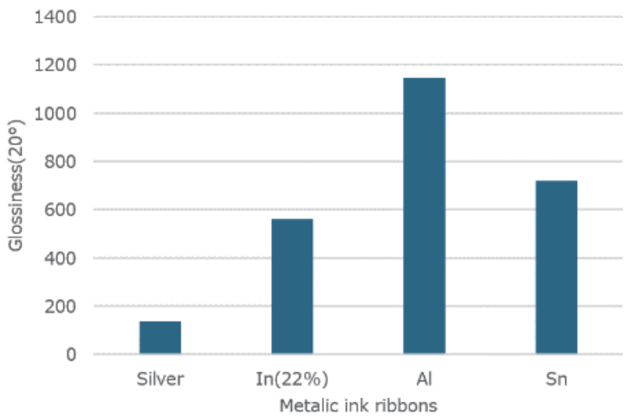

Figure 4. Glossiness of metallic ink ribbons.

By using metallic ribbons and colored ribbons, it is possible to achieve a printing expression that is both colorful and has a metallic finish.

Figures 5 (a) and (b) are examples of samples of film processed into an egg-shaped plastic, combining two-color gradation with metallic printing. By layering a two-color gradient over metallic printing, the sample becomes glossy and luxurious. Since there is no gradient in the name portion, the underlying metallic part is exposed, highlighting the logo.

(a) Appearance

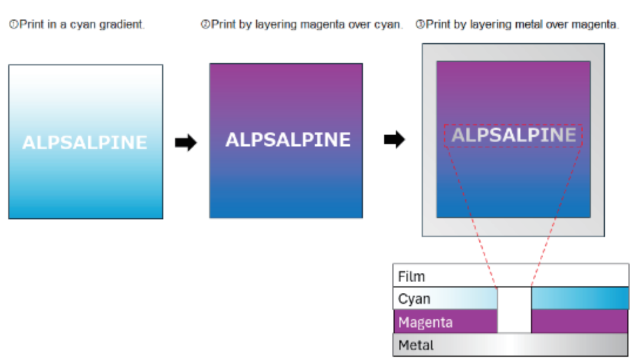

(b) The process of ink layering

Figure 5*. A film combining two-color gradation and metallic printing is processed onto egg-shaped plastic.*

2.2 Coexistence of Metallic Luster and Light Transmittance

Figure 6 is a sample using a vapor-deposited ink ribbon. Since the transmittance can be adjusted, it is possible to maintain metallic luster while allowing light to pass through. Additionally, the transmittance can be adjusted, allowing for both transparency and luster to coexist.

Figure 6. *Decorative molded products made of metallic ribbons* that allow both metallic luster and light transmission.

By combining transparent metallic inks and color inks, and installing a backlight device, it is possible to create products with a high gloss finish that transmit light while maintaining a metallic appearance. By changing the transmission rate of the metallic ribbon, the gloss can be controlled, and by using mask printing, the paths of light transmission can be controlled, allowing for color control with color printing, which also enables the creation of various designs utilizing transmitted light. (**Figure 7**)

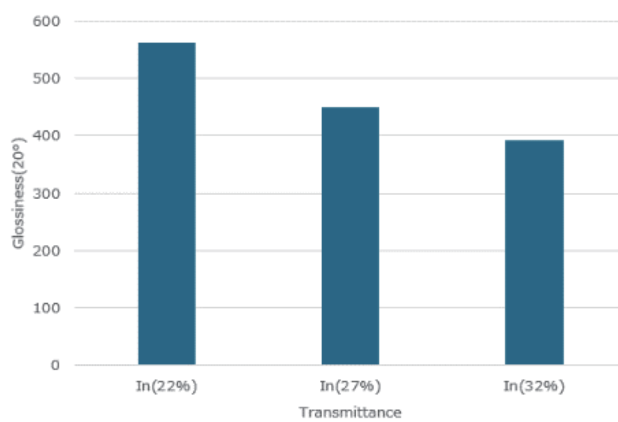

Figure 7. *Transmittance and glossiness of ink ribbons.*

2.3 Stealth Printing

Furthermore, in recent years, examples of Stealth Printing, which has been attracting attention in automotive and indoor equipment, are shown in **Figure 8**. When not illuminated, it has a metallic appearance, but when lighted, logos and symbols can be made to stand out (**Figure 9**). As shown in **Figure 10**, the gloss effect can be created by reflecting external light with metallic ink, and since metallic ink is translucent, it can also produce light expressions through backlighting. In addition, as shown in **Figure 11**, it is also possible to add color effects from white light of backlighting by placing colored ink ribbons in the transparent areas.

Figure 8. Stealth printing.

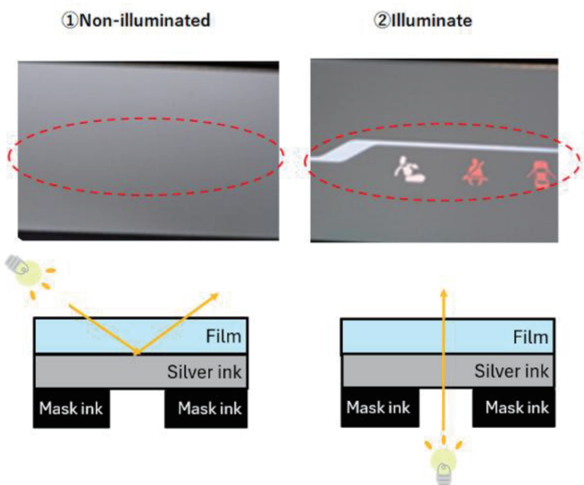

Figure 9. The appearance of stealth printing during illuminated and non-illuminated.

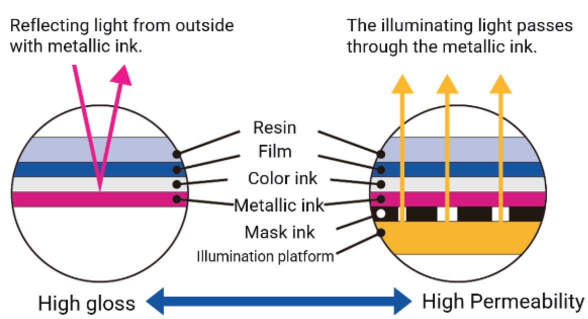

Figure 10. The mechanism of stealth printing.

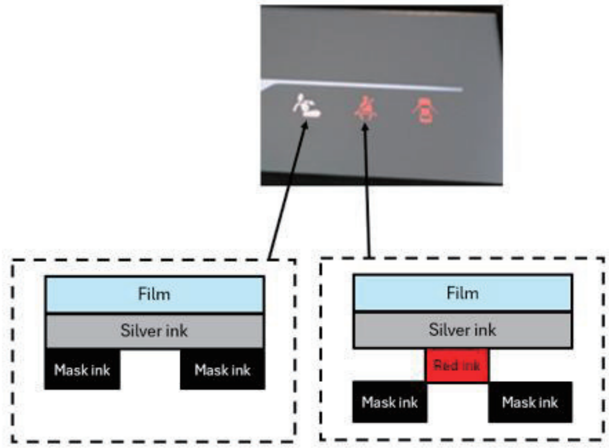

Figure 11. Control of transparency color.

As shown in **Figure 12**, by cutting the area where light passes with a laser due to illumination, it is possible to create any pattern. Since the metal ribbon has a very thin structure with an ink film thickness of about 0.1 to 2 μ, which is much thinner compared to screen printing, it demonstrates excellent processability when removing ink with techniques like laser processing. Therefore, it becomes possible to process molded products, such as hazard marks seen in vehicle emblems like in **Figure 13**, by combining laser processing with pad printing and other techniques.

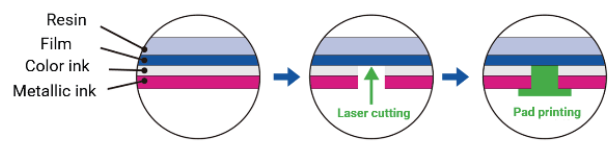

Figure 12. The process of decorative molding products using laser cutting and pad printing.

Figure 13. Laser-cut and pad-printed molded products.

2.4 Non-conductive

Normal metals are conductive, but it is also possible to create prints with non-conductive properties using metallic ink ribbons By performing non-conductive metallic printing, it enables combinations of non-conductive sensors, such as electrostatic sensors and millimeter-wave radars, which cannot be used if conductive, with metallic decorative elements. (**Figure 14**)

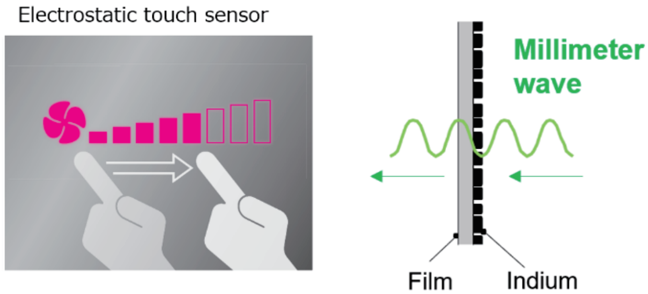

Figure 14. *The function of metallic decoration printing.*

Figure 15 is a scanning electron microscope (SEM) image of a metal ribbon that uses indium for its deposition layer. The indium nanoparticles have an island structure with gaps in the insulating structure. Therefore, it is possible to provide functionality for radio wave transmission, such as millimeter waves. In fact, the surface resistivity of the ink ribbon is over $10^9\ \Omega$, demonstrating insulating properties. Additionally, since it is an insulator, it can be combined with electrostatic operation modules without causing malfunctions, allowing for added functionality.

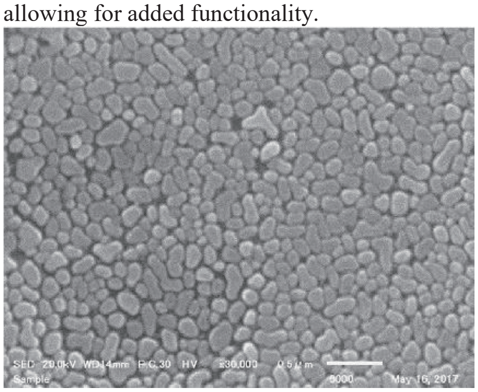

Figure 15. *SEM images of Indium ribbon.*

3. Support for large size and wide format printing

In our melt thermal transfer printing, in order to address the conventional issue of printing size limitations, we have developed a new printer that supports 12-inch printing in the width direction, and we are using both the conventional 6-inch printer [MDD (Micro Dry Decoration™)6] and the 12-inch printer [MDD (Micro Dry Decoration™)12]. Appearance photos and basic specifications of each printer are shown in **Figure 16**. The 12-inch printer can handle printing sizes up to 320 mm × 3000 mm, and the printing resolution can support up to 1200 dpi (dots per inch). This enables us to accommodate various sizes used in automotive applications, and as shown in **Figure 17**, we are advancing our support for automotive products, including customized cars under the ALPINE STYLE™.

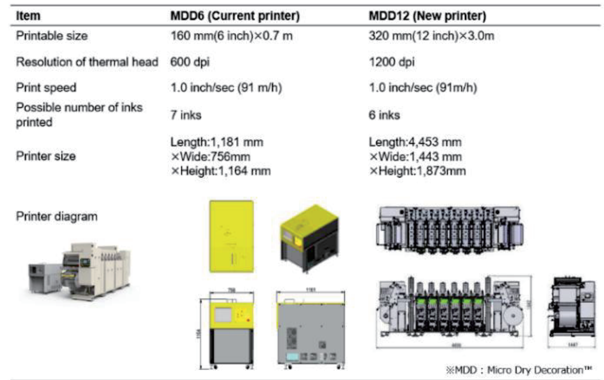

Item	MDD6 (Current printer)	MDD12 (New printer)
Printable size	160 mm(6 inch)×0.7 m	320 mm(12 inch)×3.0m
Resolution of thermal head	600 dpi	1200 dpi
Print speed	1.0 inch/sec (91 m/h)	1.0 inch/sec (91m/h)
Possible number of inks printed	7 inks	6 inks
Printer size	Length:1,181 mm ×Wide:756mm ×Height:1,164 mm	Length:4,453 mm ×Wide:1,443 mm ×Height:1,873mm
Printer diagram		

※MDD : Micro Dry Decoration™

Figure 16*. Photos of the printer's appearance and basic specifications.*

Figure 17. *The automotive product called "ALPINE STYLE™" that uses our decorative products.*

References

[1] K. Suzuki, M. Watanabe, H. Kobayashi, Y. Oishi, H. Terao, H. Sato, and K. Yamamoto, "Thermal transfer decorative printing for realistic textures feeling", Proceeding of the Imaging Society of Japan (Imaging Conference JAPAN 2019), DP7-01, pp. 239-242 [in Japanese].

Author Biography

Masaya Takahashi completed the Graduate School of Science and Technology at Iwate University in 2022, majoring in Material Science. He joined Alps Alpine Co., Ltd. in 2022. Since then, he has been engaged in the development of thermal control technology for thermal transfer printers and decorative printing technology.

Kenta Suzuki graduated from the Faculty of Engineering of Tohoku University (Department of Chemical and Bioengineering) in 2012. He joined Alps Alpine Co., Ltd. in 2013. Since then, he has been engaged in the development of thermal control technology for thermal transfer printers and decorative printing technology since 2013.

Masahito Watanabe graduated from Kanazawa University's Faculty of Engineering (Department of Electrical and Information Engineering) in 1999. He joined Alps Electric Co., Ltd. (now Alps Alpine Co., Ltd.) in 1999. He has been engaged in the development of thermal control technology for thermal transfer printers and decorative printing technology. Currently, he is responsible for technology development management across all areas of thermal transfer printing technology.

Hirotoshi Terao graduated from the Department of Metallurgical Materials of Akita University in 1991. In the same year, he joined Alps Electric Co., Ltd. He is currently the Department Manager of the engineering dept. S&C6 at Alps Alpine Co., Ltd. He holds a Ph.D. in Engineering. Since joining the company, he has been involved in the development of thermal heads and the core technology development for thermal transfer printers. He is a director of the Japan Society of Imaging Science and Technology and a director of the IS&T Tokyo Chapter.

A New 12-inch, 1200dpi Thermal Printhead for Digital Decorative Film Printing

Hiroya Nishida, Tsuyoshi Ando, Yoshiyuki Kondo, Shu Maehara, Shuusaku Higashi, Ryo Shimizu; Kyocera Corporation

Abstract

In the field of decorative film printing, there is a demand for digital methods that can handle thick film ink and metallic materials, but conventional technologies have been difficult to cope with. To address this issue, we have developed a new 12inch 1200dpi thermal print head with a unique structure.

This thermal printhead has achieved high resolution by optimizing the heater element design and has greatly improved ink over-layering performance by optimizing the height of the protrusion structure of the heater element. This solves the problems of gradient and ink over-layering performance (Ink over-printability) of conventional models and enables on-demand multilayer printing of thick-film materials that could only be handled by analog printing.

Introduction

In recent years, in the field of decorative film printing, such as for automobile interiors, there has been a demand for a shift to digital printing from the viewpoint of diversifying designs and adapting to small lots. However, digital printing has challenges in handling the thick film inks and metallic materials required for these applications, and as a result, the industry continues to rely on traditional analog methods such as gravure printing and screen printing.

To solve this problem, our company has developed a new thermal printhead for thermal transfer printing. This product enables high-precision temperature control with its unique heater element structure and is compatible with on-demand multilayer laminate printing of thick film ink that could only be handled by analog methods and metal deposition/functional materials. In addition, the wide and high resolution of 12inch width and 1200dpi is realized at the same time. Decorative film printing using a printer equipped with this thermal print head has already been put on the market for use in automobile interiors.

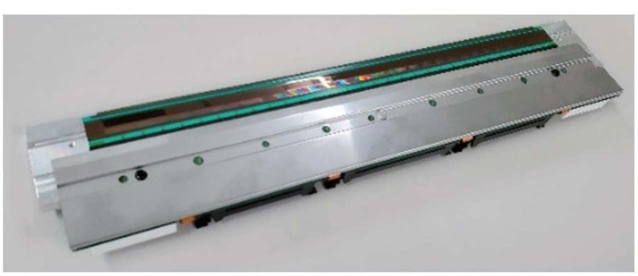

Figure 1 : New developed thermal printhead 12-inch, 1200dpi

Overview of Thermal printhead

The precise thermal control technology of thermal printhead is expanding its application to a wide range of industrial fields. One typical application is monochrome label printing in logistics and product manufacturing management. The ability to print clear barcodes and identification information at high speed and low cost is an essential foundation technology for modern supply chains. It is also widely used in the field of coding and marking, in which the best before date is printed on soft food packaging films. In this application, printing with both high followability and durability is required for the printed material moving on the high-speed production line.

In addition, the use of the sublimation thermal transfer method enables even higher quality color printing. In the card printing field, we are contributing to the formation of high-resolution face photos for government-issued ID cards and financial cards. Similarly, in the field of photographic printing, it has achieved smooth gradation expression and excellent storability comparable to conventional silver-halide photography, making it an established alternative technology. An advanced application of these technologies is decorative film printing, which adds wood grain and metal-tone designs to automobile interior components. This is an advanced application that enhances the added value of products by taking advantage of the characteristics of digital printing, which eliminates the need for gravure cylinder.

The thermal printhead is a core device that converts electrical energy into thermal energy to achieve high-definition printing. Its basic structure is precisely laminated multiple thin film layers with different functions. First, a ceramic substrate is used as the mechanical support for the entire head. This substrate has the properties of physically stabilizing the entire structure while simultaneously providing excellent thermal conductivity and electrical insulation. A glassy glaze layer (heat storage layer) formed on top of the glaze temporarily stores the thermal energy generated by the heater element. This makes the temperature-rise characteristics steeper, enabling instantaneous and concentrated heat transfer to the printing media and improving the sharpness of print dots. Heater elements that form printing pixels are arranged in a high-density array on the glaze layer. It is generally composed of a thin film resistor, which generates Joule heat in response to an external drive current, resulting in an instantaneous high temperature. These individual heater elements form the smallest printing unit, the dot.

A hard material is deposited on the top surface to protect the internal elements from physical abrasion and chemical effects caused by contact with the print media.

By organized interlocking these multilayer structures, digital electrical signals are precisely converted into physical thermal patterns, resulting in high-speed, high-quality printing.

Technical Improvements

There are two major issues related to image quality in the development of thermal printheads for decorative printing applications. The first is the lack of resolution. This has been confirmed to affect the quality of printing sharpness, the gradation of color, the reproducibility of 1 dot and line, and the smoothness of images in the current top-of-the-line 900dpi model. Gradation, which has received a lower rating in 4 points scoring, has been required an improvement.

Second is the problem of heat in the heater element. Heat directly affects the "Over-layering performance" of the ink, and even the top model received a "Not Bad" rating. It has also been found that this thermal problem affects other quality factors such as "sharpness" and "gradation." To solve these problems, we developed technologies. (See Table 1)

Table 1 : Thermal printhead performance comaprison - Conventional model

Print test check points			Result	
Category	Key Parameter	Print Image	Standard 600dpi	High spec 900dpi
Ink Over-layering performance	Heat response Local Pressure to media		3	2
Sharpness	Resolution Heat response		3	4
Gradation	Resolution Heat response		2	2
1dot line	Resolution Heat response	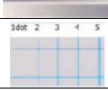	3	3
Print Smoothness	Resolution		2	3

*4-points scoring - 4:Excellent, 3:Good, 2:Not bad, 1:Poor

First, I will explain our efforts to improve resolution. We optimized the heater element design to solve the problems of conventional models.

To achieve high-definition print quality, we used heat generation temperature simulation to analyze the temperature distribution under various conditions in detail. In the temperature distribution simulation (see Table 2), we evaluated the temperature behavior at 1 dot, 10 dot, and 100 dot heating as the width (A, B, C) and length (D, E, F) of the heater element were changed based on 600dpi. Temperature concentration was observed under the condition of the smallest heater element width and length, but the optimum balance had to be searched. Based on these simulation results and the examination of the internal structure described later, we determined the optimum design value that can achieve both high resolution and higher quality printing.

Table 2 : Heat distribution map by simulation test

	Heating (Pulse) frequency		
	After 1 pulse	After 10 pusle	After 100 pusle
Ref. 600dpi	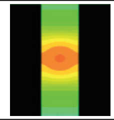		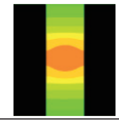
Optimized Heater size for 1200dpi	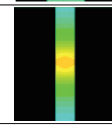	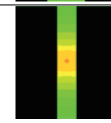	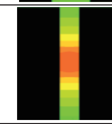

Next, we are working to eliminate the heat problem and improve ink over-layering performance.

To optimize the thermal effect from the heater element, we adopted a method of adding a protrusion structure to the heater element and optimizing its height. (See Figure 2) A detailed evaluation was conducted on a sample in which the height of protrusion of the heater element was changed to "h0 (no protrusion), h1, h2, h3". The two primary evaluation items are the percentage of ink miss-over-layering and the percentage of media residue remaining. As for ink over-layering performance, the evaluation standard was that the ink can be over-layered stably regardless of the applied energy differences. (E < F < G)

The key here is to optimize the trade-off between better ink over-layering performance and media residue remining. (See figure 3) The horizontal axis shows the height of the protrusion of the heater element, the left vertical axis shows the ink miss-over-layering ratio, and the right vertical axis shows the remining ratio of the media residue. As a result of the evaluation, it was confirmed that the ink over-layering performance improves in proportion to the height of the protrusion of the heater element, but at the same time, the remining ratio of the media residue increases.

As a result of examining this trade-off, we determined that the height of the protrusion "h2" is the optimum value for suppressing the generation of media residue while ensuring the ink over-layering performance. As a result of this optimization, the target value of "ink miss-over-layering ratio of 0.5% or less" was achieved for all applied energy conditions E, F and G.

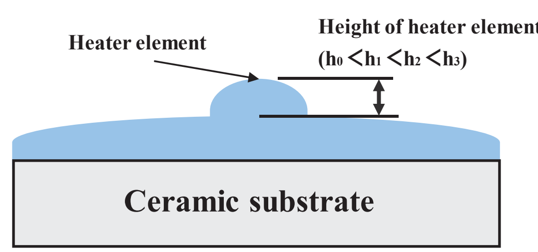

Figure 2 : Thermal printhead (Heater element) Cross Section
***Rough image (Free scale)**

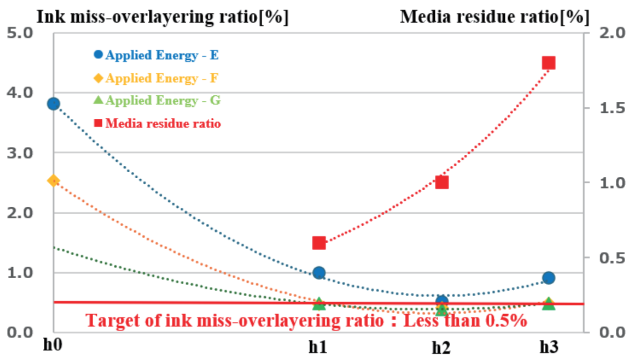

Figure 3 : Ink miss-over-layering and media residue ratio by height of heater element

The technical improvements described below (See table3), namely, higher resolution by optimizing the heater element design and improved ink over-layering performance by optimizing the height of the protrusions of the heater element, have greatly solved the image quality problems of the conventional models.

As shown in the evaluation results table, the following results were confirmed when comparing the current top-of-the-line model (900dpi) with the prototype head (1200dpi).

- Ink over-layering performance:
Improved from "Not bad" to "GOOD"

- Sharpness:
Keeping at "EXCELLENT"

- Gradation:
Improved from "Not" to "Good "

-1 dots and lines and print smoothness:
Improved from "GOOD" to "EXCELLENT"

This improved overall print quality and enabled us to respond to the market demands.

Table 3 : Thermal printhead performance comparison - New developed model

Print test check points			Result		
Category	Key Parameter	Print Image	Standard 600dpi	High spec 900dpi	New develped 1200dpi
Ink over-layering performance	Heat response Pinpointo Pressure to media		3	2	3
Sharpness	Resolution Heat response	 5pt	3	4	4
Gradation	Resolution Heat response	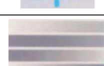	2	2	3
1dot line	Resolution Heat response	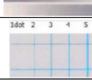 1dot 2 3 4 5	3	3	4
Print Smoothness	Resolution		2	3	4

*4-points scoring - 4:Excellent, 3:Good, 2:Not bad, 1:Poor

Conclusion and the future vision

In this research, we developed a new thermal print head with the aim of achieving both high resolution and ink over-layering performance, which were technical issues with conventional models. There are two main technological breakthroughs.

1. By optimizing the heater size based on heat generation temperature simulation and making full use of fine patterning technology, we achieved a high resolution of 1200dpi.

2. The protrusion height of the heater element was optimized. As a result, we have succeeded in controlling thermal energy transfer precisely and significantly improving ink over-layering performance.

In conclusion, we have simultaneously established both the size of the heater element and its structure in terms of the high-definition drawing performance and the excellent heat transfer efficiency for thick-film ink, which had previously been a trade-off. The high-resolution and high-definition technology established in this development is an important technological foundation to achieve the next-generation requirements of the digital decorative film printing market.

In the future, this application is expected to need even higher speeds in addition to wider print width and higher print quality. Based on the knowledge obtained in this development, we will further advance these elemental technologies and promote research and development aiming at overall performance improvement.

Author Biography

Hiroya Nishida joined Kyocera Corporation in 2013.
After joining Kyocera, he has been involved in the development of thermal printhead process and design.

End of report.

Peripheral Technologies for Enhancing Print Quality in the ID Photo Booth "Ki-Re-i"

Nobuyuki Kamitani, Dai Nippon Printing Co., Ltd., Tokyo, Japan

Abstract

The "Ki-Re-i" ID photo booth is equipped with a dye-sublimation printer and incorporates a range of peripheral technologies to achieve high-quality prints. This presentation outlines the evolution of "Ki-Re-i" from silver halide-based systems to the current digital format and highlights key image processing technologies such as optimized lighting design and ICC-based color reproduction.

These technologies enable the faithful rendering of natural skin tones and shadows, meeting the stringent quality standards required for official documents such as passport photos. Additionally, the system features network connectivity for enhanced user convenience and remote quality management, as well as robust enclosure design for outdoor use and security.

Through specific case studies, we demonstrate how these technologies maximize the performance of dye-sublimation printers, contributing to improved customer satisfaction and reduced downtime.

Introduction

Since the late 1990s, ID photo booths have transitioned to dry systems with the adoption of dye-sublimation printers. Following the transfer of the ID photo business from Konica to DNP in 2008, all "Ki-Re-i" booths have been equipped with dye-sublimation printers.

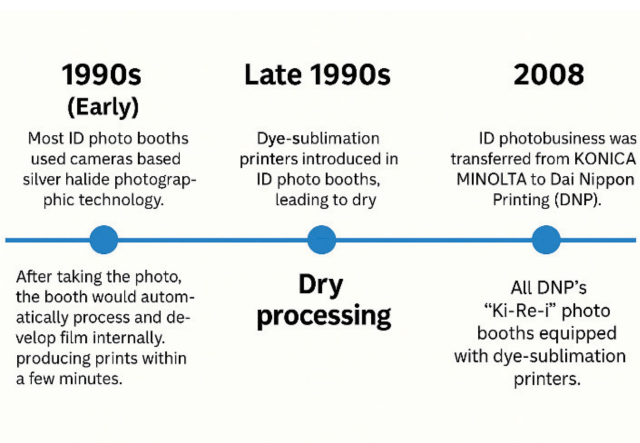

Figure 1. *History of dry processing in ID photo booths*

DNP has consistently prioritized high print quality, developing not only the booth hardware but also proprietary techniques for optimizing in-house print media. In response to societal needs, the system has evolved to support electronic payments, multilingual interfaces, and more recently, applications for Japan's "My Number" identification system. The development of the "Ki-Re-i" booth emphasizes the following key elements.

Figure 2. *"Ki-Re-i" supports electronic payment*

Figure 3. *"Ki-Re-I" enables photo capture and application for My Number Card*

Booth design optimized for ID photography (lighting, surface coating, security features)

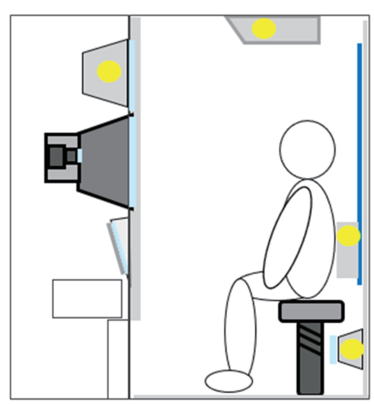

Figure 4. *Lighting and other enhancements suitable for ID photos*

Image processing tailored for ID photos (tone curve optimization, ICC-based color management). The captured images are deployed to two services.

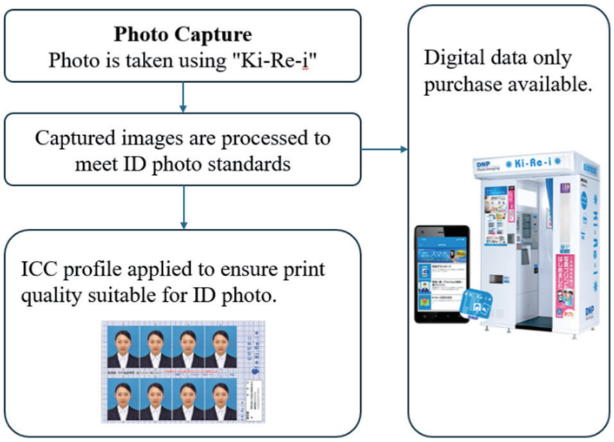

Figure 5. The captured images and two services

Network integration for enhanced service and maintenance (online applications, remote diagnostics)

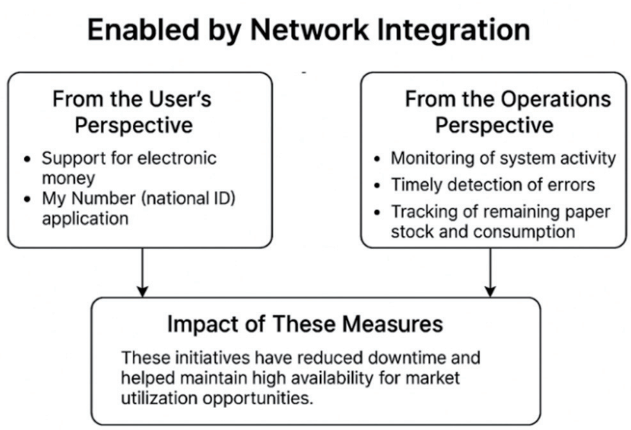

Figure 6. Advantages of network integration

Booth Design Optimized for ID Photography

Lighting is strategically placed at the front, top, and rear of the booth to utilize reflected light within the shooting chamber, creating natural shadows and a sense of depth while avoiding harsh contrasts on the face and neck.

To maximize lighting efficiency, the interior has been painted white.

Figure 7. A white interior was chosen to maximize the effectiveness of the lighting system

Lighting is strategically positioned to reduce shadows created by facial contours.

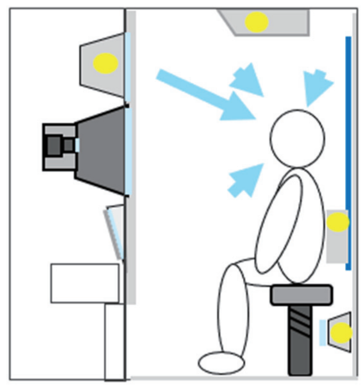

Figure 8. Contour-aware lighting design

Given that many booths are installed outdoors, the design incorporates measures against rain leakage, corrosion, and vandalism, drawing on extensive know-how in weatherproof and security-conscious design.

"Ki-Re-i booths are designed for diverse environments, including coastal areas with salty air, rainy and windy locations, and snowy regions with heavy accumulation.

Figure9. Outdoor installation subject to wind, rain, and snow exposure

An Electrostatic powder coating is applied to the surface to prevent rust-induced corrosion, providing the benefit of a thicker and more durable film.

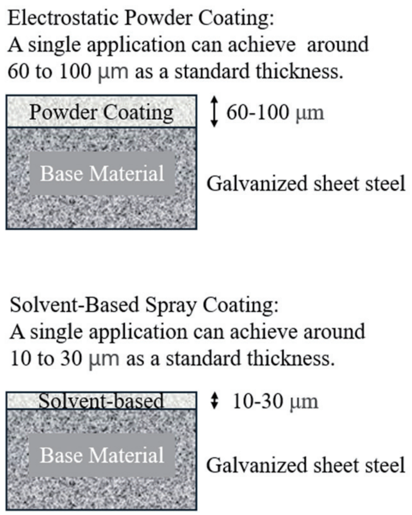

Figure 10. *The thickness of the coating protects the enclosure from corrosion*

“Ki-Re-i” features a strong-looking lock and built-in security measures based on proprietary know-how. With the adoption of comprehensive anti-theft measures, there have been no reported theft attempts in recent years.

Figure 11. *All “Ki-Re-i” units feature a lock designed to appear robust, enhancing its security presence*

In the printing industry, there exists a unique expertise characterized by the principle of making printed materials appear “slightly better than the original.” This know-how has been cultivated through the process of responding to client requests—typically editors or publishing houses—regarding image and color adjustments. The objective of this approach is to deliberately enhance the visual impression of printed images, thereby achieving a more refined appearance than the actual subject.

Such accumulated expertise includes techniques such as optimizing facial skin tones using specific ratios of CMY (cyan, magenta, yellow), or rendering cherry blossoms in landscape photographs with a soft pink hue to evoke a stronger emotional impact. These practices reflect a deep understanding of how subtle color manipulation can influence perception.

Figure 12. *An example of a slight improvement*

With a clear understanding of the general purposes and applications of ICC profiles, our closed system leverages color management systems and ICC profiles to achieve desirable color reproduction effectively. Built upon this technical foundation, we incorporate the printing industry’s know-how of “making things look slightly better than reality.”

For example, in skin tone reproduction, we aim for natural hues that avoid extreme shifts toward reddish or bluish tones, while also ensuring that facial shadows caused by contours do not appear overly pronounced. Similarly, in hair rendering, particular attention is paid to preserving detail in darker areas by carefully managing tonal gradation in the shadow regions.

By integrating technical precision with industry experience, we continue to pursue improvements in image quality that inspire users to “want to print again”.

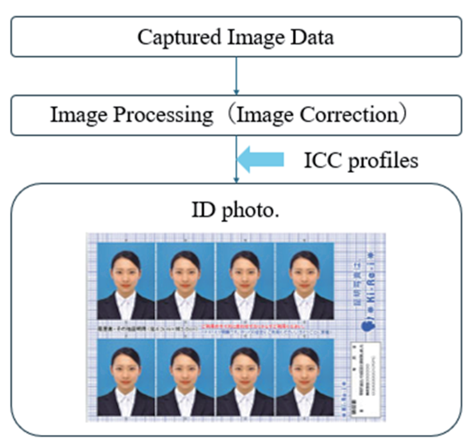

Figure 13. *Color workflow with ICC profiles*

Conclusion

The "Ki-Re-i" ID photo booth delivers consistently high quality from capture to print through its comprehensive design, which emphasizes image quality, color fidelity, user convenience, and security. The system supports natural skin tone reproduction and accurate color expression tailored to the characteristics of dye-sublimation media and complies with international standards for passport photos (ICAO). The low rejection rate in passport applications attests to its high quality. Furthermore, network connectivity enables support for My Number applications, automatic software updates, remote monitoring, rapid troubleshooting, and improved maintenance efficiency. Through these technologies and operational capabilities, "Ki-Re-i" continues to provide value to society.

Author Biography

Nobuyuki Kamitani received his B.E. in Mechanical Engineering from Waseda University in 1994. He began his career at Sony Corporation, where he was involved in the mechanical design of thermal printers for medical and professional dye-sublimation applications. In 2011, he transferred to Dai Nippon Printing Co., Ltd., where he has since been engaged in system development.

Enhancing Quality and Standardisation in Flexographic Printing: the need to embrace Big Data

Enn Kerner, EUR ING, board member of Engineers Europe

Abstract

The most valuable asset of a printing company lies with the optimal technical performance of the printing machine, and this must be given the highest priority in ensuring quality. Whilst flexographic (flexo) printing for flexible packaging has seen significant growth, notably with the integration of ECG, itself reducing costs by minimising the need for spot colour inks and supporting sustainability by reducing ink waste, many companies still lack the in-house expertise to manage the complexity of Big Data required for ECG implementation, often relying on third-party advisors. This article explores advancements and challenges in flexographic (flexo) printing, particularly those related to managing quality and achieving standardisation requirements when implementing Extended Colour Gamut (ECG) printing, often reverting to third-party support. The core challenge lies in the plethora of variables reported by the flexo printing machine, forming the record of running performance long term, effectively summing to constitute a repository of Big Data. In the context of this paper, Big Data refers to the extensive array of physical and chemical variables mining and recorded by the flexographic printing machine throughout its operational lifecycle. Big Data, in this sense, provides the foundation for process optimisation, predictive maintenance, quality assurance, and colour standardisation across production runs. Other variables, such as printing plates, double-sided adhesive tapes, and anilox rollers, play an important role in the process, they are regarded as consumables with significantly shorter lifespans compared to the printing machine itself, and their impact on quality can be more readily judged and corrected in real time. Unlike other printing methods like offset, which benefit from clear ISO guidelines to achieve standardisation, flexo printing in comparison lacks a formal standardisation process, making it difficult to maintain consistent control of image quality and colour reproduction arising from factors such as pressure settings and image raster adjustment. To eliminate this contradiction, a corresponding process has been initiated in cooperation with market leaders and FOGRA, which will be launched in 2025.[3] Companies need to tackle these challenges by establishing internal capabilities for handling their machine reported Big Data, including machine fingerprinting and monitoring of critical variables within the production process. To adopt ECG effectively, companies need to assess factors such as data availability, internal plate production, and compliance with quality standards. The significance of skilled in-house engineers who are experts in colour management, quality control, and data analysis cannot be underestimated. As digitalisation advances in flexo printing, the role of these professionals becomes vital for maintaining consistent quality and operational efficiency through the control of Big Data, requiring a comprehensive understanding of the entire value chain and precise control over all variables in the printing process. The article concludes that with appropriate standards and in-house expertise, companies can successfully implement ECG, ensuring the quality and consistency of their printed products worldwide. This is reflected already in those cases where companies successfully implement ECG printing systems.

Index terms – *Flexographic (flexo) Printing Technology, Process Standardisation, Colour Management, Machine Fingerprinting, Continuous Quality Control, Big Data.*

Introduction

Modern technologies in flexible packaging printing have reached new heights with the implementation of an extended colour gamut. The latest digital inkjet technology streamlines this process, as advanced printhead nozzles enable precise pixel manipulation and complete control over process colour ink application on various substrates.

For advertising and publications printed using offset technology, process monitoring has been achieved to a high standard by adhering to ISO 12647-2 [6] and Process Standard Offset (PSO) [7] requirements. These standards outline comprehensive value-chain datasets and colorimetric values specific to each printing technology.

In contrast, this standard-based advantage is absent when discussing meeting the quality requirements in gravure and flexographic (flexo) printing. This is particularly evident in the specific issue of how well print providers can control image raster Colour Value Increases (CVI) and their relation to the applied pressure on printing forms and substrates. We are consistently confronted with the challenge of assessing how effectively these processes can be standardised to ensure a unified value chain and repeatable production outcomes in daily manufacturing. While these ongoing challenges are often disregarded, flexo printing for flexible or corrugated packaging continues to lack progress in standardising processes, leaving many companies to depend on in-house management and external expertise to analyse and define suitable colour spaces for their key investments, including those for new printing machines. Only a few major players in the global flexible packaging market appear to be positioned to value their assets fully by controlling their flexo printing machine reported Big Data, thereby minimising risks associated with third parties.

This article discusses the advancements and challenges in flexographic (flexo) printing technology, particularly those related to managing Big Data to provide full process control when implementing Extended Colour Gamut (ECG) printing.

This article aims to address the following issues:

1. Do flexo printing companies manage their value chain and printing machine reporting Big Data, and if so, how?
2. Are flexo printing companies fully aware of their most critical assets—specifically, printing machine fingerprint conditions—and able to control them daily?

During undersigned visits to various flexographic printing providers, it was observed that data management is frequently outsourced to third-party reproduction houses. Historically, reproduction house services were convenient for supplying flexographic printing plates; however, with the digitalisation of printing processes, in-house expertise has become essential for monitoring and adjusting printing variables daily.
With the digitalisation of printing processes and the advent of high-tech flexographic common impression cylinder (CI) presses (or modular presses), in-house expertise is essential to monitor and adjust printing variables daily. Therefore, having skilled printing technology engineers on-site is becoming a critical asset for any significant print service provider. These professionals must possess comprehensive knowledge of colour management and the entire value chain, as well as the ability to analyse data and implement corrective measures to eliminate issues and maintain or improve quality. Use of the Simplex method to optimize CMYK input values so that, after printing, the measured TVI matches a target TVI curve (such as ISO 12647-2 and 12647-6 standards). The Simplex Search is based on Nelder-Mead Simplex Method, is a direct search method used to find the minimum (or maximum) of a function in a multi-parameter (n-dimensional) space.
Notably, parallel to the analytical needs of the print service provider sector, many flexo machine manufacturers now operate their own repro and plate-making departments—a further indication of the growing importance of pan-industry Big Data control.

Factors to consider before adopting ECG in flexographic printing

In the early 2000s undersigned participated a project at a world-leading flexo print service provider pioneered the Extended Colour Gamut (ECG) printing process using the Opaltone system. This company successfully implemented ECG across all group operations by controlling their entire value chain's Big Data. This innovation significantly reduced costs, mainly by minimising the need for spot colour inks, and supported sustainability by reducing leftovers of waste inks. Due to the implementation of ECG technology in flexo technology and in cooperation with creative agencies, the aforementioned printing service provider did not have to deal with mixing spot colours and could leave ECG printing inks in the machine. As a result, machine downtime due to wash time for colour changes was reduced and production throughput increased.

Implementing ECG in flexographically printed packaging has become a significant trend, yet many companies lack in-house expertise and turn to third-party advisors. There are many consulting companies, but the standardization process and continuous quality improvement require daily presence.

Before adopting ECG, factors to consider include the availability of comprehensive Big Data, in-house production of flexographic plates, adherence to quality standards, and expertise in colour management.

Today, approximately 25 years later, the implementation of ECG in flexo-printed packaging has become a significant trend. Still, often the majority of companies feel compelled to give up the quest because of the lack of access to in-house competence. This has led to a growth in resorting to third-party advisors offering ECG implementation services. Despite specific expertise residing with such advisors, the essential connection between raw materials, machine design, parameters and reproducibility of graphic requirements is, by definition, lacking when the expertise is not physically in-house and on-board daily. Especially in the case of remote monitoring, the parameter input remains insufficient whilst the quantity becomes overwhelming.

Before implementing ECG (Extended Colour Gamut) printing, companies must carefully evaluate the following factors, grounded in logical reasoning and deductive analysis by Nelder-Mead Simplex Method.

Applying the first stage Nelder-Mead method into a 4-colour printing process:

a. Start with 5 CMYK combinations;
b. Simulate or measure the TVI response from each;
c. Compute the sum of squared errors to the target;
d. Iterate via reflection, expansion, contraction, or shrink;
e. Stop when ΔTVI is minimized.

1) The availability of comprehensive printing machine Big Data for four-colour process printing
a. A **critical challenge** in four-colour process printing is maintaining stability daily. The in-house quality department must monitor the following key variables:
b. **Pressure setting** based on the machine fingerprint data, which directly affects colour reproduction during printing

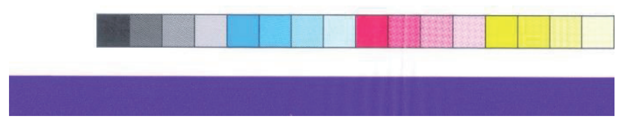

Figure 1 Four colour printing control patches. [1] [3]

c. **Achieving stable pressure values** to establish a correlation between the pressure settings during the fingerprinting process and the optimal colour shades on the substrate.
d. **Accuracy** in the secondary colours is required to monitor consistent print quality in four colour process printing.

Figure 2 Four colour printing control patches with overprint control patches [1] [3]

2) Consistency in the in-house production of flexographic printing plates [2]
a. Producing flexo plates internally offers advantages such as increased speed, security for proprietary processes, and intellectual property protection.
b. In-house production allows for faster resolution of non-conformities, minimising interruptions to manufacturing processes.

3) Adhering to four-colour process printing quality standards (i.e. ISO 12647-6)
a. The correlation between ink pigmentation and printing ink viscosity. Defining the ink pigmentation percentages and their relationship to ink viscosity settings are essential for the standardisation of the print process.

b. The correlation between the chosen anilox rollers and press performance. Using the appropriate anilox roll specification (lines per cm or lines per inch) ensure optimal ink performance and consistent ΔE values.

Substrate ΔE_{00}	All patches ΔE_{00}		Maximum ΔC_h
	Mean	95% quantile	composed grey
A.0	B.5	C.0	D.5

Table 1 List of optimal ΔE values during the print process [3]

c. Monitoring critical variables Colorimetric Tone Value (CTV) needs to align with the pressure settings (1b.) and stability measures (1d.)
d. Ensuring compatibility between the smallest dot size and the chosen anilox roller results in effective print reproduction and avoids dot dunking.

4) In-house colour management expertise
a. Establishing in-house standards that align with international requirements (ISO 12647-6) ensures print uniformity.
b. Having the necessary tools available for daily quality assurance like spectrophotometers, dot size and dot shape evaluation devices, and ICC profiling tools ensure consistent print quality.
c. The quality control personnel should possess expertise in optical physics and colour theory so they can perform logical and deductive analysis of the daily manufacturing data.

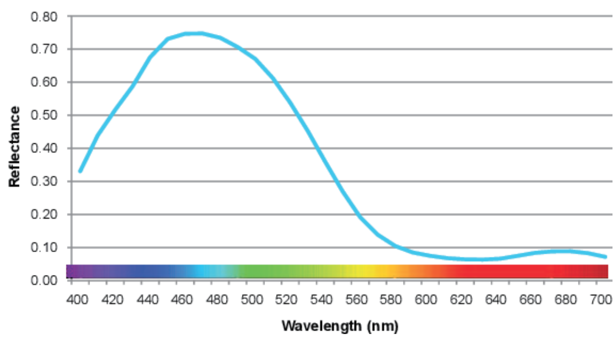

Figure 3 Example of spectral reflectance curve used during the quality control process [8]

5) Control of key variables
a. Clear decision-making rules for material procurement and quality control need to be established.
b. Changes in materials such as inks or adhesives require thoroughly evaluating variables, including supplier data on ink pigmentation levels.
c. Decisions should not only be cost driven. Reduced ink costs must be evaluated against pigmentation percentages (changes in ΔE towards the standard ink profile) and print mileage per kilogram.

6) Stability across shifts and over time
a. All shifts must maintain uniformity in process management, especially in multinational enterprises.
b. Key parameters must be recorded and documented during shift handovers to ensure continuity.
c. Quality control teams and management staff should track and analyse logged data inputs effectively.
d. The printing company's engineer's must be able to continuously improve the printing machine printing and speed setting curves, in daily routine.

7) Current percentage of non-conformities
a. Recorded non-conformities should undergo a systematic case-by-case analysis using logical and deductive methodologies to determine the root cause of the problem.
b. Findings must be communicated to the shop floor personnel and documented by key quality management stakeholders.
c. Critical technological and quality risks should be clearly defined and methodically assessed.

8) Additional operational risk considerations
a. The process of onboarding and offboarding employees must be well organised to ensure the continuity of in-house quality requirements.
b. Training and mentoring processes should be thoroughly recorded and updated regularly.
c. Ongoing training programs, both in-house and from third-party providers, are essential for theoretical and practical advancements.

By employing inductive reasoning, which derives conclusions from observed data, and deductive analysis, which validates these conclusions against logical frameworks, companies can make informed decisions about adopting ECG in their printing operations while guiding customers on best practices to optimise material usage in manufacturing.

Figure 4 Colour control bar used in expanded gamut (ECG) printing

Conclusions

Companies can use inductive reasoning and deductive analysis Nelder-Mead Simplex Method to make informed decisions about adopting ECG in their printing processes while advising customers on best practices to optimise material usage. Implementing ECG should not be difficult if companies adhere to clearly defined printing standards and develop in-house expertise.

If these requirements are met, implementing ECG should not be overly challenging. The key factors are installing or adhering to existing, well-defined printing standards and building in-house expertise with technology engineers' support, adopting best practices throughout. With consistent efforts, customers and brand owners will appreciate knowing that their trademarks are safely and reliably printed using flexographic technology worldwide.

The next time you consider standardising flexographic printing processes, don't hesitate to say, **"YES!"** Standardisation becomes a valuable investment. By controlling your big data and monitoring all printing variables daily, you can ensure your company's long-term success and competitiveness.

References:

[1.] Graphic technology — Process control for the production of half-tone colour separations, proofs and production prints ISO 12647-6:2020;
[2.] Flexo Printing Technology, COATING 2000, ISBN3/85599-005-0;
[3.] Project – Process Standard Flexo (PSF) (under development) Fogra, Grafitek 2025;
[4.] Media Standard Print – Bundesverband Druck und Medien e. V. (bvdm)
[5.] Workflow management and standardisation of the printing industry – EUR Ing. Enn Kerner, International Circle, California US, 2015;
[6.] Graphic technology — Process control for the production of half-tone colour separations, proof and production prints ISO 12647-2:2013;
[7.] Process Standard Offset (PSO), Fogra Forschungsinstitut für Medientechnologien e.V.
[8.] The Color Guide, X-Rite, P/N XRC550 B-12-96

Author Biography

During 30 years of entrepreneurship as CEO of an engineering company in the printing and packaging industry.

Awarded by title of EUROPEAN ENGINEER (EUR ING) by ENGINEERS EUROPE (engineerseurope.com).

Currently working as a FOGRA auditor for Process Offset & Flexo Standardisation, contributing to the integration and comparison of EU, North American, Japan Colour quality standards in study curricula for print operators and printing technology engineers.

Executive Board Member of ENGINEERS EUROPE and Vice President of the Estonian Association of Engineers.

Vice Chair of the International Circle of Educational Institutes of Graphic-Media Technology and Management (IC).

GREEN, a sincere approach to Ecology applied to inkjet printing

Patrick Le Galudec, PLG Consultant, Zürich, Switzerland

Abstract

Inkjet printing integrated into wide-format has contributed to a rapid development of advertising, with massive production of banner, plastic display films. It has unfortunately also ignored the consequences and contributed to growing mountains of non-recyclable waste.

As the industry matures, it tries to adopt a more responsible approach to printing and recycling the printed materials. The paper is about DiatecX, a client of the author, focusing on materials made from renewable resources, printable, recyclable and the implications for inkjet media coaters.
GREEN is a private, pragmatic initiative to ensure that recycled materials are affordable and recyclable to a large extent, made available to a wider public. It documents the difficulties met, both technical and organizational and provides an overview of the next challenges faced by inkjet media developers committed to reduce the footprint of their industry without punishing the consumers.

European industry started with recycled textile, grew with the industrial revolution, converted to wood pulp and now largely uses leftovers and least valuable pieces of wood to produce FSC and soon EUDR papers in a sustainable way. With 60 to 80% of paper being recycled and recycled paper covering around half of demand, it offers a good base for sustainable inkjet printing.

Coating predated inkjet. It grew together with inkjet, enabling superb printing on porous and non-porous substrates. Enhanced coating coupled with substrates made from recycled materials, recyclable themselves, can have a major positive impact on practical Ecology.

Priced at same level as FSC virgin fiber media, GREEN papers developed by DiatecX combine a proven 100% FSC recycled post-consumer paper base and a functional inkjet receptive coating. GREEN media insert themselves into a Produce – Print - Collect – Recycle – Print again look that should contribute to carbon footprint reduction and reduced wastage of resources.

We hope to see more of such initiatives to facilitate change towards a more sustainable economy, one small contribution to the resolution of a large problem at a time.

Before inkjet – background and legacy

From its beginning in the middle-age (1289 Xativa, Spain) to the industrial revolution (1801 to 1843 in the case of paper), European paper was made from recycled textile fibers. Poor Europe was then quite efficient at recycling every possible leftover.
Unlike China/Japan/Korea which have been using cultivated or harvested tree bark fibers, Europeans went first through a shortage of recycled materials at the beginning of the industrial revolution: that forced them to introduce and adopt wood pulp for mass manufacturing of paper.

Industrial paper manufacturing was quite a polluting process, ruining rivers and resulting even today into high costs of land decontamination when reclaiming vintage paper areas. Productivism, with always larger and faster paper machines was the standard philosophy.

Volume analog printing on offset, heliogravure or typo presses was generating always larger quantities of printed goods, recycled into folkloric yet efficient ways (from fish & ships to toilet paper). Recycling progressed through the shortage of resources during the 2 worlds wars, and large scale recycling of paper became a reality in Europe in the late 50's.

From the 60's, the system had reached a certain stability with paper being manufactured for analog printing inks and machines, processed by printers into publications, then partly recycled into paper.

Next to that computer output and copy/duplication was largely perceived as fringe paper usage outside of "the printing industry".

The wild years of Digital Printing and the late start of inkjet:

Paper for digital imaging can trace its origins through 3 main sources:

1)-Duplication of documents and plans, with Xerography for documents and Diazography for documents.

2)-Computer output: digital printing started in the computer rooms of the 1950's, as a successor to the tabulating machines. Paper was there both an input device (cardboard) and an output support (listings) – consumed in extravagant quantities. Interestingly, paper makers were among the investors funding early computers and optimizing papers and cardboards for these devices (Aussedat-Rey and Companie des Machines Bull in France).

3)-Photography: combining light, coated papers and enlargers to deliver printed images in every possible format,
Paper printing was not much better, with some reproduction processes such as Diazography (with ammonia) particularly "stinky".
Paper was there both an input device (cardboard) and an output support (listings) – consumed in extravagant quantities.

All these 3 actors went from the 1950's to the end of past century through an explosive growth phase, happy to produce and waste increasing quantities of materials and finished products.

Digital printing remained a province of copy/Duplication and computing until 1990 to 1995. From 1974 to 1990 it started absorbing publishing (composition software), document duplication (adoption of scanners and then introduction of Xerox Docutech), plan copy (wide-format scanners and electrostatic plotters), computer output (from personal printer to large high-speed document printers) and even photography (films scanned and then imaged digitally on silver halide photopaper).

Among digital printing technologies, electrophotography was first to emerge as reasonably reliable and user-friendly. Paper treated for “Xerox” became the de-facto standard there. Recycled paper was available while still largely ignored outside of Germany (Steinbeis).

Inkjet came later, plagued by difficult start (unreliable printheads and inks). As later arrival it was at a disadvantage when facing electrophotography (normal paper designed for Xerox would not perform as well with liquid inks). It gained however acceptance on certain markets where it was fast (Scitex digital printing for billing and statement printing) or could provide affordable color.

Several industries were quick to notice that, when combined with adequately coated media, inkjet could deliver photographic level color output. CAD & Reprography on one hand, Visual Communication on the other hand are worth following into more details.

They both triggered the emergence of wide-format printing, replacing Diazo, quick printing, art photography through the combination of reliable inkjet printing devices and media (paper and other materials) coated to match the inks and deliver colorful stable output.

Diazo coating factories switched to inkjet media coating. For photopaper manufacturers, the change proved painful as it implied moving for high-value complex paper making to much simpler and cheaper productions.

When it came to environment, paper making factories had fixed several of their issues (water treatment and reuse, used water cleaning stations, smoke filters, removal of most toxic chemical components: Chlorines, Sulphurs, Mercury, Phenols to name a few.

For the rest it was more of a “wild west” culture, with focus on the race between technologies and machines and profits that could be obtained from selling always more. Compliance with state bureaucracies such as fulfilling demand for recycled paper printing was performed reluctantly at best. As for inks and coating chemical composition, inexpensive and efficient formulations and processes were used, with non-toxicity tests kept at minimal levels.

Inkjet media safety – Reach, California and Greenpeace

From 2000, Inkjet had established itself as the leading technology in home printing and in CAD & Light Graphics and Viscom. Large format photography with water-based pigmented inks (Epson 9500) started delivering artist photographic prints.
All sorts of inkjet receptive formulations were developed, then applied as receptive coatings on papers and other substrates to match with the new inks.
Home printing became soon the province of electronic giants (HP, Canon, Epson, Brother) which enforced tighter electronic safety compliance (RoHS) and safety compliance (OSHA) on to their subcontractors. The sheer importance of their OEM supplies contracts forced the media industry to take notice and upgrade rapidly their processes and formulations.
The industry acted partly out of sincere respect for the health of end-user consumers, partly to anticipate and remove the threat of activist organizations (see Greenpeace activists staging a protest on the roof of Hewlett-Packard's (HP) headquarters in Palo Alto on July 28, 2009).

Around the same time, the European Union released a REACH white paper, listing and rating all industrial molecules and establishing a European Agency in Helsinki to manage the termination of substance proven to be health damaging, listing suspect Chemicals well in advance of test results, so that manufacturers would have a chance to qualify in time alternatives. The determination of the agency paid and the coaters integrated the REACH lists to avoid using chemicals listed as dangerous or even just suspect/under investigation.

Thanks to the combined pressure of the largest order-givers and the EU regulators, much progress was achieved in the ink and media domains. Many solvent-based formulations were replaced by water-based coatings, phenolic components were phased out.

There were tough choices, for example in the areas of fire-retardant surface treatments, needed to deliver mandatory M1 fire resistant indoor advertising media in France. Classic proven formulations containing Borates, Brome or Ammonium had to be replaced and that proved challenging.

By 2010, solvent inks had almost disappeared from developed countries, with water, eco-solvent and new Latex inks providing cleaner solutions when combined with modern coated media.

It had grown into a large industry producing in a cleaner way more healthy products. However, all these inkjet prints had to be discarded at a point or another, and there, increasingly large quantities of media posed new environmental issues.

Towards Circular Economy - Producing on demand, collecting and recycling discarded printouts

As inkjet became the preferred technology for Visual Communication, volumes of printed materials (paper and plastics mainly, including PVC) became significant.
We have to admit that there was not much discussion between the techies, eager to digitize the world and sometimes ignorant of the past and the recycling industry.
The issues generated by the growing volume of digitally printed media started to emerge slowly. There were cases of large lots of

digitally printed paper landing at a recycling factory and ruining a complete batch of recycled papers. There were concerns about PVC coated materials being burned at lower temperatures and releasing toxic dioxins. There was the rapid filling up of landfills in Europe, and the cost of incineration of media, followed by catalytic filtering of exhaust fumes.

The generalization of digital printing alone should have generated huge economies of media: 30% of books, unsold, unread, repulped into recycled paper, probably the same percentage of posters, labels, business forms and other goods ordered by lot of 1000 to 50000 pieces to be on the safe side and benefit from staircase discounted prices.
However, while printers and their clients did take advantage of the more flexible production features, they often kept the old pricing habits, continuing wasteful overproduction.
The media mix also shifted to increase more plastics, harder to sort out and recycle – for a mix of technical and financial reasons.

Last, simplistic anti-paper campaigns created a gap between the environmentalists and the paper makers, coaters and vendors. Exchange of emotion-loaded opinions replaced partly constructive debate.

The author believes that at that stage home office inkjet printer industry passed its peak and faced other urgent priorities than environmental issues. Wide-Format inkjet, while still busy with fast technological development pace was also looking for new market applications as Viscom showed signs of saturation.

So, after a phase of rapid progress, where digital inkjet had cleaned up their production processes and their media, inkjet industry was probably making less progress than conventional printing, where the Forest Stewardship Council (FSC) had paved the way to the implementation of a circular paper economy maximizing the usage of sustainable resources and its recovery and recycling.

Some of the first attempts to catch up and release recycled paper products did not go too well: makers asked for a price premium and the digital market rejected it in most cases. Several alternatives to PVC films and banners proved costly and less efficient – vendors learning that good intentions did not deliver markets. It was probably time for rethinking environmental approach.

GREEN a sincere approach to Ecology applied to digital printing

Many of the inkjet media manufacturers are mid-sized companies with limited human resources. They don't carry the weight of paper manufacturers, chemical industries and advertising lobbies when it comes to influencing and preparing European Union environmental policies.
Unlike part of America, European electorate and thus politicians were endorsing the concept of a single planet with a finished stock of resources, where overexploitation was progressing at an alarming rate.
There was little discussion on the need to privilege media made from sustainable, renewable resources, to put in place a product lifecycle ensuring recycling of a large extend of used resources while minimizing energy consumption and heat & carbon emissions.

The question was rather how to do it while maintaining or increasing one's position in what was turning into a very competitive industry, often under price pressure from new manufacturers from China.

Printer manufacturers are doing their share of efforts with machine refurbishing and rebuilding programs; inks delivered in bulk mode or in recyclable.
Media manufacturers could also bring their contribution, mainly through the replacement of plastic materials through paper and cardboard, or the switch to recyclable mono-component plastics instead of complex multi-materials laminates.

DiatecX, an independent French-based, Italian-Owned media manufacturer decided to elaborate recycled media alternative to mainstream FSC paper-based inkjet media and to offer the recycled product at exactly the same price. The idea was to be fair to early supporters of recycled media, often public sector collectivities faced with budget constraints – being GREEN should not cost them extra money.

Technically speaking, it implies the deposition of thin receptive inkjet layer, free of plastic or other substances that would compromise recycling after usage. The imaging properties are identical to those achieved on FSC paper, the difference being the shade of paper (slightly greyish when it comes to recycled).

Defining the right paper shade took some efforts together with the recycled paper manufacturers. Recycled paper portfolio ranges from grey or green (not that good for graphic rendering) to as white as FSC virgin paper (this step requiring more washing cycles, ie. more energy, more water and also possibly reducing the recyclable value of the paper through fiber shortening).

Sincerity implies the usage of post-consumer waste paper resources. While waste from paper mills or printers are of best quality (almost virgin paper ready for repulping), user vision of recycling implies using the paper they have just discarded after usage. We believe that honesty and sincerity can partially replace advertising money when promoting a product "really better than previous options for the planet health.

First feedback from market is encouraging. We look for more adoption, experimentations outside of Europe and duplication or adaptions worldwide to contribute collectively to Ecology.

Conclusion: GREEN developments and getting even greener

The short-term horizon is well defined: zero stock, production on demand using a number of qualified base mono-materials – paper, non-woven, textiles made from renewable resources (plants, animals, wood pulp chemistry…) – adding functional layers and image receptive layers compatible with industrial recycling processes.

This does not fix societal issues – the thrive for cheap and disposable goods, be it fast fashion, furniture, stationary, low-budget inkjet media with questionable pedigree… The urge to consume is human, the e-commerce omnipresent and the budgets too tight for many.

Inkjet media industries still have progress to do: shift to renewable energies, improvement on coating and drying energy usage, replacement of chemicals originating from oil & coal industry by bio-manufactured materials. Incentive to do so will grow together with the acceptance of GREEN media.

As for inks themselves, changes of pigments, binders and possibly biocides would be anticipated. In the case of UV, special attention to the choice of photo-initiators and plasticizers would help too.

We believe that coaters, with their manufacturing expertise and understanding of digital industries could be the missing link and contribute to the greening of the digital inkjet/imaging industry. While state programs and administrative constraints can help, a sincere and persistent approach of clients with constructive, no-added cost approach can deliver faster acceptance of more "good for the planet" inkjet media.

References

[1] How bad are bananas Mike Berners-lee 2020
a fun and no-nonsense approach to carbon footprint and consumption

[2] Wasteland Oliver Franklin-Wallis 2023
a great introduction to "real" recycling industry and associated issues

[3] No More Plastic (in French) Rosalie Mann 2024
all reasons to move into substitutes to oil & coal-based plastics

[4] Greenpeace activists vandalize HP headquarters
2009 article on Wired, Reuters---

[5] Print unchained Edward Webster 2000
unfortunately there is no second volume to cover the years 2000 to 2025…

[6] Bitten by the bitch fever Lucinda Hawksley 2023
How wallpaper makers fought successfully to keep producing toxic wallpapers

And the Europa.eu for their huge library of texts on Reach, EUDR, PPWR plans and application procedures

Author Biography

Patrick Le Galudec graduated from « Hautes études Commerciales » Paris, France in 1982, worked as marketing manager for Bull Periphériques, then Nipson on high-speed magnetic toner printing machines. He then joined the Sihl,, then Sihl-Diatec, as OEM manager, Business developer and Asia-Pacific Sales Director. He lives now in Zürich, Switzerland and continues consulting work on inkjet media development and on Asia-Pacific developments for DiatecX, the inkjet media division of Diatec group, Italy.

The Enduring Value of Electrophotography in the Digital Age: Pioneering New Frontiers

Katsuhiko Nishimura; Minato-ku, Tokyo JAPAN

Abstract

Electrophotography redefines printing value in the digital age. At ICJ 2025, CrossMINDS' Laxerop technology enabled vibrant 7-color printing, including gold, on washi, silk, and gold glass, earning praise like "Electrophotography can do this?!" Inkjet's dynamic adaptability excels in high-speed printing on diverse substrates. However, electrophotography offers precision, durability, low-gloss, and high-gamut for cultural heritage, like Manshoji Temple fusuma, though thin paper and wide-format solutions are scarce. Seven-color scanners are also lacking. This talk envisions enhanced on-demand printing equipment and data for electrophotography's future.

1. Introduction

A wide variety of media are used in art works, including traditionally Japanese paper, Western paper, and silk, as well as many mixed-media works combining these materials. Meanwhile, stained glass and Bohemian glass, for example, are often used to create art by coloring glass or glass, and many works are created using glass paints. This presentation will first introduce the main features and examples of full-color printing on glass plates and glass using our proprietary Laxerop glass printing technology. We will then introduce examples of canvas printing, silk printing, seven-color printing, and printing on Japanese paper using Laxerop technology.

2. Laxerop Glass Printing Technology

Figure 1 illustrates the principle of Laxerop full-color glass printing. A full-color reverse image is formed on a Laxerop glass sheet using an art-grade laser printer. The toners used include YMCK, as well as gold, silver, white, and clear toners. Subsequently, only the toner image is transferred onto a glass plate or glassware.

The toner transfer efficiency from the Laxerop glass sheet to the glassware is effectively nearly 100%, enabling the near-perfect transfer of fine images and halftones. Currently, full-color image formation is commonly applied to items such as rock glasses and wine glasses. Depending on the design, partial white toner at 80% density may be used to create photographic images, or 100% white toner may be applied for specific areas. Full-color glass printing is performed to meet various customer requirements.

3. Examples of full-color glass printing

Fig. 2 shows a photograph of Laxerop full-color glass printing.The original image is a full-color print of "Style Taste," a masterpiece by Malaysian artist Daniel Liau Wee Seng, on both the front and back of a Zwiesel rocks glass.

The on-demand printing equipment used was a DocuColor 1450GA manufactured by Fujifilm Business Innovation Co., Ltd. Subsequently, only the toner image is transferred onto a glass plate or glassware.

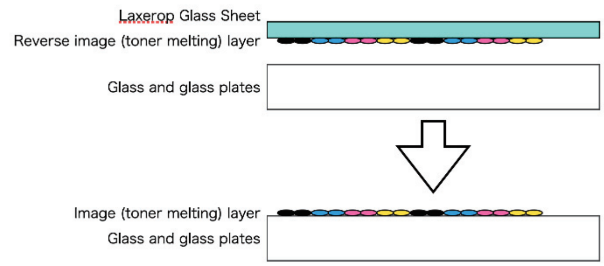

Figure 1. *Principles of Laxerop full-color glass printing*

Figure 2. *Laxerop full color glass printing examples "Style Taste"*

4. Laxerop full color glass printing color gamut and gloss

The color gamut of images created using Laxerop glass sheets was applied to various media, and gamut and gloss were measured using an X-Rite Ci64 portable integrating sphere spectrophotometer in D65/10 SPIN mode. Fig. 3 shows the gamut of an image formed on a glass plate using Laxerop glass technology. Fig. 4 also shows the results of scanning an image at 600 dpi using an Epson ES-G11000 flatbed scanner in transmission mode and measuring the gamut using Adobe Photoshop.

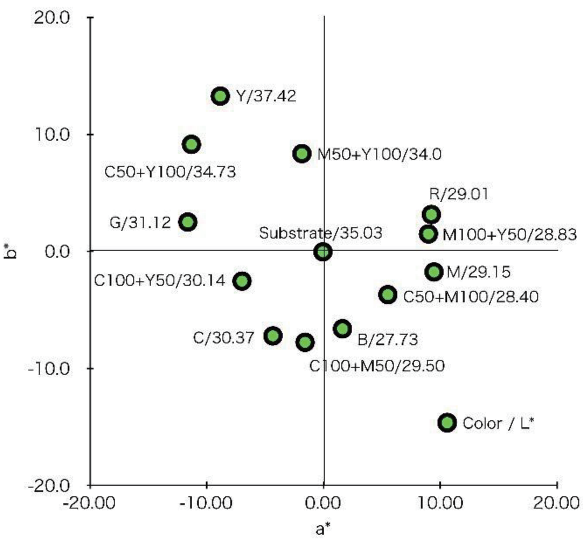

Figure 3. *Laxerop Glass Printing Gamut (Reflection)*

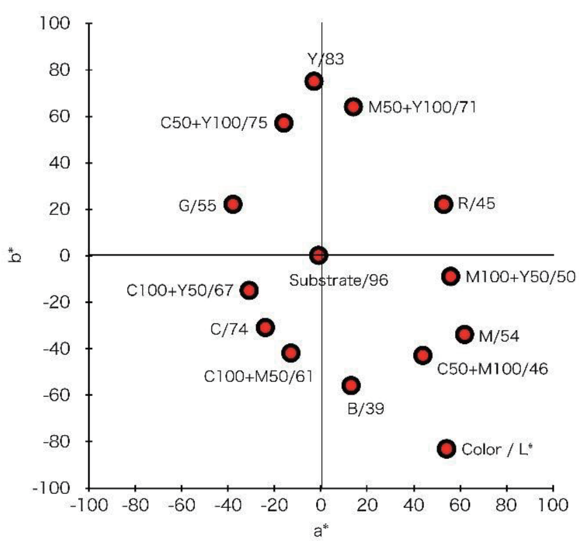

Figure 4. *Laxerop Glass Printing Gamut (Transparent)*

Based on the above, the practical gamut of glasses needs to be considered from the perspectives of reflection, transmission, visibility, etc.

5. Laxerop: Future developments in full-color glass printing

In addition to being used for events and gifts, our products are currently being adopted by beer halls, izakayas, and coffee shops for a variety of glassware, including wine glasses, champagne glasses, Copa glasses, and beer glasses.Full-color printing on glasses can create a unique and valuable experience. Printing unique artwork in full color on glasses can bring laughter, emotion, and healing.Fig. 5 shows photos of Austrian and German-made wine glasses with Daniel Liau Wee Seng's "Helpless Explanation" and "Changes as we go along" printed in full color. Needless to say, we want to maintain image quality for a long time, and we are continuing to evaluate various aspects.

Figure 5. *Laxerop Glass Printing on Wine Glasses Left: “Helpless explanation” Right: “Changes as we go along“*

Figure 6. *The image on the left shows the GOLD Glass delivered to Bar CENTIFOLIA, and the image on the right shows Bormioli Rocco Sorgente Old300 with flowers printed using Laxerop Glass technology.*

The owner of the bar "CENTIFOLIA" requested that we print a gold logo on glasses to enhance the brand's luxury and uniqueness. Spot-color printing was required for both visual appeal and durability. By using Laxerop glass printing technology, we were able to achieve a vivid gold color that would be difficult to achieve with inkjet printing. This provided high-quality glass befitting the bar space and met customer expectations. Additionally, there was a request for full-color printing on textured glass, which Laxerop glass printing technology made possible. Fig. 6 shows an actual image.

6. Laxerop Canvas Print

Canvas printing using Laxerop achieves a wide color gamut with low gloss. The matte toner brings out the texture of the fabric, making it ideal for reproducing artworks that look almost authentic. Normal laser printers are not suitable for printing on canvas. Inkjet printers use a canvas that is suited to their technology, and we look forward to further developments in the future in terms of low gloss and color reproduction suitable for art.

Fig. 7 shows the principle of Laxerop canvas. A full-color reverse image is printed on a Laxerop sheet using an art laser printer. In addition to YMCK, gold, silver, white, and clear toners are also available. The toner image is then printed onto the canvas or tile using Laxerop film. The toner transfer efficiency to the Laxerop sheet is virtually 100%, allowing for nearly perfect transfer of fine images and halftones. The thickness is a few microns, depending on the process.

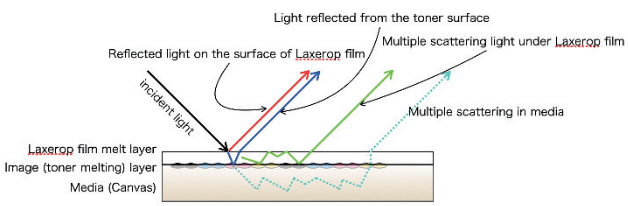

Figure 7. Principles of Laxerop Canvas

7. Laxerop Canvas Printing Examples and Techniques

Fig. 8 shows a photo of a Laxerop canvas print.The original image is a full-color print of "Goal Forward," a masterpiece by the artist, Malaysian artist Daniel Liau Wee Seng, on canvas. The on-demand printing equipment used was a DocuColor 1450GA manufactured by Fujifilm Business Innovation Co., Ltd.

The color gamut of images printed using Laxerop sheets was applied to various media, and gamut and gloss (60°) were measured using a Konica Minolta CM-26dG portable integrating sphere spectrophotometer in d/8° SCE mode. Figures 9-11 show the gamuts printed on each dedicated matte paper using the Laxerop method, the Fujifilm Business Innovation DC1450GA laser method, and the Canon MG7530 water-based inkjet method.

From the above, we can see that the gamut of Laxerop canvas prints is low gloss but has a wide color gamut. As a result, as shown in Fig. 12, the three-dimensionality and reproducibility are so high that even when enlarged, they are indistinguishable from the original. With laser printers, the gloss is slightly higher this time due to the toner melting process. With inkjet printing, the color gamut is not as wide as with paper, with some exceptions.

Figure 8. Laxerop Full color Canvas Printing Examples
Daniel Liau Wee Seng “Goal Forward” F6 size

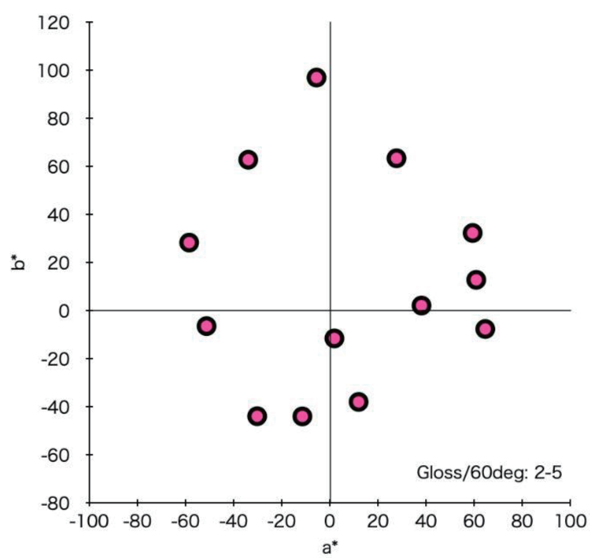

Figure 9. Laxerop Matte Printing Gamut (matte paper)

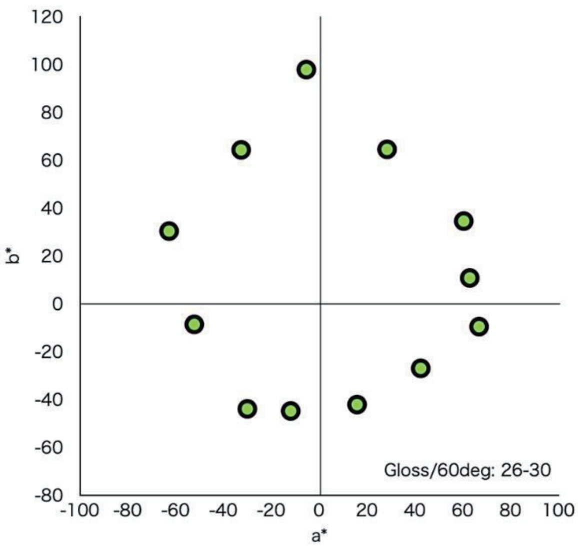

Figure 10. Laser Matte Mode Printing Gamut (matte paper)

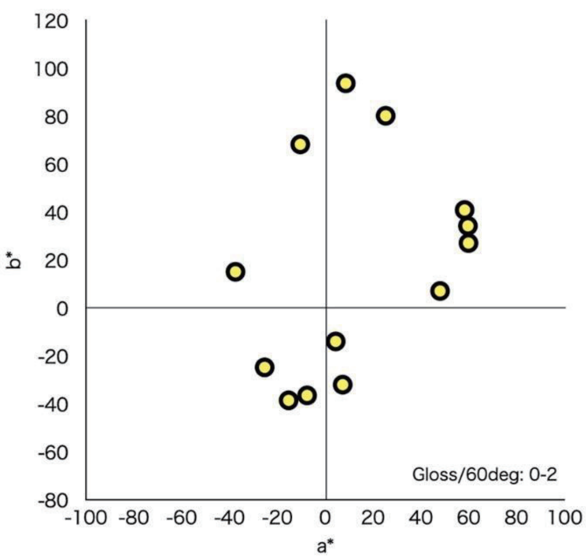

Figure 11. Inkjet Matte Mode Printing Gamut (Inkjet matte paper)

From the above, we can see that the gamut of Laxerop canvas prints is low gloss but has a wide color gamut. As shown in Fig. 12, this results in a three-dimensional effect and reproducibility so striking that many art producers can touch it with their fingers, and even enlarge it to the point where it's indistinguishable from the original. For laser printers, the gloss is slightly higher this time due to the toner melting process. For inkjet printers, the low gloss, similar to that of paper, means that the color gamut is not as wide as for either, with some exceptions.

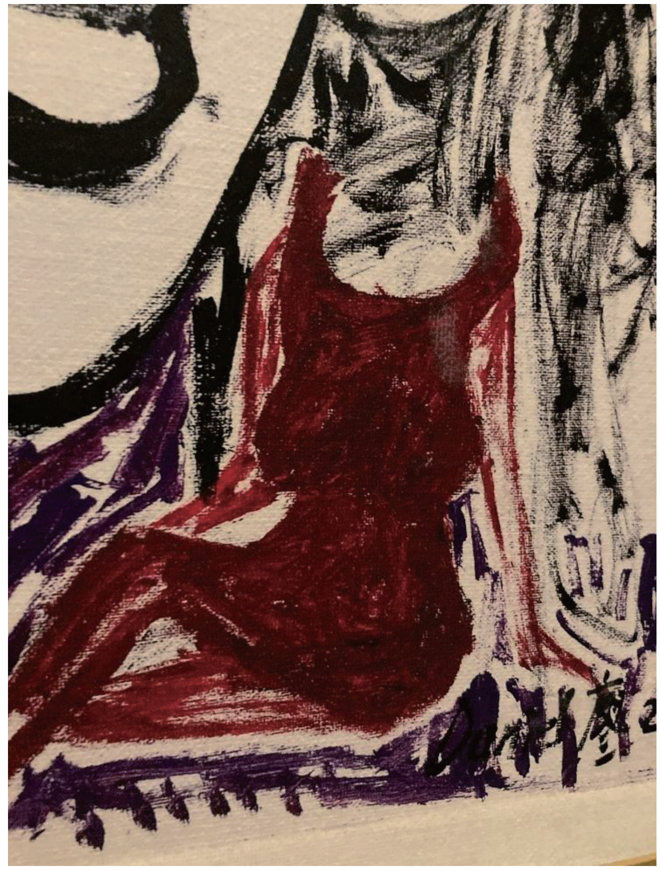

Figure 12. Laxerop Full color Canvas Printing Examples
Daniel Liau Wee Seng "Goal Forward" Enlarged

Using the Laxerop canvas printing technique, Fig. 13 shows a full-color print on silk laid over gold leaf paper.
Furthermore, you can feel the texture of the silk book by touching it with your hands.

Figure 13. Laxerop Full color Canvas Printing Examples

8. Regarding special color printing

Spot color printing combines full color with special colors like gold and silver to create a luxurious and visually appealing look. This presentation will introduce a full-color and gold reproduction of a drawing by world-renowned designer Junko Koshino and provide a tour of the accompanying exhibition.

We also showed photos of our delivery of gold logo glasses to the bar "CENTIFOLIA." Gold and silver logos are in high demand in the beer industry, but designers lack experience with spot color designs, so YMCK full-color printing is the norm. Gold and silver spot colors are becoming increasingly important in art and glass printing, and Laxerop glass printing, using electrophotographic technology, will achieve this effect, which is difficult to reproduce using inkjet printing.

Fig. 14 shows the processing screen for turning Junko Koshino's drawing into a spot color GOLD. The laser printer used was a Fujifilm Business Innovation Revoria Press PC1120, and the software used was Adobe Photoshop and Illustrator. While referring to the original and closely examining the data for the "Fujin" drawing, I selectively added spot color GOLD settings as a new spot channel. The spot color instructions vary depending on the printer used.

Special color printing is becoming increasingly important in the art and premium markets. We are also working on applying it to gemstones such as sapphires and improving the durability of line drawings, with the aim of further technological innovation and market expansion in the future.

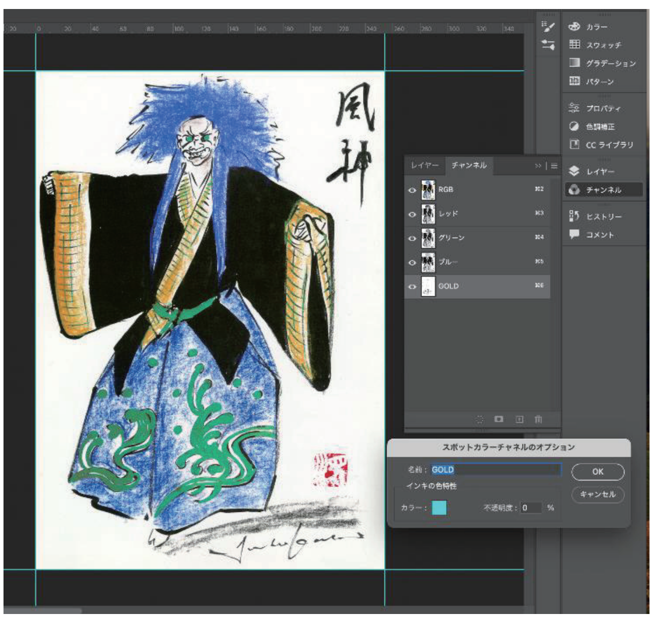

Figure 14. Junko Koshino's "Fujin" drawing feature GOLD instruction screen

9. Laxerop folding screen printing on Shin Torinoko washi paper and expectations for the future

The sliding screen paintings by painter Saito Kaishin (two Cloud Dragons, one Pine Tiger, and one Landscape) housed at Manshoji Temple in Yokosuka City are a valuable heritage site designated by Yokohama City and open to the public once a year. They represent the culmination of a major project by the Kano school from the late Edo period to the Meiji period. This study presents a case study in which these paintings were digitized at a resolution equivalent to over 600 dpi and then used our proprietary Laxerop technology to create a four-panel folding screen. Approximately 400 photographs taken with a Canon EOS digital camera were composited to reproduce the delicate brushwork of the sliding screen paintings. Using electrophotography, the images were printed on the newly developed Laxerop media, which was then transferred 100% onto medium-weight Shin-Torinoko paper, typically used for folding screens, achieving the low gloss, high color saturation, and durability of ink painting. After much trial and error, we discovered a method for forming images on washi paper by chance, and developed specialized materials with multiple manufacturers. The folding screen, halved in size (120cm high x 360cm wide), combines elegance with portability. It features four layers of washi paper, 15 sheets per panel, for a total of 60 sheets, and is crafted with precision cutting techniques using specialized Japanese knives. Overcoming the challenges of color and alignment, the screen embodies the spirit of the artist and mounter.

This presentation will discuss how Laxerop technology goes beyond simple reproduction and combines new technology and craftsmanship to create "Japanese art," as well as the innovative potential of electrophotography.

Fig. 15 shows the shooting conditions. The digital cameras used are listed below. For photographing the early Cloud Dragon sliding door paintings, a Canon EOS Kiss X7 and a TAMRON 16-300mm F/3.5-6.3 Di ll VC PZD MACRO For works No. 2 and later, a Canon EOS 1DX Mk II and an EF 24-70mm F2.8L II USM and an EF 70-200mm F2.8L IS II USM were used. For lighting, a blackout curtain was used, and four lights were used. A light meter was used to adjust the lighting settings so that each sliding door had nearly uniform illumination. The sliding door paintings were to be unveiled on November 3rd, but the photographs had to be taken within a short timeframe, either before or after that date. Shooting time was limited. In reality, it took about two hours to set up the lighting, and about two hours to photograph the entire sliding door painting.

First, a full-length photograph was taken of each sliding door, followed by nine separate photographs and approximately 100 enlarged photographs (400 photographs of the entire sliding door painting).

Figure 15. The situation of photographing the sliding door paintings (2nd work)

Fig. 16 is a close-up of an 2nd work (Cloud Dragon). Data of 600 dpi or higher like this is composited one by one in Adobe Photoshop.

Figure 16. The situation of photographing the sliding door paintings (2nd work)

Fig. 17 shows the process of aligning and cutting A3 Nobi-sized Japanese paper, and Fig. 18 is a photograph of the finished folding screen.

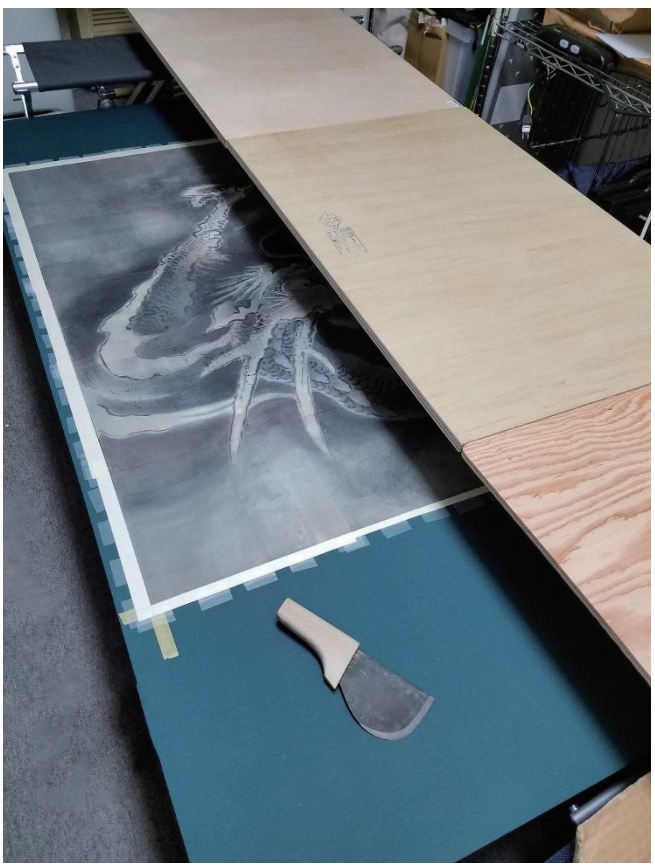

Figure 17. Aligning the washi paper and the cutting process used only for the first work.

Figure 18. Laxerop Cloud and Dragon Screen (second work)

Summary

Based on my experience designing laser printers, I believe that developing stable printing technology that can be applied to traditional Japanese washi paper and art will be key to expanding the reach of electrophotography.

Going forward, I hope to advance research and development into utilizing a variety of washi paper, including its distinctive features, and commercializing on-demand printing and scanners, opening up new horizons in cultural heritage preservation and artistic reproduction.

This Laxerop technology was developed in-house following the approval of a 2017 grant from Minato Ward, Tokyo, for the New Product and Technology Development Support Project.

I would like to express my gratitude to all those involved for their cooperation.

References

[1] K Nishimura, Color Systems, Electrophotography, Edited by the Imaging Society of Japan, Process and Simulation, Chapter 4, pp.133-148 2008 ［in Japanese］.

[2] K Nishimura ” Full-color glass printing using the Laxerop technology”. Imaging Conference JAPAN 2024 G-08 (2024)［in Japanese］.

Author Biography

Katsuhiko Nishimura

In 1981, he completed his master's degree in applied physics at the Graduate School of Engineering, Kyushu University. That same year, he joined Asahi Optical Co., Ltd. In 1986, he joined Canon Inc. mid-career and worked on the development of laser printers. In 2013, he received the Minister of Education, Culture, Sports, Science and Technology Award (one of five recipients) at the 2013 National Invention Awards. In 2014, he founded Cross Minds Co., Ltd., where he is now Representative Director and CEO.

RGB workflow and high-value-added decorative printing initiatives

Yoheita Yoshihara (Digital On-Demand Center); Director; Shinjuku Ward, Tokyo
Yoshihiro Miura (Printing Director) Nishi-ku, Osaka

Abstract

Around 2000, as digital camera accuracy improved, implementing an RGB workflow became a challenge for printing companies. Since then, each company has been improving its workflow, and today, an increasing number of printing companies can implement an RGB workflow. Furthermore, printing presses capable of reproducing RGB have also been released, adding the value of wide color gamut printing to printed materials, and techniques for adding decorative printing to surfaces have also emerged. We will explain this using examples from Kenbunsya, a company that practices both of these methods.

About Kenbunsya Co., Ltd.

Our company was founded in Osaka shortly after the end of World War II in 1946. We expanded alongside Japan's rapid economic growth, responding to customer needs and pursuing technological innovation without taking on orders from competitors. One example of this is our pioneering switch to offset printing in the 1960s, when letterpress printing was still the norm. In the early 1990s, we established a fully digital DTP department for typesetting and platemaking, transitioning to a fully digital approach. Since then, we have digitized maps using Illustrator, back when layers were not yet available, and begun work on the practical application of multi-channel PANTONE Hexachrome at a time when Photoshop was not yet capable of supporting multiple colors. In 1999, we introduced Osaka's first thermal positive CTP system, enabling color management with a printing press equipped with a Hyper System. In 2001, we were certified by PANTONE, Inc. of the United States, as the first company in Japan to implement PANTONE Hexachrome technology.

Among our various initiatives, we were also one of the first to embrace digital printing. In 2020, the company launched a digital on-demand center at its headquarters factory, which is fully digitally printed and digitally decorated, and in 2024, it opened a lab, which it continues to operate to this day.

Standardization of high-resolution printing

Standardizing High-Resolution Printing In 1993, when our company first became able to output film directly from DTP, the mainstream output method was photographic paper. Initially, we were limited to 130-line and 175-line output. However, when printing maps, the current RIP took four hours per plate. Therefore, we tested various manufacturers' RIPs. Only the HQ-RIP produced satisfactory results. We switched to the HQ-RIP and introduced a 400-line mesh at the same time. Standardizing high resolution was quite challenging in the era of plate-making and flatbed proofing, but we achieved this standardization in an environment where we were producing catalogs for automobile manufacturers.

Equipment installation

In 1999, after high-definition printing had become standardized, we installed a new drum scanner, thermal positive CTP, spectrophotometer, profile mechanism, a 6-color press equipped with a hyper system, and multicolor spectral separation software. This created an environment where color management could be performed from prepress to press in one go.

Encounter with PANTONE

Encounter with PANTONE: In 1999, after installing various equipment, we initially adjusted the orange and green of six-color printing based on complementary colors. PANTONE Hexachrome was patented in 1995, but Photoshop was not yet capable of multi-channel deployment, and information was extremely limited. Through exhaustive efforts, we were able to ask PANTONE about our questions, hold several meetings in Tokyo when we visited Japan, and then travel to the United States for technical training. There, we learned about PANTONE's thinking and operations, working with PANTONE's technical team. We then worked together as software testers in Japan, building a solid track record.

RGB Workflow

Use RGB First, PANTONE Hexachrome has a wider color gamut than sRGB and can reproduce nearly the same color gamut as AdobeRGB. It can reproduce PANTONE spot colors by multiplying them by about 90%. It balances all CMYK, K, and G inks, and does not treat OG as complementary colors. If AdobeRGB, which has the same color gamut as the NTSC LCD monitor standard, can be reproduced, it is essential to use AdobeRGB. I also created a workflow in which image retouching is performed using AdobeRGB profile data.

Launch of the consortium organization

Launching a Consortium Organization Our company shared information with PANTONE on its own and built up a track record. We modified each product, which should have been operated in the RGB color gamut, to achieve success, such as a nine-color calendar with original artwork and five complementary colors, and a jigsaw puzzle by a digital artist who painted in RGB. However, we also needed cooperation from manufacturers in various situations, and a manufacturer engineer suggested that we should instead establish a consortium organization. Thus, in 2003, the PANTONE Hexachrome Consortium, an organization recognized by PANTONE, was established. Our company's President, Mr. Amino, served as the first chairman, and author Miura participated as the technical director. Activities were held each month on various topics, and we continued to raise awareness. As a result, 1. Establishment of a workflow 2. Development of an original profile 3. Publication of the PANTONE Hexachrome White Paper, summarizing the technical details of PANTONE Hexachrome. 4. He has given seminars at domestic and international equipment exhibitions, and even hosted a successful exhibition in Aoyama, Tokyo.

Development of pre-simulation software for submitted data

Pre-Simulation Software for Manuscript Data When developing multicolor printing, one important consideration is the color gamut of the original RGB data. There was a common misconception that RGB has a wider color gamut than CMYK. (The color gamut that can be reproduced varies greatly depending on which RGB is used, as SRGB has a narrower color gamut in some areas than CMYK.) So we developed software that plots the color gamut of manuscript data on a CIEXY chromaticity diagram and shares it in advance. This enabled us to simulate manuscript data in advance, dramatically improving accuracy. Our company now conducts image analysis in advance for important projects, not just multicolor ones, because we recognize the importance of this multicolor advance confirmation.

Expanding to value-added printing

RGB Workflow Today, the practice of RGB workflow not only enables the multicolor development of offset printing, but also leads to added value development of digital printing presses. From here on, we will introduce our value-added printing efforts that utilize digital printing.

Digital printing initiatives

Our company began working on digital decoration in 2020. From the early 2000s, digital printing machines (toner type) began to appear in the printing industry, marking a period when traditional offset printing began to shift to an era of small lots with a wide variety of products. Our company is a company that has pursued the possibilities of digital printing from an early stage. In the commercial printing industry, which is our business market, the digital shift has progressed rapidly, and printed materials, which had been the top promotional media, have been overtaken by various digital channels due to the spread of the Internet. As digital technology has become more widespread, the main focus of customer promotions has shifted to digital channels such as the web, e-commerce, and social media, and it has become necessary to consider new value for printed materials.

Encounter with the digital decoration machine

The first time we saw a digital decoration machine was at the Konica Minolta booth at Drupa, the world's largest printing equipment exhibition, held in 2016. The digital decoration machine was demonstrated alongside a digital inkjet printing machine, which was still a new technology at the time. Both machines could output directly from digital data, and were exhibits that defined the new value of printing. The digital decoration machine in particular differed from conventional hot stamping in that it could output directly from digital data without using a foil plate. This technology did not use the traditional debossed foil stamping, but instead produced an embossed foil that you could almost touch. Four years later, our company has now installed the same equipment consisting of the digital printing machine and digital decoration machine we saw back then.

Equipment installation

After that, in October 2020, we installed a digital printing press and digital decoration machine, and began building a new value-added business. Initially, we made proposals to our main clients targeting promotional tools such as high-value-added direct mail and posters. However, in 2020, the year we installed the equipment, COVID-19 spread around the world, and promotional printed materials disappeared. Although our company was hit hard, having never anticipated this situation, we used this time to develop new technologies and began challenging ourselves to create new printing expressions using digital printing presses and digital decoration machines.

Branding of digital decoration technology

By utilizing digital printing machines and digital decoration machines, we set out to develop new printing expressions never before seen. Digital decoration generally involves applying decorations on top of printed paper. However, we decided to pursue new expressions by changing the printing order. Furthermore, in 2022, as COVID-19 gradually subsided and business began to move forward again, we were able to win silver and bronze awards in four categories at the Gold Leaf Awards competition hosted by the American FSEA (Foil & Specialty Effects Association).

Promotion using social media

As we were exploring new business markets after introducing our digital printing and digital decoration machines, we decided to promote our technology on social media to spread awareness among many people. In recent years, many companies have been using social media as a business tool, using Instagram and X to promote their products. We decided to also post about our digital decoration technology on social media. By doing this, we were able to meet new people who had not known about us before. We also began business relationships and learned about new printed materials and markets that we had never imagined.

Changes in consumer sentiment

The COVID-19 pandemic has dramatically changed consumer sentiment around the world. In an environment where social contact is extremely limited, people have stepped up their consumption of the things they love. One of the most notable trends among these is trading cards. With Pokémon cards at the forefront, the generation of children at the time saw a surge in spending on things they love due to the stay-at-home demand brought on by COVID-19.

Changing mindset in the printing industry

As printing companies, we tend to think of printed materials as the main focus when doing business. Looking back, we can see that before the rise of the web, printed materials reigned supreme as a promotional medium. At the time, business negotiations were conducted with the goal of producing printed materials. However, since the late 1990s, when the web began to become popular, various channels have emerged to replace printed materials, and as consumer behavior has changed, promotional methods have become more diverse. The value of printed materials themselves has been reevaluated, and they have become an effective means of promotion. Our printing industry is now being called upon to transform from a corporate structure that primarily focuses on creating products to a service provider that provides the means within solutions and services.

Trading Card Challenge

When trading cards became popular all over the world, our customers started asking us for advice on trading cards. The trading card industry is always looking for new technology, and it's an industry where new technology is recognized for its true value. This made it a good fit with the keyword "added value" that our company was looking for. The cards we made were never-before-seen cards using the latest technology, so they were well-received by customers. Demand began to increase around 2022, and in recent years they have become a new source of sales for our business.

Obtaining a technical patent

After gaining market recognition for our trading cards, we next applied for a patent to protect the value of our technology. Generally, it's difficult for printing companies like ours to obtain patents, as they primarily use printing technology to produce replica products. However, we succeeded in creating a new printing expression by combining a digital printing press with a digital decoration machine. As a result, we were able to obtain a patent. Our patented technology is based on an expression that takes advantage of the high film thickness of digital inkjet UV ink. Compared to oil-based offset printing, the ink film thickness is thicker, giving the impression of floating on the surface of the paper, which some people find concerning. However, by combining this characteristic with digital decoration, we have turned this into a positive expression. By applying this technology, we have been able to create a variety of new printing samples.

Printing as a material

Furthermore, we began to think not only about printing as a commodity such as trading cards, but also as a material. We aimed to develop sheets of paper with new processing applied as components rather than as finished products, and to provide them to the manufacturing industry as product components. This initiative was entered into the Tokyo Business Design Awards, a competition hosted by the Tokyo Metropolitan Government in 2023, and won the Theme Award. This is an example of moving from a mindset of aiming to create a finished product to thinking of printing as a means. I believe that discovering new value by exploring the possibilities of printing from various angles will be very important in the printing industry going forward.

To expand printing culture

We opened the lab to let more people know about this technology, which combines digital printing and digital decoration. Here, we exhibit samples that use the various techniques and expressions we have created, allowing you to see them in real life. It is a real experience that you cannot get from social media or the web. The greatest appeal of printed matter is that you can own it. In recent years, new digital assets have been born, such as NFTs and the metaverse. However, these cannot be touched with your hands. We will continue to pursue printing technology while exploring the possibilities of paper. Thank you for your attention.

Author Biography

Yoheita Yoshihara joined Kenbunsha in 2006. After joining the company, he worked on typesetting as a DTP operator, and from 2014 he worked hard to establish a department centered on digital printing, developing W2P systems for major banks and expanding the digital printing business centered on DX. He currently promotes digital printing technology as the Director of the Digital On-Demand Center, and works to solve customer issues.

APT2025 Committee

General Chair

Masahiko Fujii (Keio University Institute at SFC)

Lead Program and Organizational Chair

Natsuko Minegishi (Konica Minolta, Inc.)

Program Chairs

Ramon Borrell (borrell.uk Technology Management)

Takashi Fukue (Kanazawa Institute of Technology)

Hirotoshi Terao (Alps Alpine Co. Ltd.)

Atsushi Tomotake (ATI-C Consulting)

TOKYO - JAPAN
CHAPTER